NEURAL NETWORK APPLICATION FOR IONOSPHERIC STUDY

KORNYANAT WATTHANASANGMECHAI

A THESIS SUBMITTED IN PARTIAL FULFILLMENT
OF THE REQUIREMENT FOR THE DEGREE OF
MASTER OF ENGINEERING IN TELECOMMUNICATIONS ENGINEERING
FACULTY OF ENGINEERING
KING MONGKUT'S INSTITUTE OF TECHNOLOGY LADKRABANG
2011

NEURAL NETWORK APPLICATION FOR IONOSPHERIC STUDY

KORNYANAT WATTHANASANGMECHAI

A THESIS SUBMITTED IN PARTIAL FULFILLMENT

OF THE REQUIREMENT FOR THE DEGREE OF

MASTER OF ENGINEERING IN TELECOMMUNICATIONS ENGINEERING

FACULTY OF ENGINEERING

KING MONGKUT'S INSTITUTE OF TECHNOLOGY LADKRABANG

2011

KMITL-2011-EN-M-010-090

NEURAL NETWORK APPLICATION FOR IONOSPHERIC STUDY

KORNYANAT WATTHANASANGMECHAI

A THESIS SUBMITTED IN PARTIAL FULFILLMENT

OF THE REQUIREMENT FOR THE DEGREE OF

MASTER OF ENGINEERING IN TELECOMMUNICATIONS ENGINEERING

FACULTY OF ENGINEERING

KING MONGKUT'S INSTITUTE OF TECHNOLOGY LADKRABANG

2011

KMITL-2011-EN-M-010-090

คณะวิศวกรรมศาสตร์

สถาบันเทคโนโลยีพระจอมเกล้าเจ้าคุณทหารลาดกระบัง

ใบรับรองวิทยานิพนธ์

หัวข้อวิทยานิพนธ์ โครงข่ายประสาทเทียมเพื่อการศึกษาชั้นบรรยากาศไอโอโนสเฟียร์

Thesis Title Neural Network Application for Ionospheric Study

นักศึกษา นางสาวกรยณัฐน์ วัฒนะแสงมีชัย

รหัสประจำตัว 52611215

ปริญญา วิศวกรรมศาสตรมหาบัณฑิต

สาขาวิชา วิศวกรรมโทรคมนาคม

อาจารย์ที่ปรึกษาวิทยานิพนธ์ รศ.ดร.พรชัย ทรัพย์นิธิ

หมายเลขวิทยานิพนธ์ KMITL-2011-EN-M-010-090

คณะกรรมการสอบวิทยานิพนธ์		ลายมือชื่อ
รศ.ดร.สุวิพล	สิทธิชีวภาค	
รศ.เกรียงไกร	วงศ์โรจนภรณ์	
รศ.ดร.ประยุทธ	อัครเอกฒาลิน	
รศ.ดร.พรชัย	ทรัพย์นิธิ	

วัน / เดือน/ ปี ที่สอบ วันอังคารที่ 24 พฤษภาคม พ.ศ. 2554 เวลา 11.00 – 13.00 น.

สถานที่สอบ ณ อาคาร A ชั้น 5 ห้องประชุม 1

คณะวิศวกรรมศาสตร์ รับรองแล้ว

(รองศาสตราจารย์ ดร.สุชัชวีร์ สุวรรณสวัสดิ์)

คณบดี คณะวิศวกรรมศาสตร์

วันที่ 24 พฤษภาคม พ.ศ. 2554

หัวข้อวิทยานิพนธ์	โครงข่ายประสาทเทียมเพื่อการศึกษาชั้นบรรยากาศไอโอโนสเฟียร์
นักศึกษา	นางสาว กรยณัฐน์ วัฒนะแสงมีชัย
รหัสนักศึกษา	52611215
ปริญญา	วิศวกรรมศาสตรมหาบัณฑิต
สาขาวิชา	วิศวกรรมโทรคมนาคม
พ.ศ.	2554
อาจารย์ที่ปรึกษาวิทยานิพนธ์	รศ. ดร. พรชัย ทรัพย์นิธิ

บทคัดย่อ

ไอโอโนสเฟียร์เป็นชั้นบรรยากาศที่ประกอบไปด้วยอิเล็กตรอนซึ่งไม่เสถียร ส่งผลให้ไอโอโนสเฟียร์ประพฤติตัวเป็นตัวกลางที่ไม่ปกติ สัญญาณดาวเทียมใดใดที่เคลื่อนที่ผ่านไอโอโนสเฟียร์จึงเกิดการแตกกระเจิง นำไปสู่การลดทอนของสัญญาณ บางครั้งเกิดการสูญเสียการล็อคของสัญญาณ ส่งผลให้ปราศจากการสื่อสารผ่านสัญญาณดาวเทียมในช่วงเวลานั้นๆ อีกด้วย ไอโอโนสเฟียร์แปรปรวนอย่างมากบริเวณเส้นศูนย์สูตรดังเช่นบริเวณจังหวัดชุมพรของประเทศไทย ซึ่งทุกวันนี้การประยุกต์ใช้สัญญาณจากดาวเทียม GPS ในด้านต่างๆได้เข้ามาเกี่ยวข้องกับชีวิตประจำวันอย่างมิอาจหลีกเลี่ยงได้ เช่น การประยุกต์ใช้สัญญาณ GPS เพื่อการระบุตำแหน่ง หรือเพื่อการนำร่องในกิจการการบิน เป็นต้น ดังนั้นความแปรปรวนของอิเล็กตรอนในชั้นบรรยากาศไอโอโนสเฟียร์อันเป็นสาเหตุหลักของปรากฏการณ์ต่างๆในไอโอโนสเฟียร์ ซึ่งสามารถถูกศึกษาได้ด้วย TEC นั้น จึงถูกเลือกเพื่อศึกษาในวิทยานิพนธ์ฉบับนี้ นอกจากนี้แล้ว ข้อมูล TEC ที่ถูกเก็บจากจังหวัดชุมพรซึ่งถูกพิจารณาว่าเป็นสถานีเส้นศูนย์สูตรของประเทศไทยนั้นยังไม่เคยถูกสร้างเป็นแบบจำลองมาก่อน อีกทั้งโครงข่ายประสาทเทียมเป็นระบบการจัดการข้อมูลที่สามารถเรียนรู้และแก้ปัญหาที่ซับซ้อนอย่างเช่น TEC ได้ ดังนั้นวิทยานิพนธ์ฉบับนี้จึงนำเสนอการสร้างแบบจำลอง TEC ด้วยโครงข่ายประสาทเทียมสำหรับสถานีชุมพร ประเทศไทย สำหรับโครงข่ายประสาทเทียมที่นำเสนอนั้นเป็นโครงข่ายประสาทเทียมแบบหลายชั้นโดยอาศัยข่ายงานประสาทแบบแพร่กระจายย้อนกลับ เพื่อเป็นการทดสอบประสิทธิภาพของโครงข่ายประสาทเทียมที่นำเสนอจึงทำการเปรียบเทียบ TEC ที่ทำนายได้จากโครงข่ายประสาทเทียมด้วย TEC อ้างอิง (GPS TEC) และ TEC ที่ทำนายมาจากแบบจำลองมาตรฐาน IRI-2007 จากผลการทดลองสรุปได้ว่าโครงข่ายประสาทเทียมที่นำเสนอนั้นสามารถทำนาย TEC ที่สถานีชุมพรซึ่งเป็นสถานีบริเวณเส้นศูนย์สูตรได้ค่อนข้างดี ถึงแม้ข้อมูล TEC ที่มีจะค่อนข้างจำกัดก็ตาม

Thesis	Neural Network Application for Ionospheric Study
Student	Miss Kornyanat Watthanasangmechai
Student ID.	52611215
Degree	Master of Engineering
Program	Telecommunications Engineering
Year	2011
Thesis Advisor	Assoc. Prof. Dr. Pornchai Supnithi

ABSTRACT

The Earth's ionosphere is an irregular and dispersive medium, through which the satellite signals passing are subject to scatter. This property leads to the degradation of the communication signal or causes the loss-of-lock. GPS signal is rapidly involved in the daily life for positioning and navigation system, for instance. In an equatorial region, the ionosphere condition is typically affected by the severe disturbance. TEC can reveal the nature of the electron density variation in the ionosphere which contributes to a number of ionospheric phenomena. The TEC data collected in Thailand, covering an equatorial region, have never been modeled. The neural network is the information processing system which can tackle the non-linear and complex data like the TEC. It is increasingly accepted as a technique to model the TEC data in many latitudinal zones. This thesis presents the TEC modeling based on the NN as the single station model for Chumphon. We employ the multilayer neural nets with the backpropagation algorithm in this work. The proposed NN effectiveness is investigated by making the comparison of the proposed NN TEC, the GPS TEC and the IRI-2007 TEC. The results reveal that the proposed NN can well predict the TEC over Chumphon, the equatorial latitude station in Thailand, even with the limited amount of the available TEC data.

ACKNOWLEDGMENTS

With his warmly welcome since the first day we have met when I was a junior student at King Mongkut's Institute of Technology Ladkrabang (KMITL), I would like to take this opportunity to sincerely express my gratitude to my supervisor, Assoc. Prof. Dr. Pornchai Supnithi. His overwhelming encouragement as well as his high standards and expertise have inspired me to be my best. I have been very fortunate being under his supervision. This thesis work was done at the Communication and Storage Research Group (CSRG) in KMITL during the years 2009 – 2011. I, therefore, wish to thank the CSRG and KMITL for providing the space, computer and internet resources. I also thank everyone at the CSRG as well as Assoc. Prof. Narong Hemmakorn and Assoc. Prof. Nipa Leelaruji for being like my family.

I would like to acknowledge National Institute of Information and Communications Technology (NICT) in Japan for the funding support through the SEALION project under the NICT-KMITL collaboration. Moreover, it is a great honor to have been awarded as a trainee researcher, during my last semester, in Japan. I have gained the knowledge and the excellent experience which surely play a part in defining my future.

I devote my warmest thanks to Dr. Takashi Maruyama, NICT executive researcher, for lending a hand whenever he could and for all the wonderful supports he afforded me. I impossibly fail to thank Dr. Takuya Tsugawa, NICT senior researcher and my supervisor during my stay in NICT, for his utmost obligingness and appreciated assistance during the crucial period of my life. Both of them have motivated and sparked me to do the things that I only dreamed of doing. Thank you very much.

For being such a dear friend, I need to express my thanks to Dr. Kaori Sakaguchi. Through all the trials and challenges which I have faced over the last year; her friendship has been an anchor to me, keeping me strong and happy. Without her and her family, living and training far away from home would be difficult for me.

Lastly, I am indebted to my beloved family for their patience, dedication and unconditional love which are endless and invaluable.

Kornyanat Watthanasangmechai

TABLE OF CONTENTS

TABLE OF CONTENTS (to)

TABLE OF CONTENTS (to)

LIST OF TABLES

Table **Page**

LIST OF FIGURES

LIST OF FIGURES (to)

Figure **Page**

LIST OF FIGURES (to)

Figure **Page**

Chapter 1

Introduction

1.1 Literature Review of TEC Modeling

The Earth's ionosphere is a dispersive medium which is irregular, through which the satellite and/or radio signals passing are subject to scatter and refract [1]. Since the Earth's ionosphere is unstable, the electron density drastically changes, a number of phenomena such as ionosphere disturbances and plasma bubble frequently occur, especially in the low-latitude region like Southeast Asia. These phenomena lead to a degradation of the communication signals. Total electron content (TEC) is one of the important parameters, which can describe the ionosphere ionization content and varies over place and time. The TEC derived from the GPS satellites has been collected to construct empirical models. Neural network (NN) techniques, for instance, have recently been applied to various topics in the study of the upper atmosphere [2].

Previous works focus on the NN development for the study of temporal and spatial forecasting of the foF2 values in advance [3], [4], ionospheric variability and electron density profile studies [5], retrieval of in situ electron density in the topside ionosphere from cosmic radio noise intensity [6], the Schumann resonance intensities forecasting [7] as well as GPS-TEC modeling for Turkey [8], Canada [9], South Africa [10] to [13], Japan [2], [14], and Thailand [15], [16].

1.2 Motivation and Significance

At present, there exist a number of ionosphere models, including IRI-2001 and IRI-2007, the empirical standard models, which allow calculations of the electron density profile as well as TEC. The TEC is directly related to the satellite delay time and other ionospheric phenomena. IRI-2007 now offers various options to compute the electron density in the topside ionosphere, the region above the F2 maximum, which was improved from the limitations in the previous versions of the model [17], [18]. In addition, IRI-2007 is now being developed and tends to employ the neural network as one of the potential tools for ionospheric parameter prediction since it can learn from the prior data, which are limited and complex.

The equatorial and the auroral regions are anomaly areas where the most significant discrepancy of experimental and modeled data was observed [19]. At the equator and the low latitude, changing in the Earth's electric field induces the dynamical change of the TEC [20]. Thailand is located on the equatorial ionization anomaly (EIA) zone, which is the important area for the ionosphere study. However, the data covering this region are still scant.

In the recent years, TEC computed from the GPS data have become available in Thailand and some neighboring countries through SEALION project among others. The availability of historical TEC data is important to the development of the IRI model [21] as well as the NN model which can learn from the prior data. It provides the opportunity for archiving and collecting the TEC to develop the TEC model over Thailand. Hence, we focus on the NN development for TEC modeling over Chumphon, equatorial latitude station in Thailand.

1.3 Objective of the Study

- Observe the nature of the Earth's ionosphere in an equatorial latitude region.
- Model the TEC as the single station model based on the NN.
- Verify the developed NN by making the comparison of the GPS TEC, the proposed NN TEC and the IRI-2007 TEC.
- Investigate an effectiveness of the IRI-2007 model by considering the discrepancy between the IRI-2007 TEC and the GPS TEC.

1.4 Scope of Research Work

In this thesis, the TEC data derived from the dual-frequency GPS receiver installed at Chumphon campus of King Mongkut's Institute of Technology Ladkrabang (KMITL) are investigated. These TEC data are operated and supported by National Institute of Information and Communications Technology (NICT), Japan, according to the SEALION project collaboration. They are employed as the source of the input space for the proposed NN. Another crucial source for the input space, the daily sunspot number, is the website of National Oceanic and Atmospheric Administration (NOAA), USA. The TEC over Chumphon station on solstice and equinox days, in

March and September equinox seasons, in June and December solstice seasons, and for all studied-year, are predicted. The IRI-2007 model-derived TECs are used to compare with the NN-predicted values as well as the GPS-derived TEC in order to examine the effectiveness of the proposed NN.

1.5 Thesis Outline

This thesis is divided into six chapters. Chapter 1 introduces the literature reviews of TEC modeling, the motivation and the significance of this research work, the objective of the study, and the research scope.

The related theories, including the Earth's atmosphere and ionosphere, the solar cycle, the total electron content (TEC), as well as the GPS-derived TEC are given in Chapter 2.

Chapter 3 provides the review of related models, International Reference Ionosphere (IRI) model for example, and GPS receiver networks both in Thailand and the world.

The research methodology can be found in Chapter 4 regarding to an artificial neural network theory and the proposed neural network model. The details of NN algorithm and architecture, parameters selection, NN process, and the output of the model are also discussed.

The results and discussions are in Chapter 5. The hourly, diurnal, seasonal and yearly comparisons of the NN TEC with the IRI-2007 TEC and the observed are discussed.

Chapter 6 concludes the overall NN processes and its results. The effect from the Earth's ionosphere and TEC in the equatorial latitude area to the communications system is deduced. Finally, the future work is discussed.

Chapter 2

Atmosphere and GPS-Derived TEC

In this Chapter, the neutral atmosphere and the ionosphere are reviewed. The ionosphere structure which depends on the height from the Earth, and the latitude are described. The prereversal enhancement phenomenon which causes suddenly increasing in an electron density and leads to the generation of an ionosphere instability that contributes to a number of ionospheric effects is introduced. The ionospheric effect on positioning, navigations and communications systems is mentioned. The solar cycle which relates to the TEC variation, the definition and significant of the TEC, and the methodology to derive the GPS TEC are reported.

2.1 Neutral Atmosphere

Above the Earth's surface, the region extending beyond 1,000 km is the neutral atmosphere. It is the rudimentary source of the ionospheric plasma. To stratify it, the temperature profile in Kelvin (K) is used and demonstrated in Figure 2.1. In the troposphere, the temperature decreases with altitude to the minimum value at about 10-km height that confines its boundary, named the tropopause. The atmospheric weather and other turbulences exist in this layer. Above this, the temperature turns to increase due to the solar UV radiation absorbed by ozone. At about 50-km height, the temperature reaches the maximum before reversal again at stratopause. The next layer is the mesosphere extending from the stratopause to 90-km height, approximately. Radiative cooling brings about the sharp decrease in temperature. At the mesopause, the temperature touches the minimum of around 130 – 190 K. The mesosphere is the coldest region among others in the terrestrial atmosphere. Below 100-km height, the atmosphere is quite uniform in composition due to a variety of turbulent mixing phenomena.

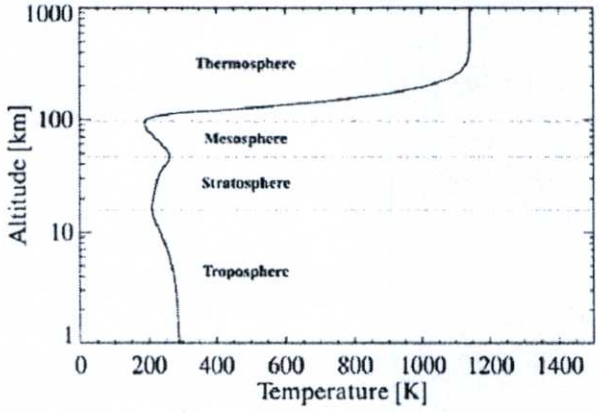

Figure 2.1 The temperature profile of the neutral atmosphere [22].

In the region above the mesopause, the dramatic increase in temperature reveals. It is due to the absorption of solar protons even with the energy above 1,000 K, on average. This region is unsurprisingly termed the thermosphere and is the hottest region in the terrestrial atmosphere. The temperature increase in the thermosphere is explained by the absorption of solar UV and EUV radiation. In sunlit hemisphere with sufficient solar energy, since the EUV radiation plays an important role in the plasma production, equal numbers of protons and electrons are produced from the neutral atmosphere.

2.2 Ionosphere

The Earth's ionosphere is an ionized portion of the upper atmosphere constituted both of the neutral and charged particles. The charged particles including free electrons and ions, so-called "*plasma*", are originated from molecules and atoms ionized by ultraviolet (UV) and X-ray radiation emitted from the Sun. These vary over space and time, and contribute to a number of ionospheric phenomena that affect on an electromagnetic wave propagation for satellite communications.

Even though the upper boundaries of an ionosphere are not well-defined yet, the ionosphere is roughly considered extending around 60 – 1,000 km altitude for the most practical purpose. It is well-known that a regular ionospheric activity depends on hourly, diurnal, seasonal, and solar cycle

variations. An irregular one such as travelling ionospheric disturbances (TID) is affected from a geomagnetic activity caused by solar storms.

2.2.1 Vertical Structure of the Ionosphere

Since the different portions of the solar spectrum are absorbed at different altitudes, it is sensible to exhibit the ionospheric layer by the plasma density as illustrated in Figure 2.2. Several layers of the ionosphere with different ion densities known as the D, E, F1 and F2 layers are demonstrated. In daytime, the plasma exponentially increases with decreasing altitude due to the solar radiation absorption of the neutral atmosphere. It causes the solar flux decreases. The combination of the decreasing solar flux, increasing neutral density, and diffusion provides a simple explanation for the basic large-scale vertical layer of ionization which is shown in Figure 2.3. At night, without the solar radiation effect, the ionization and recombination depend almost only on the chemical and collision processes. The plasma density is dramatically reduced even though some plasma can flow back from the high altitude region called "*plasmasphere*".

The D-region is adjacent to the Earth's surface and coverage is in the range of about 60 – 90 km. It is produced by the hard X-rays of the sun during daytime and rapidly disappears during nighttime. The layer above the D-region at 90 – 150 km apart from the Earth is termed the E-region. The name of which is given from the electric field in the radio wave reflected by the ionosphere. Since the E-region is produced by soft X-rays, the electron density reduces at night.

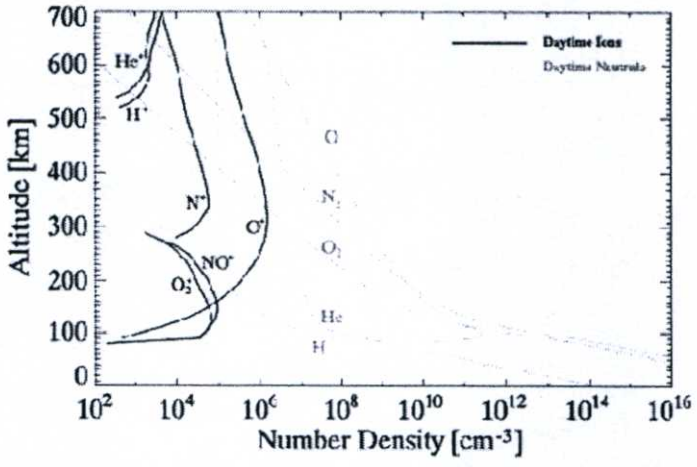

Figure 2.2 Ion density profile. [22]

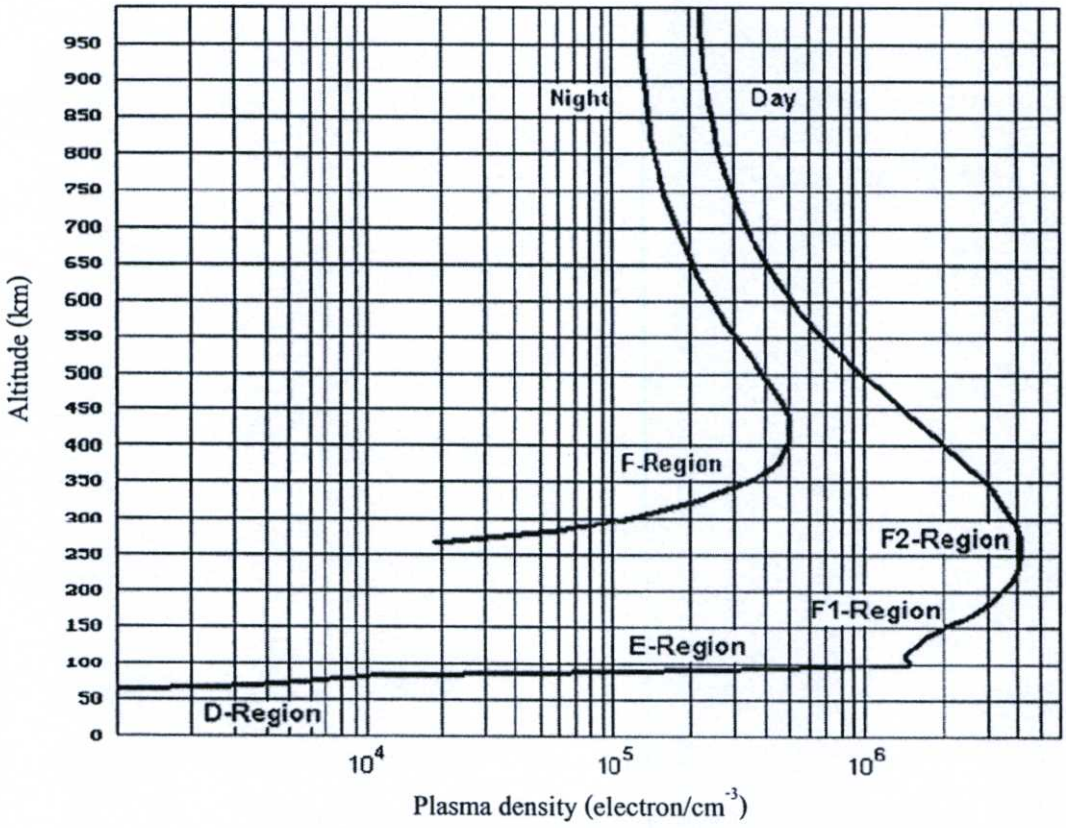

Figure 2.3 The vertical layer of ionization. [23]

The F-region is in the altitude range of 150 – 500 km above the Earth's surface. The maximum plasma density in the ionosphere occurring in the so-called F layer is termed F-peak and marks the bottom side of the ionosphere. During the daytime, the F-region is separated into F1 and F2-layers due to EUV radiation-produced ions. These two F-layers combine into the F-region at night.

2.2.2 Latitudinal Structure of the Ionosphere

The plasma density variation of the Earth's ionosphere depends on not only the processes in the vertical profile but also the different physical processes associated with the different geomagnetic field lines configurations. These incur the latitude variation of the ionosphere.

At high-latitudes, the magnetic field is nearly vertical. The ionosphere is thus connected with the magnetosphere via the magnetic field lines. Along them, ion and electron transition is generally gradual. In this region, since the electric force dominates the pressure gradient and gravitational forces, the ionosphere condition is drastically changed by the intense enhancement of the

magnetospheres' electric field and the auroral precipitation during active geomagnetic conditions such as geomagnetic storms and sub-storms.

At mid-latitudes, the magnetosphere condition does not directly contribute to the plasma drift due to a significant dip angle of geomagnetic fields. Without restriction of the geomagnetic field, the collision between the charged particles and neutrals becomes important process. The plasma promptly flow along the magnetic field lines and escape to the conjugate ionosphere. Also, Neutral wind, gravity, and pressure gradient cause the parallel drift of the plasma. These short the high-density plasma along the length of magnetic field lines and contribute to the plasma instability.

At low-latitudes, the plasma flow perpendicular to the geomagnetic field which is nearly horizontal. At dawn, the E-region dynamo electric fields are dominant in the E and F-region, and result to uplift the plasma due to the $E \times B$ drift with an eastward electric field at the magnetic equator. Two crests with maximum ionization density considered as the "*fountain-like pattern*" appear approximately at geomagnetic ±15 degree latitudes from the magnetic equator due to the plasma diffusion. The plasma drifts downward along the magnetic field lines at dawn because of the Earth's gravity and the becoming dominant westward F-region dynamo electric fields with the low conductivity in the E-region. The plasma enhancement regarding to the eastward electric field before reversal is called "*prereversal enhancement*", and the irregular ionization in this region is considered the "*equatorial ionization anomaly*" (EIA).

2.2.3 Prereversal Enhancement

The prereversal enhancement simulation has firstly been accomplished by a general circulation model named as the National Center for Atmospheric Research thermosphere/ionosphere/electrodynamics general circulation model (TIEGCM). In equatorial region, the plasma mobility is generally upward in the daytime and downward in the nighttime due to the $E \times B$ drift. As illustrated in Figure 2.4, the downward vertical electric field, $E = -U \times B$, is generated by the effect of neutral wind dynamo in E-region. The electric field maps along B to an equatorward electric field component. This field drives a westward Pedersen and Hall currents, J_P and J_H, on the both sides of the terminator. The hall conductivity in the dayside is 10 times more than that in the night side. It results to the building up of a negative charge density near the terminator, creating the

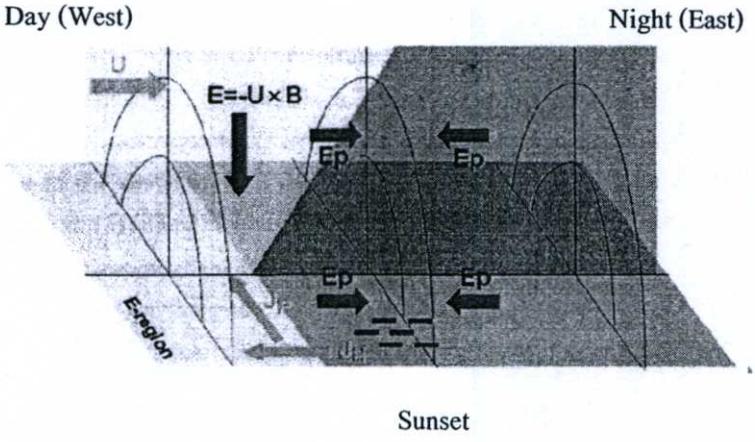

Figure 2.4 The prereversal enhancement generation. [24]

localized zonal electric field perturbation toward the terminator in the E region. The electric field is then mapped to be eastward and westward in F-region at dawn and dusk, respectively. The enhance of the eastward electric field before turning to westward is called "*prereversal enhancement*" or "*evening enhancement*".

Since the F-region dynamo acts as the constant current source with high internal resistance, it is promptly short-circuited by Pedersen conductivity before sunset. During the night time, decreasing of electron density in the E-region influences the reduction of the conductivity and creates the F-region downward electric field. This electric field induces the plasma to drift with the same direction as the thermospheric winds. Two hours prior the drift reversal, the plasma-dynamic-derived electric field in F-region results in the non-uniform E-W plasma diffusion in the E-region, it causes the immediately intense of the eastward electric field.

The prereversal enhancement, in summary, is an important ionospheric phenomenon. Besides significantly causing the plasma instability in low-latitude especially at the equatorial region, it may play a crucial role in the generation of plasma bubbles as well.

2.2.4 Ionospheric Effect on Positioning, Navigations and Communications Systems

Nowadays, the radio wave technologies are unexpectedly embedded in our daily life which make a mankind more convenient and enrich our community. Various applications are applied for different situations such as the utilization of the Global Navigation Satellite System (GNSS)

including the GPS for land surveying and mapping, earthquake study, meteorology, air traffic control, car navigation, atmospheric research, telecommunications and others. However, increasing in the propagation delay and the fluctuation of the signal passing through the Earth's ionosphere induced by the ionospheric disturbances is a great concern for those who focus on the high-precision satellite navigation system. The modulations between the ionosphere irregularities and the passing-through signal not only render the time delay persistence, but also deteriorate the signal integrity. While the observation from single station is hard to capture the ionospheric phenomena, networks can overcome. Accordingly, the idea and data sharing in the field of ionospheric study especially the GPS-based applications thus becomes useful and important. The ionospheric effects on radio applications are illustrated in Figure 2.5.

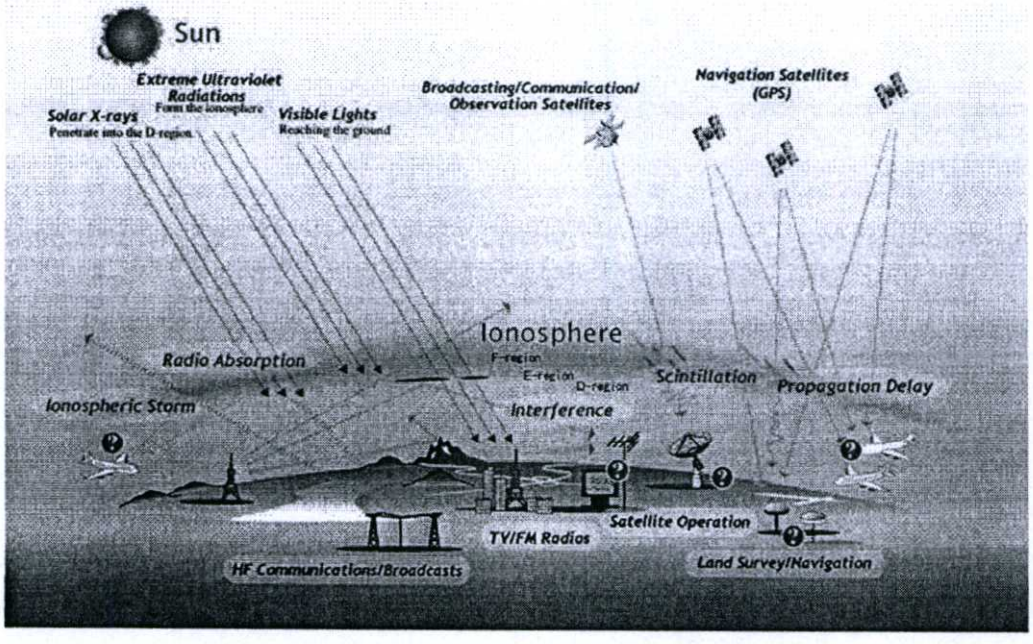

Figure 2.5 Ionospheric effects on radio applications [25].

The Earth's ionosphere contains tons of ionized portions called "*electrons*" and "*ions*" which are non-stable. If we consider in the aspect of the communications systems, whenever the radio wave propagates through the ionosphere, it is affected from the fluctuation and the instability. These communication systems include the GPS satellite for positioning system and the high-speed satellite communication which is considered the wireless broadband, for example. Since the refractive index

inside the ionosphere is drastically different from that of the outside, the satellite signal travelling through the ionosphere refracts from the satellite-receiver-path (the dash line) as shown in Figure 2.6. It is due to the non-uniform electron density which leads to the suddenly change in an amplitude of the signal known as the "*radio-wave scintillation*". The situation without satellite communications is considered the "*loss-of-lock*" (LOL) occurrence. Also, it leads to the irregular delay which affects on the satellite data transmissions, the communications between the satellite and the airborne system, and the accuracy of the GPS. The drastic change in signal amplitude known as the scintillation is the phenomenon that the satellite signal changes in its amplitude and phase when it propagates through the Earth's ionosphere as depicted in Figure 2.7. The scintillation affects the satellite communication system in the VHF and UHF bands. The motive of the scintillation appearance is strongly believed as the instability of the electron density in the E and the F region of the Earth's ionosphere. One of the parameters which can be used to study the ionosphere refractive index variation and its ionization is the total electron content (TEC).

Two types of the TEC effects on positioning, navigation and communications signals can be distinguished. Firstly, TEC is directly related to the time delay. It causes the positioning error; hence, it affects the applications which require the high-precision accuracy such as air-traffic navigation, land mapping and others. Secondly, an immediate TEC depletion is considered the "*plasma bubble occurrence*". It includes several of ionospheric irregularity scales which lead to the LOL and cause the scintillation of the radio signal. Consequently, the GPS measurement becomes impossible for a while. In the worst case, loss of communications will be more frequent during the high solar activity in the near future.

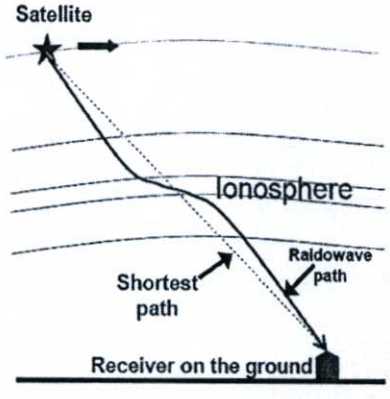

Figure 2.6 The satellite-receiver propagation path.

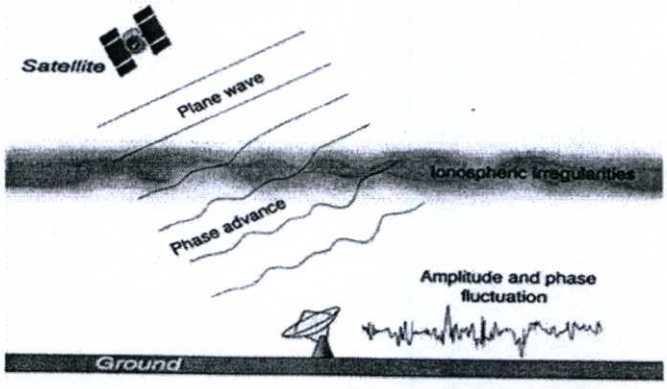

Figure 2.7 The radio wave scintillation [25].

The time delay due to the ionosphere called an "*ionospheric delay*" is a function of slant TEC (STEC). Meaning, the ionospheric delay is high during daytime and low during nighttime following the nature of the TEC variation. However, the ionopsheric delay is not only the delay. Tropospheric delay due to dense neutral atmosphere and water vapor is as large as the ionospheric delay. In the real measurements, measured delay time includes those caused by satellite and receiver clock error, satellite position error or multi-path noise, and relativistic effects. At equatorial and low latitude, changing in the Earth's electric field induces the dynamical change of the TEC [20]. The strong electric fields during a magnetic storm cause significant changes in an ionosphere morphology, and produces large GPS propagation delays and large carrier phase advance. Since the ionospheric delay leads to not only the error in the communications system but also the dominant errors in "*satellite based augmentation system*" (SBAS) for an aeronautical purpose which concerns with people safety issue, the study of the ionospheric effects including TEC which can describes the ionosphere ionization content thus becomes important.

An immediate TEC depletion is considered the plasma bubble. For its generation mechanism, it was believed as the Rayleigh-Taylor instability; however, it is not fully understood. Plasma bubble appears after sunset and causes the TEC fluctuations. So we can notice the plasma bubble by monitoring the rate of TEC change index or ROTI. The plasma bubble generally moves eastward and has the structure extending along the magnetic field line. Its horizontal scale is about more or over 200 km in longitude and 1000 km in latitude. The large TEC gradient appears at the edge of the

plasma bubble. In this area, the TEC is dense. This causes the ionospheric delay as mentioned above. Inside the plasma bubble, it includes various ionospheric irregularity scales. One of the important irregularity scales is that which leads to the radio scintillation appearance affecting on a temporary unavailable of the satellite communications. When the plasma bubble occurs, the TEC depletion appears, the drastic change of the ROTI is noticed, and then the LOL becomes visible.

2.3 Total Electron Content

Total electron content (TEC), the line integral of the electron density along the propagation path from a satellite to a receiver, is one of the quantities which can describe the ionospheric ionization content and the ionosphere variability that affects to the GPS signal. Not only the utility for the ionosphere and atmosphere study or the space weather the TEC gives, it also acts as the useful parameter for other aspects like satellite communications, for example. When the differential TEC is analyzed together with other device-derived data such as all-sky imager data, the plasma bubble can be studied. The plasma bubble is the plasma density depletion region generated by the plasma instability after sunset, and severely disrupts the radio signal. It includes several of the ionospheric irregularity scales. One of them causes the radio wave scintillation which performs as the barrier of the satellite communications. As shown in Figure 2.8, the radio wave scintillation most severely occurs at ±20 degree latitude and polar region. To understand the generation and evolution of the plasma bubble, and the scintillation occurrence, the TEC data are needed.

The TEC is the temporal and spatial variation parameter. For temporal variation, TEC depends on hour, day, season, year, solar cycle, solar activity and geomagnetic activity, for example, leading to day-to-day variation and day-to-night variation. For spatial variation, it causes the different TEC levels and characteristics among different locations in the world. One of the most important locations for the ionospheric study is known as "*equatorial ionization anomaly*" (EIA) region where the drastic change in TEC amplitudes can be observed. The EIA region is the area within ±15 degree latitude extending from the geomagnetic equator, and the area in the polar region. It is well known that Thailand is located on the EIA region. However, the TEC-related research works over Thailand have just recently been started. Five years have passed since the first observation has been launched from the research collaboration between National Institute of Information and Communications

Technology (NICT), Japan and King Mongkut's Institute of Technology Ladkrabang (KMITL), Thailand through the Southeast Asia Low-Latitude Ionospheric Observation Network (SEALION) project.

TEC can be derived from various techniques such as ionogram and GPS data. We focus on the GPS-based TEC which can be derived from code or carrier phase advances or delays of the radio wave. Those derived from carrier phase advances or delays give more precision because of its wavelength which is two to three times shorter than that of the code. Thus TEC derived from the carrier phase advances or delays are suggested for the work which requires high precision such as the aeronautical navigation. TEC is an integral value of the electron density along the propagation path with one-m^2 surface. For Chumphon station, TEC data were derived for all ray paths between GPS satellites and the receiver whose elevation angle is larger than 45 degrees. The GPS TEC data used in this thesis are derived and supported by NICT. The details of GPS-derived TEC methodology can be found in the paper titled "*A new technique for mapping of total electron content using GPS network in Japan*" [26] which will be described hereafter.

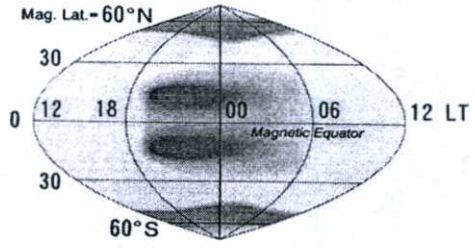

Figure 2.8 The radio wave scintillation pattern.

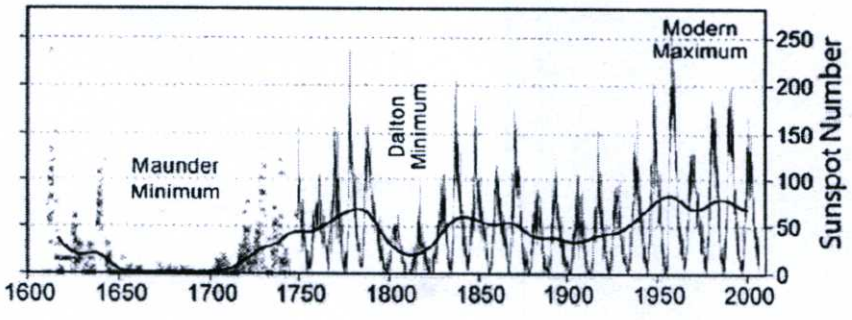

Figure 2.9 The 400 – year sunspot history. [28]

2.4 Solar Cycle

The solar cycle or solar magnetic activity is the periodic change of the solar radiation projecting from the Sun to the earth. The period of one cycle is approximately 10.7 years. Solar variation effects on the space weather changing causes slight changes in the Earth's weather. The solar cycle is observed by counting the frequency and the placement of the discernible sunspots on the Sun. Powered by a hydro-magnetic dynamo process, driven by the inductive action of internal solar flows, the solar cycle structures the Sun's atmosphere, corona and wind, directly modulates the flux of short-wavelength solar radiation, from ultraviolet to X-ray, and indirectly modulates the flux of high-energy galactic cosmic rays entering the solar system [27].

The first discovery of the solar cycle was accomplished in 1843 by Samuel Heinrich Schwabe. Focusing on an average number of the sunspots, he noticed a periodic solar variation which can be seen from year to year on the solar disk. After that, Rudolf Wolf kept further study on the solar observations, reconstructing the cycle back to 1745. It is the time when Galileo and other contemporaries earliest observed the sunspots. The standard sunspot number index was defined and has been used up to now. The 400-year record of the sunspot number is illustrated in Figure 2.9. Also, the monthly averaged sunspot numbers are processed and available as shown in Figure 2.10.

As most of the sunspots groups have ten spots on average, the sunspot number is thus given by summing the number of individual sunspots with the number of groups. Currently, there are at least two organizations which officially observe, record and provide the sunspots number which are Solar Influences Data Analysis Center in Belgium, and the US National Oceanic and Atmospheric (NOAA). The statistical record of the sunspots number is of important for the prediction work of the sunspots activity on which some researchers put their efforts to develop the model. One of the examples of the sunspot number prediction for solar cycle 24 is shown in Figure 2.11.

The sunspot activity causes a significant effect on long-distance radio communications, particularly on the shortwave band. The high levels of the sunspot activity deteriorate the quality of the radio signal. Also, they increase the solar noise levels and the ionospheric disturbances. These impacts are mainly affected from the increase of the solar radiation on the ionosphere.

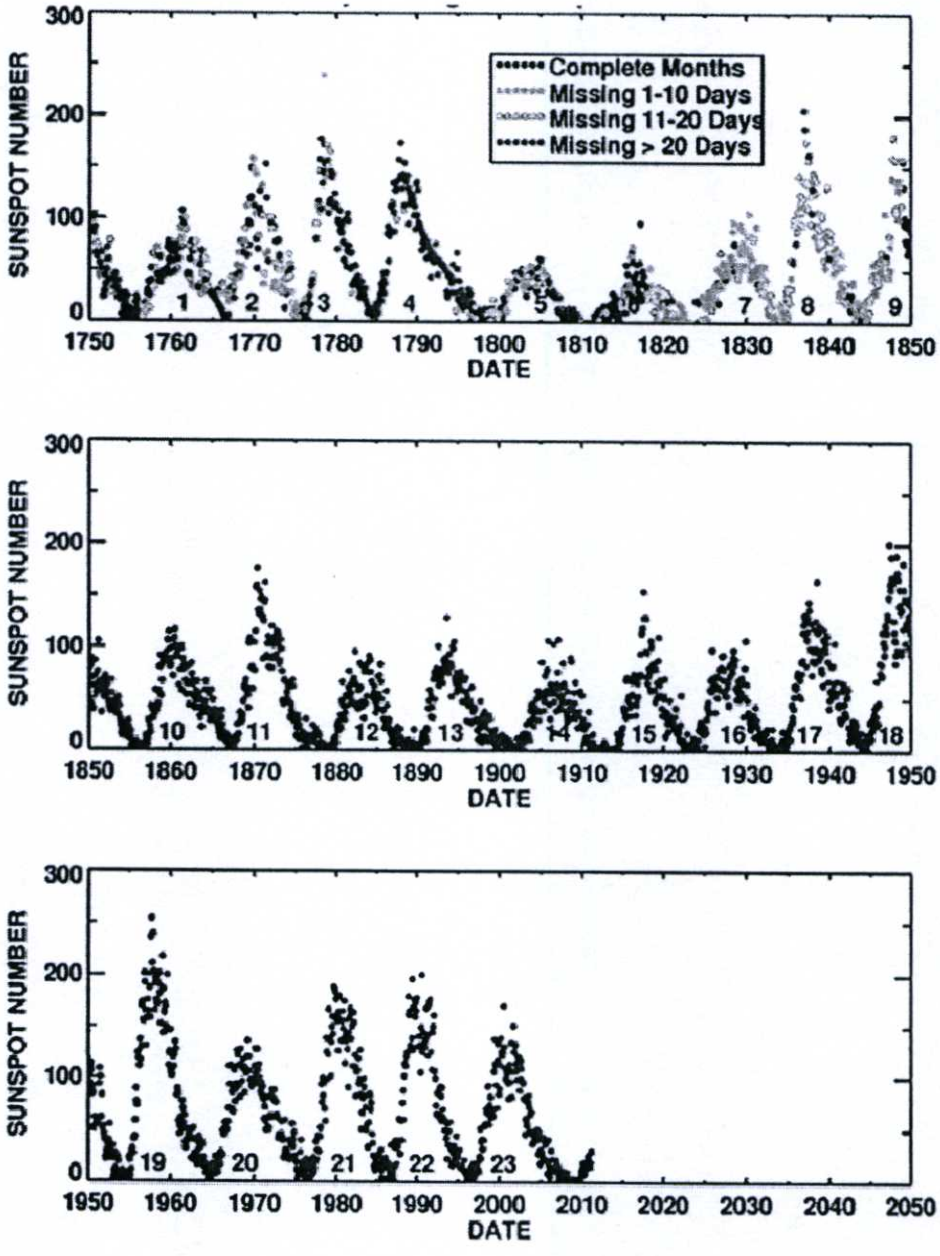

Figure 2.10 The monthly averaged sunspot numbers [29].

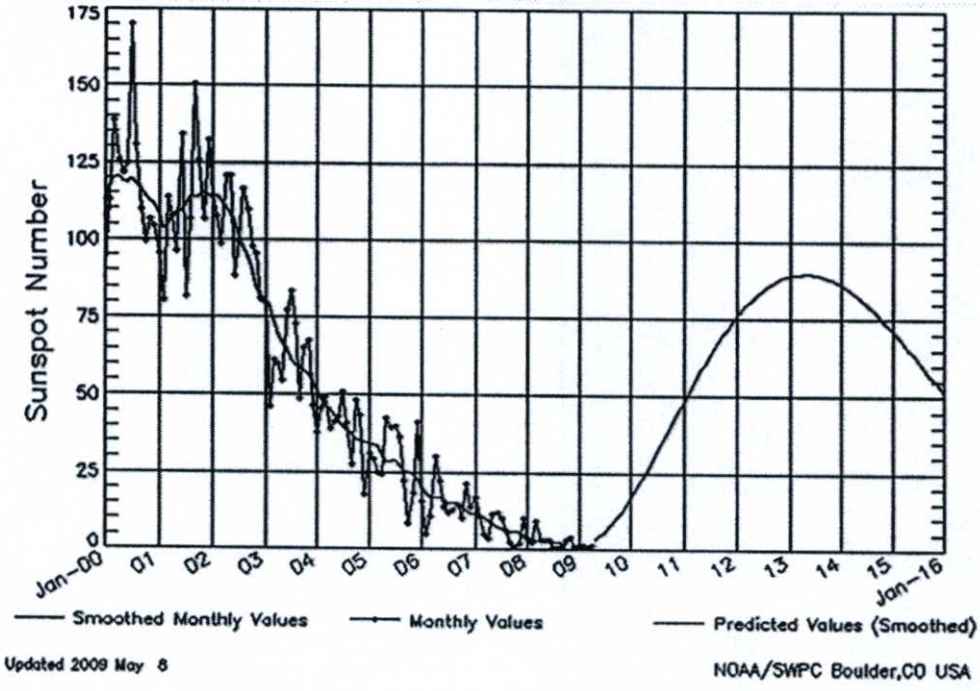

Figure 2.11 Cycle 24 sunspot number prediction. [29]

2.5 GPS-Derived TEC

TEC is defined as the total electron content (electron/m^2) of a vertical column of 1 m^2 cross-section [30], [31] called a "*vertical TEC*" (VTEC) which varies over place and time. The height of the GPS satellites is about 22,000 km which includes both of the ionosphere and the plasmasphere. The TEC measurement for Chumphon station is obtained from the JAVAD-GPS receiver which receives two GPS signals with L_1 signal (f_1 = 1575.42 MHz) and L_2 signal (f_2 = 1227.60 MHz). For this work, the TEC measurement system consists of a microstrip antenna, an amplifier, a JAVAD TEC meter, and a computer unit as shown in Figure 2.12.

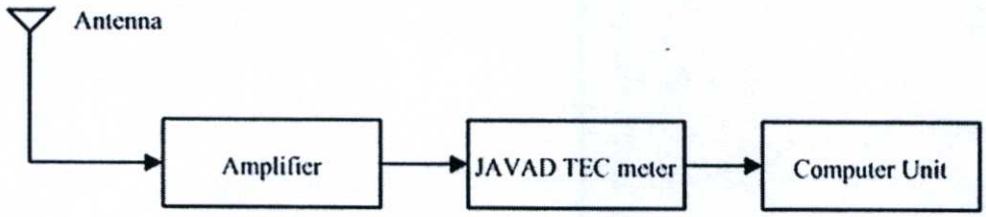

Figure 2.12 TEC measurement system.

Generally, the slant TEC (STEC) data from the satellites to the receiver can be obtained from the difference between the pseudo ranges (P_1 and P_2) or the difference between the phases ($L1$ and $L2$) of the two frequencies [32]. Then the TEC can be computed from the STEC value and the zenith angle as [31].

$$\text{STEC}=\frac{2(f_1 f_2)^2}{k(f_1^2 - f_2^2)}(P_2 - P_1), \tag{2.1}$$

or

$$\text{STEC}=\frac{2(f_1 f_2)^2}{k(f_1^2 - f_2^2)}(L_1\lambda_1 - L_2\lambda_2), \tag{2.2}$$

where k, related to the ionosphere refraction, is 80.62 (m^3/s^2), λ_1 and λ_2 are the wavelengths corresponding to f_1 and f_2, respectively. However, the TEC estimation technique for this work bases on the TEC mapping technique which is introduced by Otsuka et al [26] and will be described below.

TEC data were derived for all ray paths between GPS satellites and the receiver whose elevation angle is larger than 45 degree. The vertical TEC, in el/m^2, is computed from the mapping technique described by Otsuka et al [26]. The ionosphere is assumed to be a thin shell which is commonly used in the GPS TEC studies [33]. For Thailand, as shown in Figure 2.13, the ionospheric shell height for TEC calculation is assumed to be 400 kilometers [34]. The bottom side and top side of the ionosphere are set to be 300 kilometers and 600 kilometers, respectively.

For mapping technique, the receiver position is exactly known. Also, the satellite position can be known from orbit data which are downloaded from the NASA via ftp. Refer to the basic geometry, for the given right triangle, if two vertex angles are known, the rest one will be known.

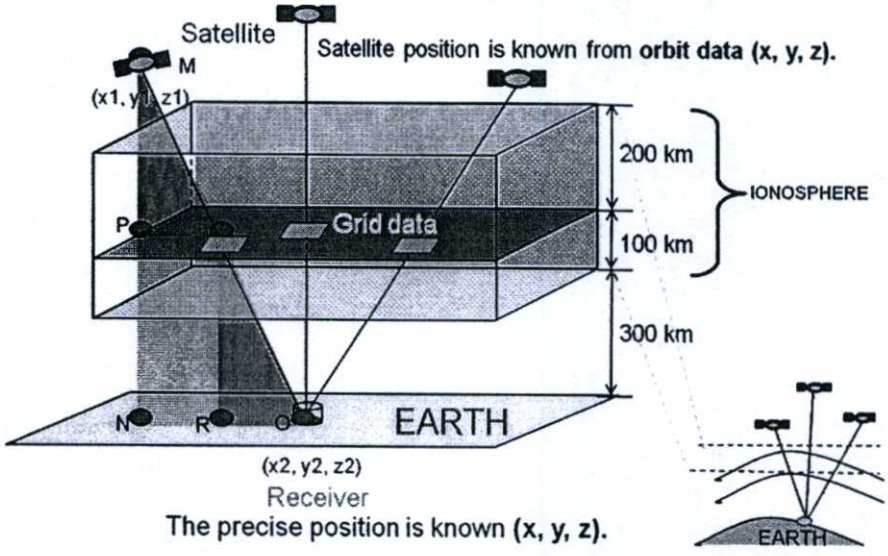

Figure 2.13 TEC mapping technique.

Here we know the satellite (M) and receiver (O) positions, thus, the point N can be known. And then we will know the P position. Finally we get the point Q called the "*ionospheric piercing point*" (IPP), which is the VTEC mapping point.

The absolute TEC, $I^i(t)$, is measured by satellite – i at epoch time t and determined from the phase and pseudorange data. It comprises of both of the slant TEC, $T^i(t)$, along the propagation path and the instrumental bias B^i.

$$I^i(t) = T^i(t) + B^i \tag{2.3}$$

The instrumental biases are assumed to be constant over several days [33]. From this assumption, the STEC at a given point in the ionospheric thin shell is thus equivalent to the VTEC. A user calculates IPPs of each satellite and interpolates to obtain VTEC at each IPP. The slant factor is then multiplied to obtain the correction in range as:

$$T^i(t) = S\left(\varepsilon^i(t)\right) V^i(t) \tag{2.4}$$

where $V^i(t)$ is the equivalent vertical TEC at the given point. $S\left(\varepsilon^i(t)\right)$ is the slant factor of each satellite at altitude h which is defined as an inverse of cosine of the satellite zenith angle at a sub-ionospheric point and given as:

$$S(\varepsilon)=\frac{1}{\cos\left[\arcsin\left\{\frac{R}{R+h}\cos(\varepsilon)\right\}\right]} \tag{2.5}$$

where $S(\varepsilon)$ is the slant factor, ε is an elevation angle of the line-of-sight along the satellite-receiver path, and R is the radius of the Earth.

Also, the slant factor, S, can be defined as the ratio of the ray path range between 300 and 600 km altitudes, τ_1, to the ionosphere thickness of 300 km for the zenith path, τ_0, as:

$$S=\frac{\tau_1^i}{\tau_0} \tag{2.6}$$

The slant factor is proportional to an error in VTEC estimation process – in other words, the estimation error increases with increasing of the slant factor at the lower elevation angle. With this reason, only the data with elevation angles larger than 45° are included in the GPS-derived TEC method for Thailand.

Consider Equations (2.3) and (2.4), $I^i(t)$ is rewritten as:

$$I^i(t)=S\left(\varepsilon^i(t)\right)V^i(t)+B^i \tag{2.7}$$

The hourly average VTEC is assumed to be uniform within the receiver-covered area. Since this technique is applied for four SEALION sites in Thailand which are Chiang Mai, Bangkok, Chumphon and Phuket, the coverage area corresponds to a surrounding of hundreds of kilometers from each receiver. Meaning, the GPS signals received from different satellites by one receiver are

the same and can be averaged to be the hourly average VTEC. To estimate the hourly average VTEC, equation (2.7) is divided by the slant factor and averaged over one hour as follow:

$$\overline{\frac{I_k}{S\left(\varepsilon_k^i\right)}} = \overline{V_k} + \overline{\frac{1}{S\left(\varepsilon_k^i\right)}} B^i \tag{2.8}$$

for $k = 1, 2, 3, \ldots, N_t$ and $i = 1, 2, 3, \ldots, N_s$ where N_t is the hourly TEC average number, and N_s is the number of satellite with the elevation angle larger than 45 degree which can be observed by one receiver.

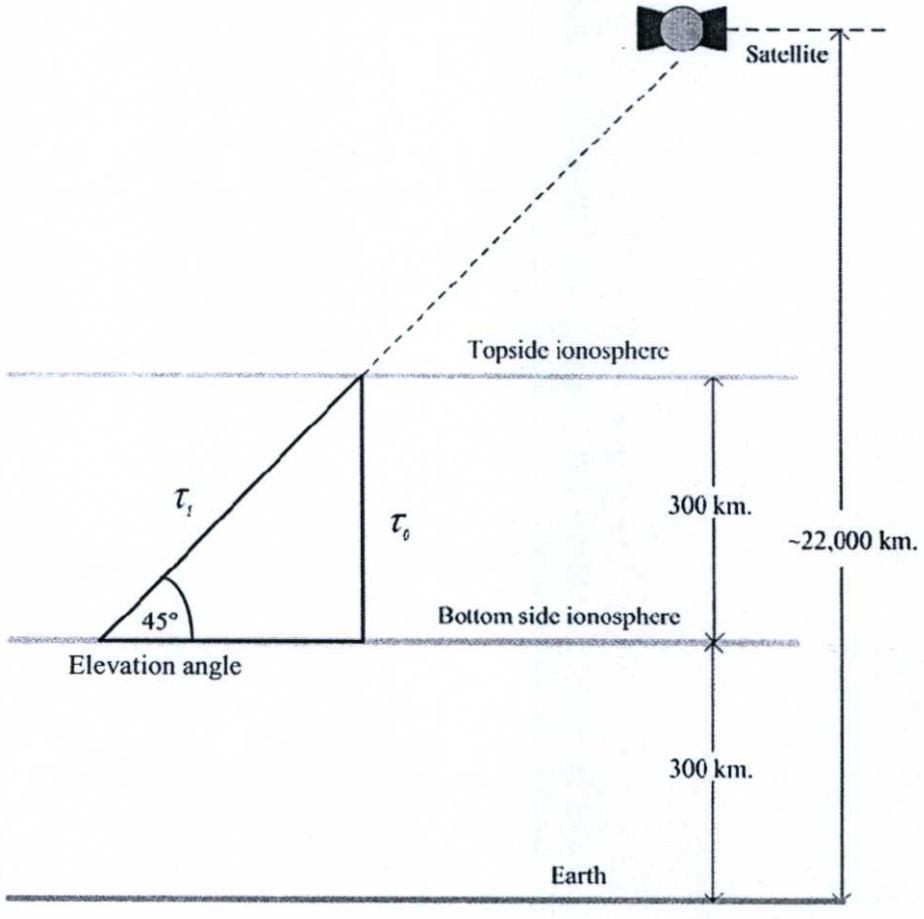

Figure 2.14 Illustration of the parameters setting for the slant factor computation.

Since the number of equations is larger than that of the unknowns, the unknowns, $\overline{V_k}$ and B^i can be solved. Applying a least square fitting technique, we get

$$E=\sum_{i}^{N_s}\sum_{k}^{N_i} W_k^i\left[\frac{\overline{I_k}}{S\left(\varepsilon_k^i\right)}-\left(\overline{V_k}+\frac{\overline{1}}{S\left(\varepsilon_k^i\right)B^i}\right)\right]^2 \tag{2.9}$$

where W_k^i is the weight function and defined as an inverse of the slant factor as

$$W_k^i=\frac{1}{S\left(\varepsilon_k^i\right)} \tag{2.10}$$

Taking the partial derivatives of E in equation (2.9) with respect to $\overline{V_k}$ and B^i and setting them equal to zero, the desired parameters, $\overline{V_k}$ and B^i, can finally be determined. Note that the GPS satellites appear over fixed receiver every about 24 hours, this procedure requires continuous data over more than 24 hours at the receiver [26].

2.6 Conclusions

The neutral atmosphere is an elementary source of the ionospheric plasma which is a group of the charged particles, including free electrons and ions. Absorbing the solar energy by molecules and atoms in the Earth's ionosphere is considered the main reason for the generation of such particles making the ionosphere to act as a dispersive medium which is irregular and unstable. It induces a number of ionospheric phenomena like prereversal enhancement and plasma bubble occurrence that affects on the satellite communication system. The modulations between the ionosphere fluctuations and the passing-through signal bring about the time delay and deteriorate the signal integrity, availability and reliability. In the worst case, the satellite communications become unavailable due to the LOL effect during an occurrence of severe radio scintillation. Since a number of GPS-based communication users are rapidly increasing and diverse satellite-based applications include not only space communications but also aeronautical navigations and communications that concern with

human life safety, understanding of the ionospheric effect on such communications thus becomes significant. TEC is one of the temporal and spatial parameters which can manifest the characteristic of an electron density variation in the Earth's ionosphere and has been demonstrated in this Chapter. TEC data over Chumphon which is used in this thesis are from SEALION project, supported by NICT, Japan. Employing the method proposed by Otsuga [26], NICT derive the TEC data from all satellite-receiver path of GPS signal whose elevation angle is larger than 45 degree for four SEALION sites in Thailand. The sunspot number, considered the solar activity effect in this research work, is described by the relationship with the solar cycle. The radio signal, particularly on the shortwave band, are degraded from high levels of the sunspot activity which are proportional to the solar radiation on the ionosphere. The TEC derived from the mapping technique based on Otsuga's method which is reported in this Chapter are used to study the ionospheric effect and feed to the proposed neural network for modeling the TEC which will be discussed in Chapter 4.

Chapter 3

Related Model and GPS Receiver Networks

In this Chapter, we review the international reference ionospheric model or IRI model, the GPS receiver networks in Thailand and the GPS receiver networks in the world, respectively. For the IRI model, it is an empirical standard model based on the observation data collected from around the world. The latest version of the IRI model is "*IRI-2007 model*". Even though the IRI-2007 model has been improved from the limitations of the previous IRI model, some significant discrepancies between the model and observed data, especially over an equatorial latitude area, are still noticeable. In this Chapter, we describe the significance of the IRI-2007 model and how to access the online version of the IRI-2007 model. We employ the IRI-2007 model in comparison with the observed data and the model data in Chapter 5. Since Thailand is located on an equatorial ionization anomaly area which is of importance for the Earth's ionosphere study and other related fields like telecommunications and aeronautical navigation as suggested in Chapters 1 and 2, the availability, reliability and accessibility of the GPS receiver networks in Thailand are mentioned. In this Chapter, we suggest two GPS receiver networks in Thailand, which are from SEALION project, and Department of Public Works and Town & Country Planning (DPT). This thesis is based on modeling of the analyzed TEC data from SEALION project. For the GPS receiver networks in the world, GEONET of Japan, CORS of the United States, IGS of international and other networks are described. As well as the list of each network, abbreviation, webpage and contact information are summarized.

3.1 International Reference Ionospheric (IRI) model

International Reference Ionosphere (IRI) [17] is an international project of NASA sponsored by the Committee on Space Research (COSPAR) and the International Union on Radio Science (URSI). The IRI is bi-annually updated during special IRI workshops. It is an empirical model based on data from the worldwide network of ionosonde stations, incoherent scatter radars, the ISIS and

Alouette topside sounders, and in situ measurement on several satellites and rockets [35]. IRI predictions are most accurate in Northern mid-latitudes because of the generally high station density in this part of the globe. The steepest gradients, sharp peaks and deep valleys, of the ionospheric parameters are found at the low and high latitudes. Where are requiring a high station density to fully record and monitor the highly variable ionosphere. Due to the equatorial and the auroral regions have rather scant ionosonde coverage, partly because of the harsh climate conditions [36], and the lack of available local GPS TEC data which can be used for the model development, thus the IRI predictions are less accurate at equatorial and auroral latitude.

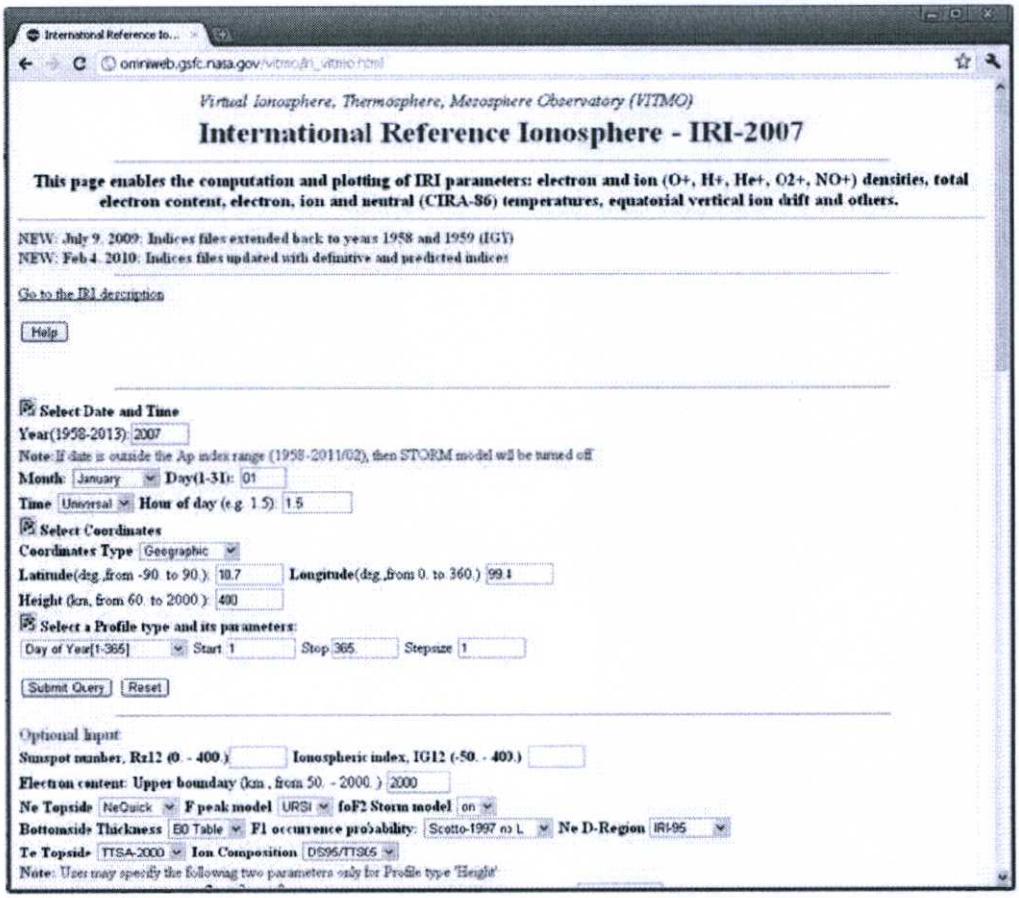

Figure 3.1 The IRI-2007 model homepage.

The IRI-2007 is the latest IRI model developed from the limitations of the previous IRI models. The topside profile which impacts on the TEC is specially improved. To overcome the shortcoming of the previous IRI models for the auroral region, one of the new features in the IRI-2007 is the NN model that was trained with a large volume of EISCAT incoherent scatter data and also with 115 profiles obtained from rocket borne wave propagation experiments [37].

The IRI-2007 TEC predictions are calculated online from the IRI-2007 model via the IRI homepage by using latitude and longitude, date, period of time, and the upper boundary height, as the model input as shown in Figure 3.1. We can access the IRI homepage at http://ccmc.gsfc.nasa.gov/modelweb/models/iri_vitmo.php. For this work, we set the upper boundary height to be 2,000 km, the maximum height of the IRI-2007 model, to include not only the ionosphere but also the plasmasphere as well. An example plot of the IRI-2007 TEC on March 11, 2011 over Chumphon station is illustrated in Figure 3.2.

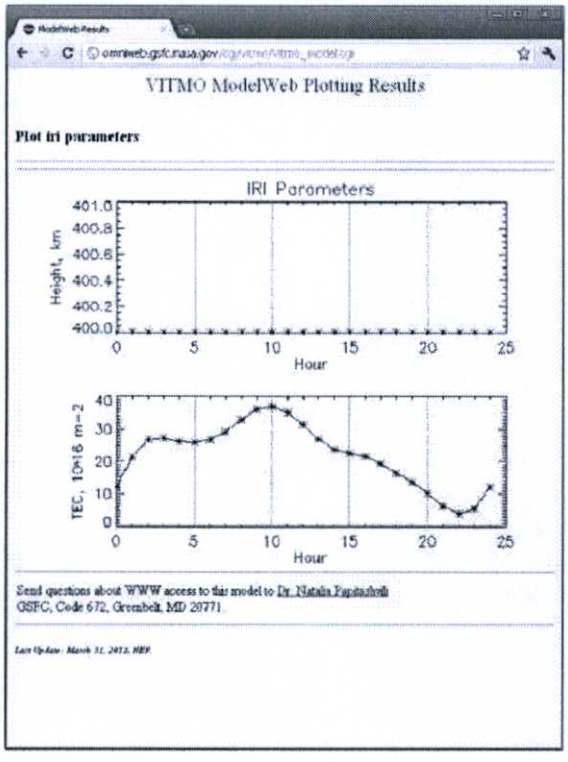

Figure 3.2 The plotting result of the IRI-2007 TEC on March 11, 2011 over Chumphon station.

3.2 GPS Receiver Networks in Thailand

In the recent years, GPS receiver networks for the ionospheric study purpose have become available in Thailand and some neighboring countries through SEALION project. This project has been conducted by National Institute of Information and Communications Technology (NICT), Japan since 2003. It is a joint project among several institutes in Japan, Thailand, Vietnam, Indonesia, and China, including NICT and King Mongkut's Institute of Technology Ladkrabang (KMITL). The project aims to study the generation and propagation mechanisms of severe ionospheric disturbances in the equatorial regions, such as plasma bubbles, and their effects on the space-borne navigation and communication systems. The availability of historical GPS data is of important for an ionosphere study.

In Thailand, there are four GPS receiver stations supported by SEALION as summarized in Table 3.1. An observation of the ionospheric conditions over the magnetic equator area like Thailand is important because the ionospheric irregularities always initiate at the magnetic equator, then expand to north and south along the magnetic field line. The available GPS receiver networks in such an important area like Thailand provides the opportunity for archiving and collecting the TEC to develop the TEC model. The GPS data are generally formatted to be the RINEX format in order to guarantee an easy exchange between different computer systems [22]. The modeling of the TEC in this thesis is based on the analysis of the GPS data from the SEALION GPS receiver networks.

Table 3.1 The GPS observation sites in Thailand supported by SEALION project.

Site	Latitude	Longitude	Dip latitude
Chiang Mai	18.76	98.93	12.7
Bangkok	13.73	100.78	6.7
Chumphon	10.72	99.37	3.0
Phuket	8.09	98.32	-0.2

Figure 3.3 The map of GPS observation sites in Thailand provided by SEALION [38].

To monitor ionospheric irregularities including their generations and evolutions, the dense GPS receiver networks are needed. However, the GPS receiver networks in Thailand are so sparse. One of the possible ways to increase the GPS receiver networks is to make the collaboration with other institutes in Thailand.

One of Thai government institutes which provides the GPS data is Department of Public Works and Town & Country Planning (DPT). The GPS data in the Receiver Independent Exchange Format (RINEX) format with 5-sec interval have been provided through an online website since 2008. The 24-hour real-time service of a differential GPS (DGPS) is available via a radio modem, telephone modem and internet IP. The baseline processing for precise computation is also served. One who is interested in the DPT service can access the DPT website at: www.dpt.go.th. For the data sharing policy of DPT, the user needs to sign up in order to get the authorized username and password. The users can be a government institute, a private company, the University, a research group, or even anyone who is interested in using the provided data. Currently, DPT maintenances 11 GPS stations which include Chiang Mai, Utaradit, Udonthani, Nakornsawan, Srisaket, Nakornrachasrima, Bangkok, Chantaburi, Prachuabkirikhan, Suratthani and Songkha as shown in Figure 3.4.

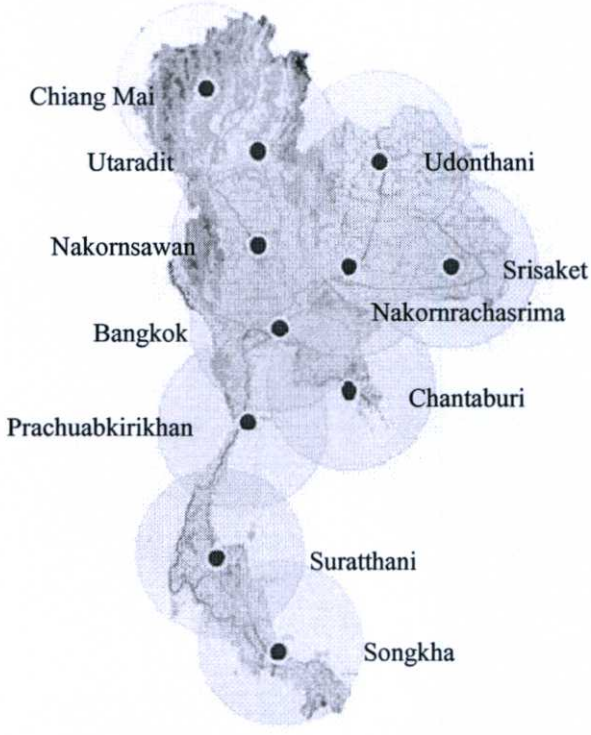

Figure 3.4 The map of GPS observation sites in Thailand provided by DPT [39].

3.3 GPS Receiver Networks in the World

Recently, several GPS receiver networks, such as GPS Earth Observation Network (GEONET) in Japan, Continuously Operating Reference Stations (CORS) in the United States, and International GPS Service (IGS) have been established and developing [22]. The GPS station distributions of GEONET, IGS and CORS in November 2003 are shown on Figure 3.5.

GEONET is the permanent observation station network covering all over Japan. Geographical Survey Institute (GSI) started to establish the GEONET in 1993. GEONET consists of about 1,000 GPS observation sites which are settled in approximate spacing of 25-30 km as shown in Figure 3.5 (a). GPS data observed by the receivers at each site are sent to the central station and analyzed once a day. Since August 1999, the RINEX format observation data can be downloaded from the homepage of GSI. However, some limitations in the service still remain. For example, only the last three-month

observed data are available in the server. Those who need the older data should send their requests to GSI by e-mail or printed letter. Also, the downloading site is operated only by Japanese language [40], [41].

(a) GEONET GPS stations

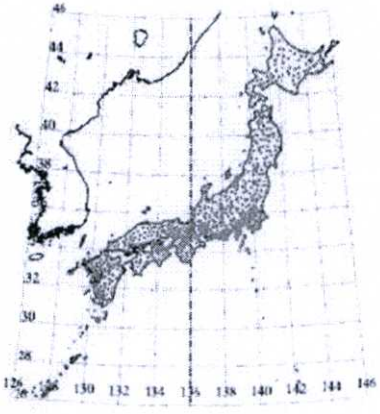

(b) CORS GPS stations

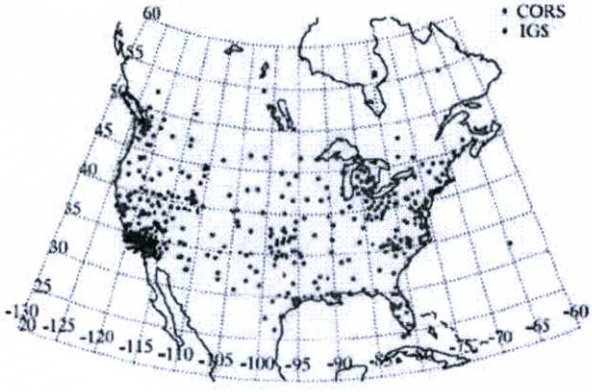

(c) IGS GPS stations

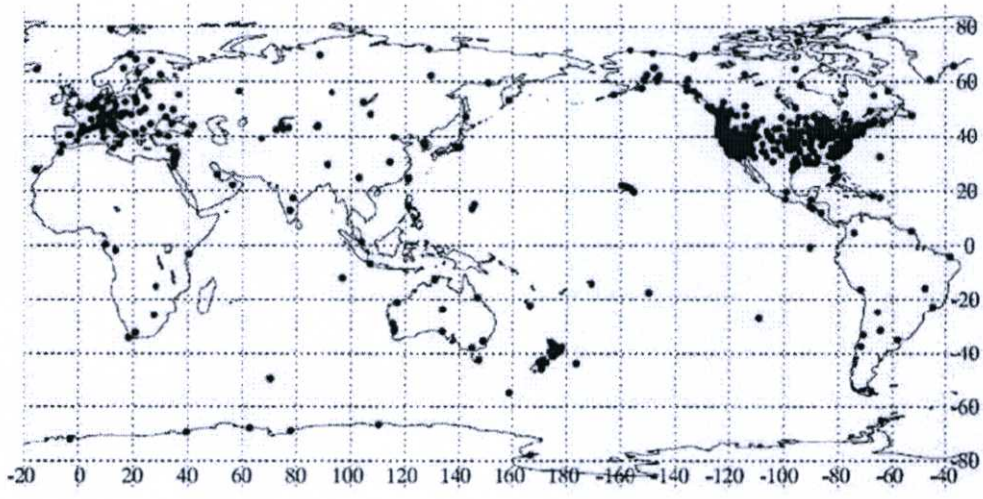

Figure 3.5 The GPS stations of (a) GEONET in Japan, (b) CORS in the United States, and (c) IGS in November 2003 [22].

CORS [42] is operated by the U. S. National Geodetic Survey (NGS). As for May 2010, The CORS network provides the GPS data as Global Navigation Satellite System (GNSS) data consisting of carrier phase and code range measurements in support of three dimensional positioning, meteorology, space weather, and geophysical applications. The data are derived from about 1,450 stations which are contributed by over 200 different organizations, and the network continues to expand. To download the GPS data, users can access the CORS website at http://www.ngs.noaa.gov/CORS. The CORS GPS stations distribution is illustrated in Figure 3.5 (b).

IGS was established by International Association of Geodesy (IAG) in 1994. 1,000s IGS stations, including one station in Thailand, are expanded all over the world as shown in Figure 3.5 (c). The GPS data and other products including the research activities are provided via the IGS website (http://igscb.jpl.nasa.gov) [43]. The provided GPS data are based on the global TEC map [44]. Those who are interested in the IGS data can freely access the IGS website to obtain the GPS based TEC map data.

The other GPS networks, such as European Reference Frame (EUREF) and Southern California Integrated GPS Network (SCIGN), also provide the data that are accessible via the SOPAC website (sopac.ucsd.edu).

A number of GPS networks in the world are accessible through the SOPAC website (sopac.ucsd.edu). List of each network, abbreviation, the webpage and contact information are recorded in Table 3.2.

Table 3.2 List of GPS networks in the world and some details.

Name of the GPS network	Abbreviation	Webpage	Contact information
Australian Regional GPS Network	ARGN	http://www.ga.gov.au/nmd/geodesy/argn/	wizard@auslig.gov.au
Bay Area Regional Deformation GPS Network	BARD	http://quake.geo.berkeley.edu/bard	bard@seismo.berkeley.edu
Basin and Range GPS Network	BARGN	http://cfa-www.harvard.edu/space_geodesy/BARGEN/	jnormandeau@cfa.harvard.edu

Table 3.2 (Cont.).

Canadian Active Control System	CACS	http://www.geod.nrcan.gc.ca/	information@geod.nrcan.gc.ca
California Passive Network	CALPAN	http://csrc.ucsd.edu	ybock@ucsd.edu
Canary GNSS Center Network	CGCN	N/A	nacho@canaryadvanceddsolutions.com
Continuously Operating Reference Stations	CORS	http://www.ngs.noaa.gov/CORS/cors-data.html	richard.snay@noaa.gov
Central Valley Spatial Reference Network	CVSRN	N/A	giana_cardoza@dot.ca.gov
Eastern Basin Range Yellowstone	EBRY	http://www.mines.utah.edu/~rbsmith/RESEARCH/UUGPS.html	rbsmith@mines.utah.edu
Estaciones de Referencia GPS/GNSS de Valencia	ERVA	http://www.gva.es/icv	Capilla_raq@gva.es
European Reference Frame	EUREF	http://www.euref-iag.net	C.Bruyninx@oma.be
Friuli Regional Deformation Network	FREDNET	N/A	dzuliani@inogs.it
Forecast Systems Laboratory	FSL	http://www.fsl.noaa.gov/	gutman@fsl.noaa.gov
Galileo Sensor Stations Network	GALILEO	N/A	Tim.Springer@esa.int
GPS Array for Mid-America	GAMA	N/A	rsmalley@memphis.edu
GeoNet New Zealand	GEONET	http://www.geonet.org.nz	info@geonet.org.nz
Geospatial Information Authority of Japan	GSI	http://www.gsi.go.jp/ENGLISH/	N/A
International GNSS Service	IGS	http://igscb.jpl.nasa.gov	igscb@igscb.jpl.nasa.gov

Table 3.2 (Cont.).

West Java / Bali GPS Network	INATEWS	N/A	csubarya@bakosurtanal.go.id
Institute for High Temperatures	IVTAN	http://helios.gdirc.ru	bragin@tiger.gdirc.ru
Mediterranean GPS Network	MGN	N/A	N/A
Nearnet	NEARNET	http://geodesy.unr.edu/networks/index.html	gblewitt@unr.edu
Northeast Eurasia Deformation Array	NEDA	N/A	steblov@gps.gsras.ru
National Geospatial-Intelligence Agency	NGA	http://earth-info.nga.mil/GandG/satthtml/	gps@nga.mil
Nepal Geodetic Monitoring Network	NGMN	N/A	John Galetzka
Geodetic Survey Division, Natural Resources Canada	NRCAN	http://www.geod.nrcan.gc.ca/	Michael.Craymer@NRCan-RNCan.gc.ca
CORSnet-NSW	NSW	http://www.corsnet.com.au	CORSnetCustomerSupport@lpma.nsw.gov.au
Oregon Real Time GPS Network	ORGN	N/A	minera@Geology.cwu.EDU
Ohio State University	OSU	N/A	kendrick.42@osu.edu
Pacific Northwest Geodetic Array	PANGA	http://www.geodesy.cwu.edu	panga@geology.cwu.edu
PBO GPS Network	PBO	http://pbo.unavco.org	anderson@unavco.org
Pacific GPS Facility	PGF	N/A	jfoster@leka.soest.hawaii.edu

Table 3.2 (Cont.).

Permanent GPS network of the Canary Islands	PGPSNCI	N/A	nacho@canaryadvancedsolutions.com
Renag	RENAG	http://webrenag.unice.fr	Gilbert.Ferhat@insa-strasbourg.fr
Azores REPRAA network	REPRAA	N/A	nacho@canaryadvancedsolutions.com
Red Geodesica Nacional Activa	RGNA	N/A	evazquez@dgg.inegi.gob.mx
Kuker-Ranken	RGPS	N/A	minera@Geology.cwu.EDU
SuomiNet Geodetic	SNG	http://www.suominet.ucar.edu/	bjorn@unavco.ucar.edu
Southern Baja Network	SOBNET	http://www.geodesy.cwu.edu	panga@geology.cwu.edu
Survey of Israel	SOI	N/A	sade_mapi@int.gov.il
South Pacific Sea Level Climate Monitoring Program	SPSLCMP	http://www.ga.gov.au/geodesy/slm/spslcmp/network.jsp	geodesy@ga.gov.au
Sumatran GPS Array	SUGAR	N/A	sieh@gps.caltech.edu
Tibet GPS Initiatives, Chinese Academy of Sciences	TIGICAS	N/A	N/A
Tribhuvan University GNSS Network	TRIBHUGNET	N/A	bnupreti@wlink.com.np
Universidad Nacional Autonoma de Mexico	UNAM	http://tlacaelel.igeofcu.unam.mx/~vladimir/gpsred/gpsred.html	vladimir@ollin.igeofcu.unam.mx

Table 3.2 (Cont.).

USGS Southern California GPS Network	USGS-SC	http://www.scign.org	dollar@iron.gps.caltech.edu
Venezia Consorzio Nuova	VENICE	N/A	viviana.ardone@consorziovenezianuova.com
Western Canada Deformation Array	WCDA	http://www.pgc.nrcan.gc.ca/geodyn/wcda.htm	mschmidt@nrcan.gc.ca
Washington State Reference Network	WSRN	http://wsrn.org	gavin.schrock@seattle.gov

3.4 Conclusions

The empirical standard model which is applied in this thesis is the IRI-2007 model which is the latest model of the IRI. It has been improved from the limitation of the previous IRI model discussed during the IRI workshop. Since the dense stations are available in Northern mid-latitude area, not in auroral and equatorial regions, the IRI prediction in an equatorial region like Southeast Asia thus becomes inaccurate. An availability of the local GPS TEC data is of importance for the model development and the ionosphere study. Also, long term analysis of GPS data can reveal the generation and propagation mechanisms of severe ionospheric disturbances in the equatorial regions, such as plasma bubbles, and their effects on the space-borne navigation and communication systems.

For the GPS networks in Thailand, Thai GPS data from four GPS receiver stations supported by SEALION project and eleven GPS receiver stations owned by DPT are accessible. The RINEX format data are available in order to guarantee an easy exchange between different computer systems. This thesis based on the GPS data over Chumphon station provided by NICT.

For other GPS networks around the world, GEONET of Japan, CORS of the United States and IGS are briefly reported. List of each network, abbreviation, the webpage and contact information are summarized. One who is interested in such data can access SOPAC website: sopac.ucsd.edu.

Chapter 4

TEC Model Based on Neural Networks

In this Chapter, we review artificial neural networks and the proposed neural network for TEC modeling. For TEC model based on the NN, the proposed NN as well as its algorithm and architecture, the input process and output, the RMSE and normalized RMSE which are used in the NN effectiveness comparison are reviewed. The results of testing the proposed NN with several parameters, and some plots related to the performance of the NN model as a function of other parameters are illustrated in this Chapter.

4.1 Artificial Neural Networks

The effort to understand the brain and to imitate some of its strengths is the motivation of the artificial neural network development. Artificial neural network is of interest to researchers and commonly seen in many research areas such as intelligent information processing, telecommunications, pattern recognition, economical analysis, medical diagnosis, mathematical modeling, scientific parameters prediction and space weather forecast, for example.

An artificial neural network is information processing system and modeled after human brain. It is composed of input layer, hidden layer and output layer. Each consists of the processing unit called "*node*", "*unit*", "*cell*" or "*neuron*". Neurons usually have the same activation function and the same connections' pattern to other neurons. The arrangement of the neurons into layers and the connection patterns within and between layers is called the "*net architecture*".

Partial work in this chapter has been published in the proceeding of ITC-CSCC 2010.

Partial work in this chapter has been accepted to be published in the Journal of Earth Planets Space.

Neural nets are often classified as a single layer or multilayer as illustrated in Figures 4.1 and 4.2. Multilayer nets can solve more complicated problems than those which can be solved by the single-layer nets. However, the training of a multilayer net is more difficult. In determining the number of layers, the input units are not counted as a layer because they perform no computation [45]. Between the slabs of neurons, the number of layers of weighted interconnect links can be defined from the number of layers in the net. Besides the neural network architecture, the weights setting method, training, is an important characteristic in order to distinguish the different learning processes. There are two different learning processes which are supervised and unsupervised learning processes.

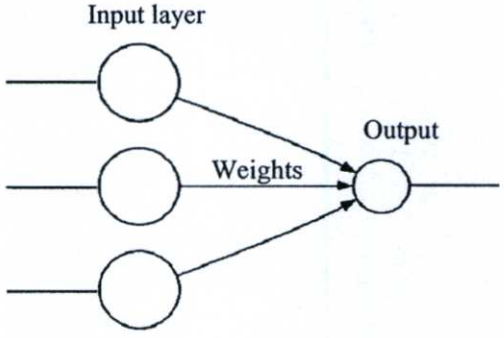

Figure 4.1 A single-layer neural net.

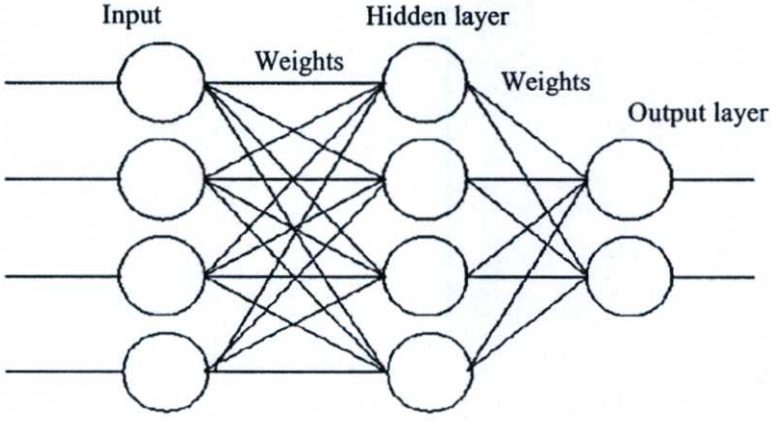

Figure 4.2 A multilayer neural net.

4.1.1 Supervised Training

The prior data are needed to teach the neural net in the training process. The training is achieved by presenting a sequence of training vectors, or patterns, each with an associated target output vector. The weights are then updated according to the learning algorithm. This process is called "*supervised training*". The simplest work which employs the supervised training is the basic pattern classification whose output is a bivalent element such as "1 and -1", "white and black", "yes and no".

The other utility is a pattern association which is another form of a mapping problem, the desired output of which is not just a "yes" and "no," but rather a pattern. A neural net which is trained by a set of input vectors corresponding to a set of output vectors is called associative memory. The net is an auto-associative memory if the desired output vector is the same as input vector, and is a hetero-associative memory if the desired output is different from the input vector. The nonlinear mapping is possible if the multilayer neural nets are trained with enough prior knowledge.

4.1.2 Unsupervised Training

An unsupervised training is for the self-organizing neural nets. An input vector sequence is provided without any specified target output vector, in other words, no historical data is needed in a training process in order to group the similar input vectors together. Unsupervised training is closely related to the density estimation problem in statistics. Among neural network models, the self-organizing map (SOM) and adaptive resonance theory (ART) commonly use unsupervised learning algorithms. The SOM is a topographic organization in which nearby locations in the map represent inputs with similar properties. The ART model allows the number of clusters to vary with the problem size and lets the users control the degree of similarity between members of the same clusters by means of a user-defined constant called the vigilance parameter. ART networks are also used for many pattern recognition tasks, such as automatic target recognition and seismic signal processing [46].

4.1.3 Common Activation Functions

The activation function is the basic operation of the neural network to define the output of the node given an input or a set of inputs. For all nodes in any layer of a neural net, the same activation

function is typically used even though it is not required. Commonly, the identify function as shown in Figure 4.3 is usually applied for the input nodes while nonlinear activation functions are applied for the others. In order to gain the benefits of the multilayer nets compared with the single-layer net limitation, the nonlinear activation functions are required in the multilayer nets.

Hereafter, three activation functions including identify function, binary step function and sigmoid function are introduced.

4.1.3.1 Identify Function

The identify function is another name of the linear function. Any result of the signal fed though the identify function will have no change compared with its input signal as shown in Figure 4.3. The identify function is defined as;

$$f(x) = x \qquad \text{for all } x. \tag{4.1}$$

4.1.3.2 Binary Step Function (with threshold θ)

The binary step function is often used in the single-layer nets to convert the input which is any continuous value to a binary (1 or 0) or bipolar (1 or -1) signal as illustrated in Figure 4.4. This activation function corresponds to a person's action, "Go to see the concert." Each input signal corresponds to some factors affecting on the decision to "go" or "not go" such as information about who is the singer, how much does the ticket cost, where is the concert place, etc.

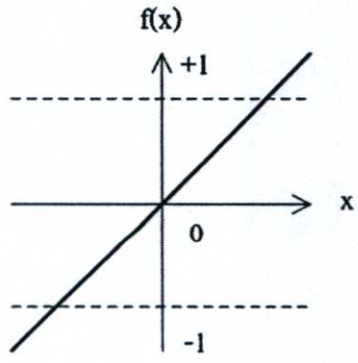

Figure 4.3 Identify function.

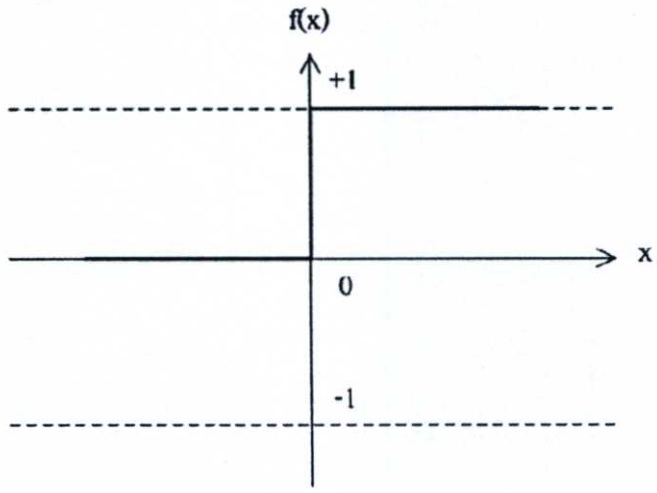

Figure 4.4 Binary step function.

The importance that the person places on each factor is equivalent to the weight on each input signal. To make a decision, a threshold value is used to indicate the person to "go" or "not go." As the significance of the threshold, the binary step function is occasionally called the "*threshold function*" or "*heaviside function*". The function is defined as;

$$f(x) = \begin{cases} 1 & if\ x \geq \theta \\ 0 & if\ x \leq \theta \end{cases} \tag{4.2}$$

4.1.3.3 Sigmoid Function

Sigmoid functions are useful activation functions especially for the neural nets trained by a backpropagation. The logistic function and the hyperbolic tangent function are the most common ones. A sigmoid function ranging from 0 to 1 is usually used if the desired output is binary or between 0 and 1. To accentuate the range of the function, this sigmoid function is called "*binary*

sigmoid" or "*logistic sigmoid*". The binary sigmoid function is illustrated in Figure 4.5 and defined as;

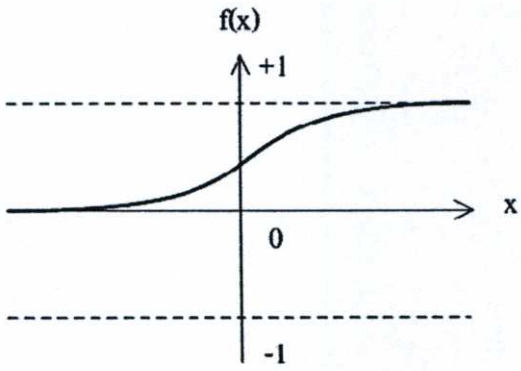

Figure 4.5 Binary sigmoid function.

$$f(x) = \frac{1}{1+e^{-\sigma x}} \tag{4.3}$$

$$f'(x) = \sigma f(x)[1-f(x)] \tag{4.4}$$

Parameter σ is the steepness of the binary sigmoid function. The logistic sigmoid function can be modified to cover any range of target values regarding to any given problem. The most common one is in the range of -1 to 1 as shown in Figure 4.6. The steepness of which can be adjusted by changing parameter σ. It is called as the "*bipolar sigmoid function*". The bipolar sigmoid function is defined as;

$$\begin{aligned} g(x) = 2f(x) - 1 &= \frac{2}{1+e^{-\sigma x}} - 1 \\ &= \frac{1-e^{-\sigma x}}{1+e^{-\sigma x}} \end{aligned} \tag{4.5}$$

$$g'(x) = \frac{\rho}{2}[1+g(x)][1-g(x)] \tag{4.6}$$

Taking Equations (4.5) and (4.6) into account, it can be noticed that the bipolar sigmoid is closely related to the hyperbolic tangent function. In order to illustrate the relation between both of the functions, let parameter ρ of the bipolar sigmoid function equals to 1. We have

$$g(x) = \frac{1-e^{-x}}{1+e^{-x}} \tag{4.7}$$

The hyperbolic tangent function is always applied for the neural nets, the desired output range of which is between -1 and 1. It is defined as;

$$\begin{aligned} h(x) &= \frac{e^{x}-e^{-x}}{e^{x}+e^{-x}} \\ &= \frac{1-e^{-2x}}{1+e^{-2x}} \end{aligned} \tag{4.8}$$

The derivative of the hyperbolic tangent is

$$h'(x) = [1+h(x)][1-h(x)] \tag{4.9}$$

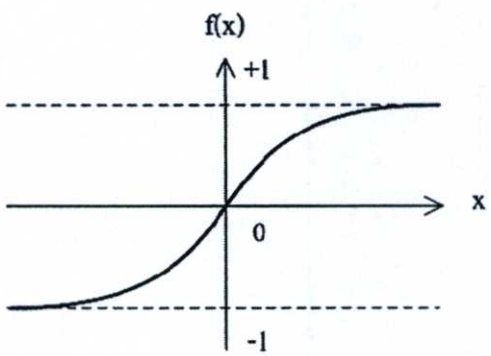

Figure 4.6 Bipolar sigmoid function.

4.1.4 Backpropagation Network

To reach the goal of the training, the weights between neurons need adjusting since they are embedded with an intelligence of the network. Backpropagation, or generalized delta rule, is known as one of the most common learning algorithms. It can learn from the prior knowledge, meaning, the sets of input–output are needed in order to teach the nets. Training a neural network using the backpropagation algorithm includes 3 steps which are feeding the training pattern input forward, calculation and backpropagation of the associated error, and adjustment of the weights.

In feed-forward network, every input neuron receives the input signal and sends it to each hidden neuron. Each output neuron produces the response or the output of the network for any given input pattern based on the current synaptic weights. Initially, the output will be randomized. The output is compared with the target value to calculate the error and the mean square error. The error is then propagated backward through the network for improving the learning ability by weight adjusting to reach the desired mean square error. In other words, small weight changes are made in each layer in order to minimize the overall errors of the network. It is not necessarily advantageous to keep training the network until it exactly reaches the minimum mean square error. As long as the error decreases, the whole process is repeatedly continued. The training will be terminated when the error starts to increase or drops below the required threshold value. At this point, it can be said that the neural network has learnt the problem well enough to memorize the training patterns or be used in the specific purposes.

4.1.5 Mean Square Error

To stop the training process, two criterions including the desired mean square error (MSE) and the acceptable maximum iteration are considered. As long as the MSE is higher than the desired MSE and the iteration does not reach the maximum iteration yet, the training process continues. The MSE is computed by taking the differences between the target and the actual neural network output, squaring them and averaging over all classes and internal validation samples [47] as defined in Equation 4.10.

$$\frac{\sum_{i=1}^{n}\left[(y_t - y_a)^2\right]}{n} \tag{4.10}$$

where n is number of samples, y_t is target of the neural network, y_a is actual neural network output. Because the neural network outputs are real numbers between 0 and 1, the MSE thus ranges between 0 and 1.

4.2 Proposed Neural Networks (NN)

Neural Networks (NN) is an information processing system composing of input layer, hidden layer and output layer. Each layer consists of the processing unit called as node, unit, cell, or neuron. A neuron is an information processing unit which consists of connecting link, adder and activation function. The neuron patterns are similar to biological neural nets and modeled after human brain [48]. NN is an important tool for nonlinear approximation when it is trained with enough historic data [10]. TEC is one of the nonlinear ionospheric parameters which have been previously predicted by using NN [1], [10], [12], [14], [15] and [16]. Among the various NN structures, we have used a basic structure known as feed forward network with back propagation algorithm, the well known algorithm, for our model. In order to achieve the optimum NN, the comparison of the "*root-mean-square error (RMSE)*" was used. RMSE is defined as:

$$RMSE = \sqrt{\frac{1}{N}\sum_{i=1}^{N}(TEC_{pred} - TEC_{meas})^2} \tag{4.11}$$

where N is number of data points, TEC_{pred} is TEC predicted by a model and TEC_{meas} is vertical TEC (VTEC) estimated from GPS observations by using the technique described above. Since the TEC_{meas} and the target TEC which is used to trained the NN are normalized before passed through the NN process, the TEC_{pred} from the NN process thus have no unit, meaning the RMSE also have no unit.

This NN comprises of one input layer, one hidden layer and one output layer. As shown in Figure 4.7, it is the schematic diagram of the proposed NN for this work. The input layer consists of five nodes or neurons corresponding to five input parameters each with 32,112 data points while the

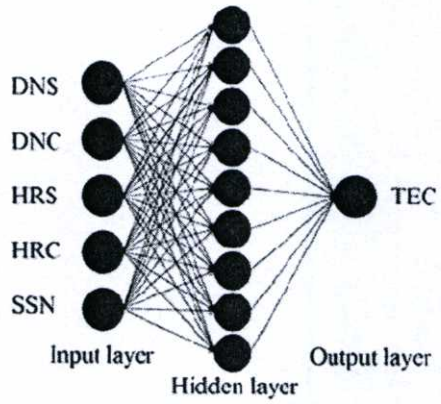

Figure 4.7 The NN architecture for TEC prediction [16].

hidden layer and the output layer consists of nine and one nodes or neurons, respectively. The expositions about NN and its algorithms are well described in 4.2.1. In this thesis, we focus on the NN application for predicting TEC over equatorial latitude station in Thailand. On the other hand, the main purpose is to model the NN and compare the NN TEC with GPS TEC and IRI-2007 TEC so as to validate the NN model. The data set is divided into training, validating and testing sets. The training and validating sets are the TEC data in 2005, 2006, 2008 and 2009 while the TEC data in 2007 are reserved for the testing process. Besides the RMSE, the performance of our NN model is also considered from the normalized RMSE to avoid the misinterpretation of the comparison result affected from the large TEC background as well. The normalized RMSE is the ratio of the RMSE to the average normalized GPS-TEC, $\overline{TEC_{meas}}$, as given below;

$$Normalized\ RMSE = \frac{RMSE}{\overline{TEC_{meas}}} \tag{4.12}$$

4.2.1 Algorithm and Architecture

In order to teach the network to know the nonlinear data-pattern, we employ the feed-forward network with the back propagation algorithm to adjust the weight. Within the context of the

algorithm, this paragraph substantially relies on the book written by [45]. For this work, the algorithm is started by setting the initial weights and biases to be the small random values. Each input node (X_i, $i = 1,\ldots, n$) receives input signal x_i and broadcasts this signal to all nodes in the layer above, hidden layer. Each hidden node ($Z_j, j = 1, \ldots, p$) sums its weighted input signals as given by

$$z_{in} = w_{0j} + \sum_{i=1}^{n} x_i w_{ij} , \tag{4.13}$$

where z_in_j is the net input to Z_j, w_{oj} is the bias on the hidden node j, x_i is the input signal from the input node i and w_{ij} is the bias from input node i to hidden node j.

We applied the hyperbolic tangent sigmoid function as an activation function for Z_j to compute the hidden output as Equation (4.14).

$$z_j = TANSIG\left(z\_in_j\right) = \frac{2}{1+e^{\left(-2\cdot z\_in_j\right)}} - 1, \tag{4.14}$$

Then, the signal z_j *is* sent to all nodes in the layer above, output layer. Each output node (Y_k, $k = 1, \ldots, m$) sums its weighted input signals as given by

$$y\_in_k = w_{0k} + \sum_{j=1}^{p} z_j w_{jk} , \tag{4.15}$$

where y_in_k is the net input to Y_k, w_{ok} is the bias on the output node k, z_j is the input signal from the hidden node j and w_{jk} is the bias from hidden node j to output node k.

The linear transfer function, Equation (4.16), is used as an activation function for Y_k to compute the output signals, y_k.

$$y_k = PURELIN\left(y\_in_k\right) = y\_in_k , \tag{4.16}$$

The Levenberg-Marquardt backpropagation (trainlm) is emploied as the training function for this work. It is not necessarily advantageous to keep the training on until the square error actually

reaches a minimum [19]. As long as the error from testing process decreases, the training continues. The error is backpropagated to the nodes in the layer below. Each node, excluding the nodes in the input layer, updates its weights and biases. The validation process will be terminated if the error begins to increase or meets the required conditions.

4.2.2 NN Input Process and Output

The input space was collected from the parameters that have an impact on the TEC data such as the hour number (*HR*, diurnal variation), the day number (*DN*, seasonal variation) and the sunspot number (*SSN*, measure of solar activity). To make data continue, the first two parameters were each split into sine and cosine components, two cyclic components [10], [11], [16] and [49] as follows:

$$\begin{aligned} DNS &= \sin\left(\frac{2\pi DN}{365.25}\right), DNC = \cos\left(\frac{2\pi DN}{365.25}\right) \\ HRS &= \sin\left(\frac{2\pi HR}{24}\right), HRC = \cos\left(\frac{2\pi HR}{24}\right) \end{aligned}, \tag{4.17}$$

where *DNS*, *DNC*, *HRS* and *HRC* are the sine and cosine components of *DN* and *HR*, respectively. The studied years include the leap year, the year having 366 days, thus the factor 0.25 is provided in Equation (4.17).

The daily SSN which indicates the solar activity is collected from the site: ftp.ngdc.noaa.gov. It is considered as one of the input parameters for the first neural network (NN1). Since the amplitude of short-term solar-proxy variations are induced by solar rotation, one solar rotation is equal to 27 days, and the long-term variations follow the 11-year solar activity period [14], we choose the 27-day mean SSN as one of the input parameters for the second neural network (NN2) to represent the solar activity. Besides, the sunspot number has more power at the periods longer than 27-day [14] for training the neural network, thus we also choose the 81-day mean SSN, three solar rotation periods, as another input parameter for the third neural network (NN3). All of the input parameters are fed into the input space for the TEC prediction. The output of each NN is VTEC. The RMSE values of which are investigated to achieve the optimum NN.

4.2.3 The Result of Testing Neural Network with Various Parameters

In this work, the NN model is developed for Chumphon as a single station model near the magnetic equator in Thailand. The dailly SSN as shown in Figure 4.8 is applied for the NN1, while the 27-day mean SSN as shown in Figure 4.9 and the 81-day mean SSN as shown in Figure 4.10 are applied for NN2 and NN3, respectively. To achieve the optimum NN, the RMSE comparison of NN1, NN2 and NN3, each with 6 to 12 cells in the hidden layer, is made as shown in Figure 4.11. All data used in NN processes are the data from 2005 to 2009. Since the achievement of the trained network depends not only on the selection of input parameters but also on the initial weights [14] which the initial random weights are used for this work, thus we run each NN ten times to choose the best NN for the best result. From Figure 4.11, we found that the NN3 with nine hidden cells performs as the best NN for Chumphon station in the studied period with the RMSE 2.269 TECU and the normalized RMSE 0.161 from the testing process. We will henceforth refer to the NN3 as the proposed NN.

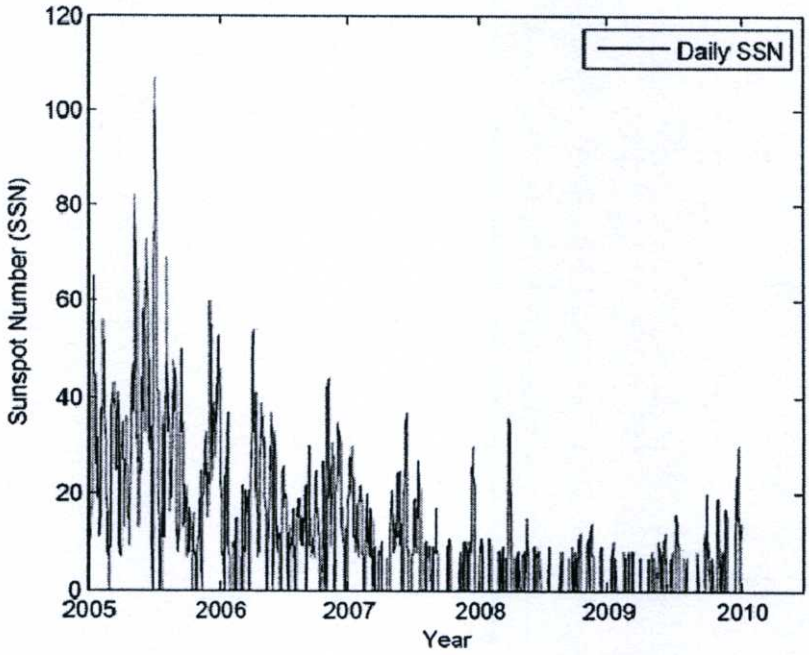

Figure 4.8 The daily SSN during 2005 to 2009 which is applied for the NN1 [16].

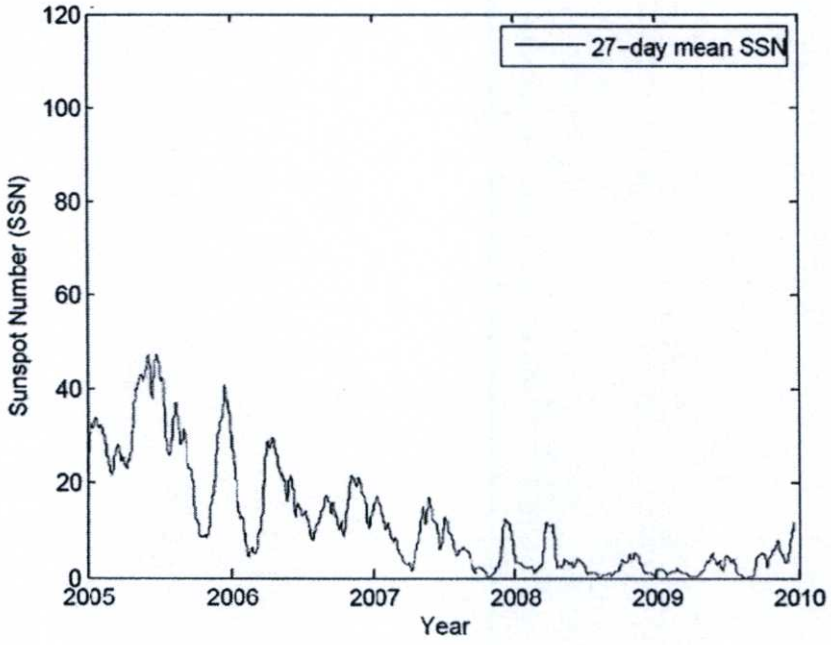

Figure 4.9 The 27-day mean SSN during 2005 to 2009 which is applied for the NN2 [16].

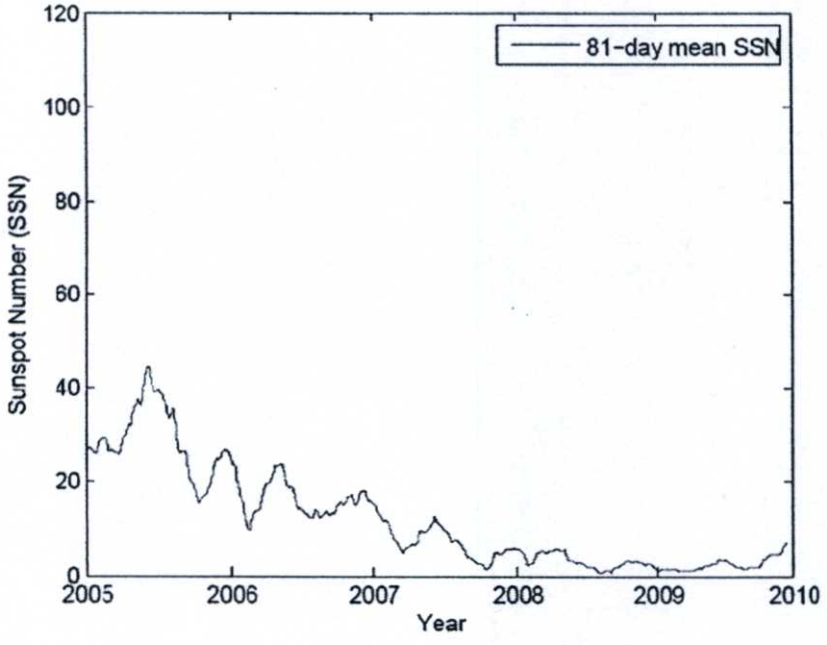

Figure 4.10 The 81-day mean SSN during 2005 to 2009 which is applied for the NN3 [16].

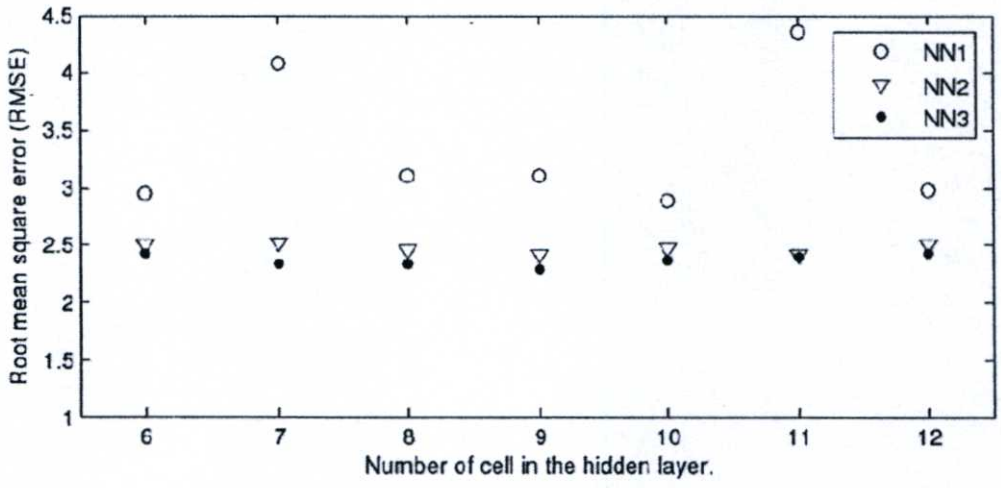

Figure 4.11 RMSE values computed for NN model with 6 to 12 neurons in a single hidden layer [16].

The proposed NN (NN3) is the feed-forward network with back propagation algorithm. It consists of five nodes or neurons in the input layer, nine nodes in hidden layer, and one output node in the output layer as shown in Figure 4.7. The input layer is fed with the sine and cosine components of the day number and the hour number, and the 81-day mean SSN. The initial weight and biases for the training process are set to be the random values. The Levenberg-Marquardt is applied as the training function. The output of the proposed NN is compared with GPS TEC and IRI-2007 TEC. We take the normalized RMSE into account for the result comparison. The normalized RMSE is the RMSE value divided by the background TEC to avoid the effect from TEC background.

To train the proposed NN, the stop condition is specified by the MSE and the maximum iteration. Generally, if we plot the MSE as a function of epoch, two periods which are transient period and stable period of the MSE can be distinct. For the transient period, the continual sharp decrease of the MSE can be seen as illustrated in Figure 4.12, for example. During the transient period, the training should not be stop because the NN has not enough learnt from the data pattern yet. The error of overall system can be decreased if the users keep training the NN until it steps into the stable period. In the stable period, the MSE will not dramatically change and the error of overall system will not be significant modified as shown in Figure 4.13. In this work, the threshold MSE is set be $10^{-3.25}$ and the maximum iteration is 100,000 iterations. The NN reach the threshold MSE at epoch 74 as shown in Figure 4.14.

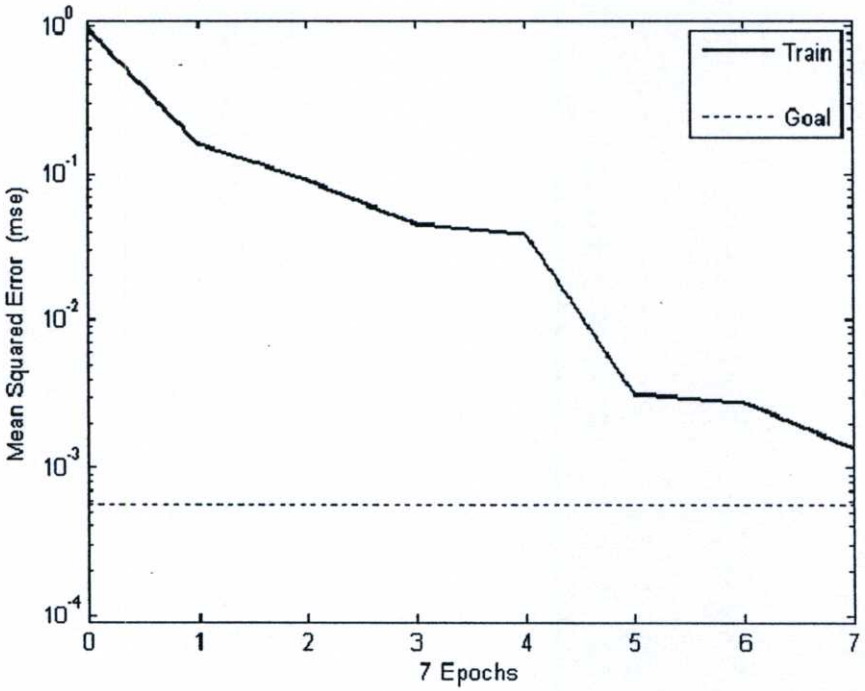

Figure 4.12 Example plot of the MSE in the transient period which can continue decreasing if the users keep training the NN.

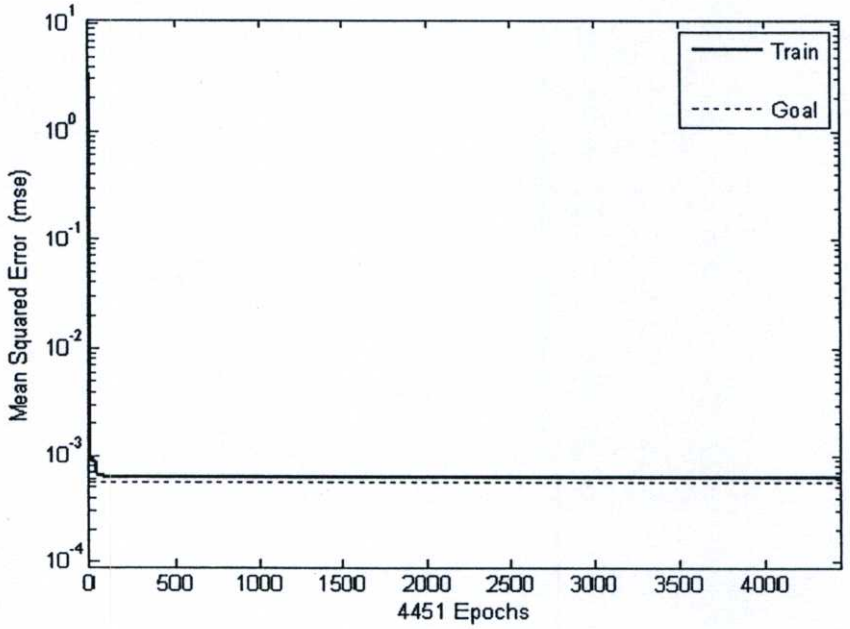

Figure 4.13 Example plot of the MSE which includes both of the transient and stable periods.

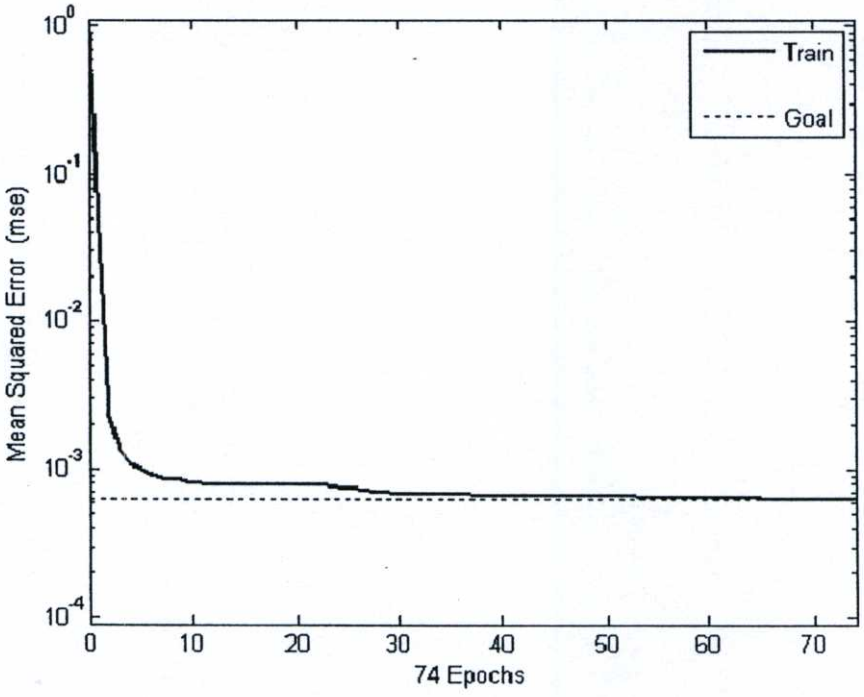

Figure 4.14 The MSE plot of the proposed NN.

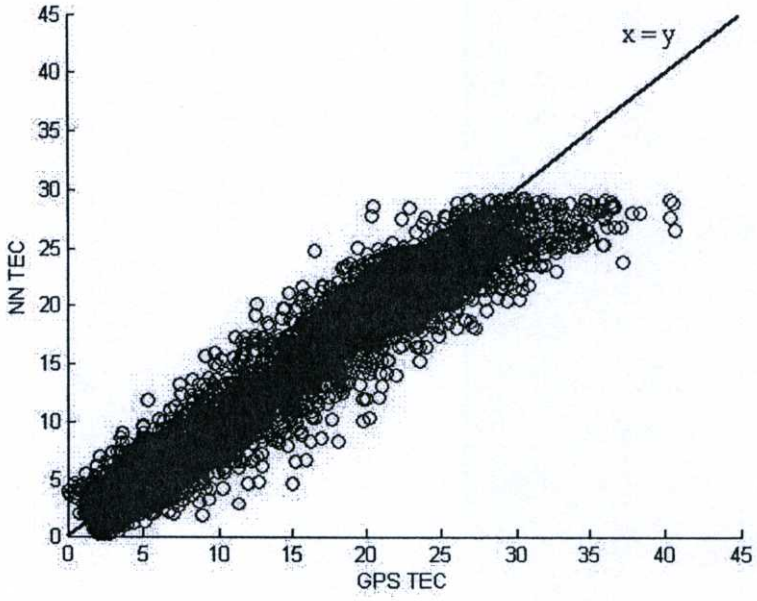

Figure 4.15 The scatter plot of NN TEC predicted from the proposed NN as a function of the GPS TEC for Chumphon station in 2007.

The scatter plot of the NN TEC predicted from the proposed NN as a function of the GPS TEC is illustrated in Figure 4.15.

In this work, we set the upper boundary height for the IRI-2007 model to be 20,000 km, the maximum value which the IRI-2007 model allows, to include not only the electron in the ionosphere but also in the plasma-sphere as well. The results in years 2005, 2006, 2007, the last period of solar cycle 23, and in years 2008, 2009, the start period of solar cycle 24, from the NN processes are plotted versus the GPS TEC and the IRI-2007 TEC at 1230 LT as shown in Figure 4.16.

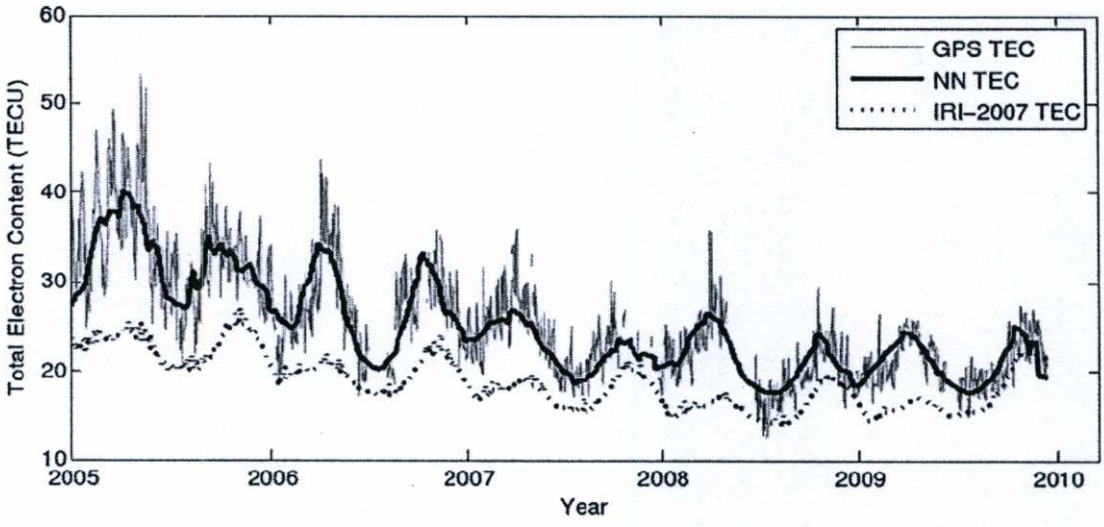

Figure 4.16 GPS TEC, NN TEC and IRI-2007 TEC over 5-year period, 2005 to 2009, at 1230 LT for Chumphon station [16].

4.3 Conclusions

The NN is developed to imitate ability and intelligent of human brain. It is an artificial intelligent system which can tackle the complex problems like the nonlinear data prediction. There are single layer and multilayer NNs with supervised and unsupervised learning. The multilayer NN with supervised learning is developed for TEC modeling in this thesis. The tangent sigmoid function with back propagation algorithm is applied for the proposed NN. The proposed NN architecture is a five-nine-one architecture, representing five input nodes, nine hidden nodes and one output node,

respectively. This architecture yields the smallest RMSE in the optimum NN architecture selection as reported. The input parameters for the NN-based TEC modeling, selected from those which affect the TEC variation, include the day number, the hour number and the sunspot number. The TEC over Chumphon, equatorial latitude station, in 2005, 2006, 2008 and 2009 are used for the NN training, while those in 2007 are used for the NN testing. Since a well-performing NN is obtained when it is trained with the small-ripple data, we did normalize the input data before passing them trough the NN process. All of the NN processes are repeatedly run until the stop condition is satisfied. To stop the training, two criteria, the maximum iteration defined by users and the threshold MSE, are considered. In this work, the NN stops training when an overall error drops to the required MSE. The output of the proposed NN is the hourly TEC. The NN effectiveness is investigated by taking into account of the RMSE and normalized RMSE, which will be described in Chapter 5.

Chapter 5

Simulation Results and Discussions

In this Chapter, to reveal the temporal variation of the TEC and investigate the NN performance, seven comparisons including hourly comparison, seasonal comparison, 0030 LT comparison, 0630 LT comparison, 1230 LT comparison, 1830 LT comparison and TEC comparison on an individual day are introduced. Each comparison describes an effectiveness of the proposed NN model in the TEC prediction or interpolation. The RMSE and the normalized RMSE are mentioned and applied for the NN performance investigation. The prediction errors caused from the solar activity are analyzed. The magnetic effect which mainly contributes to the prediction errors in this work since it is not included in the NN input space is discussed. Moreover, we suggest three mechanisms which can lead to the prediction errors. The discussions of the IRI-2007 TEC data used in the comparisons are made in this Chapter.

5.1 Hourly Comparison

To evaluate the performance of NN, the hourly model is then constructed. The data set for the learning process composes of TEC in 2005, 2006, 2008 and 2009. Following the learning process, NN output is compared with GPS TEC and IRI-2007 TEC on equinox and solstice days in 2007. In 2007, equinox days occur on March 20 and September 23 while solstice days occur on June 21 and December 22 (U.S. Naval Observatory; http://www.erh.noaa.gov/box/equinox.html), respectively. However, we compare the results on December 25 for the solstice day due to the loss of data on December 22. The hourly NN TEC is plotted with the GPS TEC and the IRI-2007 TEC to see an effectiveness of the hourly model as shown in Figure 5.1 (a) - (d).

The RMSE and normalized RMSE of the NN TEC and the IRI-2007 TEC for each of the four proposed days are shown in Table 5.1.

The work in this chapter has been accepted to be published in the Journal of Earth Planets Space.

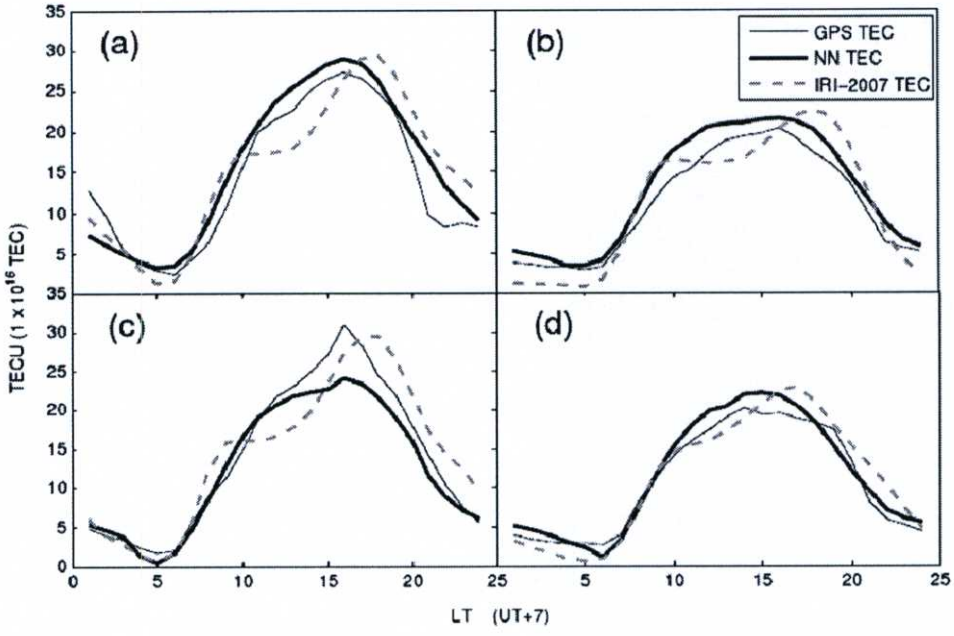

Figure 5.1 GPS TEC, NN TEC and IRI-2007 TEC at Chumphon station (a) on 20 March 2007 (equinox day), (b) on 21 June 2007 (solstice day), (c) on 23 September 2007 (equinox day), (d) on 25 December 2007 (solstice).

The NN TEC with the smallest RMSE (1.468 TECU) and the smallest normalized RMSE (0.135) is on December 25, a solstice day. The NN TEC with the largest RMSE (2.797 TECU) and the largest normalized RMSE (0.195) is on March 20, an equinox day. The average TEC values on December 25 and March 20 are equal to 10.805 TECU and 14.281 TECU, respectively, and are considered the background TEC values of December 25 and March 20.

Among various methods to predict TEC, the results prove that the hourly model behaves as one of the appropriate tools for TEC prediction purpose. Even though there is considerable difficulty for NN to learn in TEC prediction process on equinox days during this period due to the occurrence of equatorial plasma bubble which includes various ionospheric irregularity scales causing a large day-to-night variation and drastically fluctuated component of the TEC, the hourly model is still able to predict TEC quite well.

Table 5.1 Background TEC, RMSE and normalized RMSE values of GPS TEC and predicted values (NN TEC and IRI-2007 TEC) for different days (equinox and solstice days) in 2007 over Chumphon station.

Date	Background TEC (TECU)	RMSE (TECU) between		Normalized RMSE between	
		NN TEC	IRI-2007 TEC	NN TEC	IRI-2007 TEC
March 20	14.281	2.797	4.164	0.195	0.291
June 21	10.904	1.965	2.743	0.180	0.251
September 23	14.006	2.430	3.412	0.173	0.243
December 25	10.805	1.468	2.142	0.135	0.198
4 studied-day	12.499	2.165	3.115	0.173	0.249
All year 2007	14.078	2.296	3.881	0.163	0.275

If we consider in terms of the normalized RMSE as shown in Table 5.1, the normalized RMSE from the hourly model is smaller than that from the IRI-2007 model for entire year over Chumphon. We do not mean that IRI-2007 model is not appropriate to use for TEC prediction, on the other hand, we presume that the IRI-2007 database may not cover Southeast Asia data especially over Chumphon, equatorial latitude station, for example. However, our NN TEC performs well during the studied period since the NN model learns from the local TEC value. This is a reason why the hourly model can well predict TEC values as mentioned above.

5.2 Seasonal Comparison

Since the seasonal variation plays an important role in TEC variation, we also make the seasonal TEC comparison to investigate the possibility of the NN to predict the seasonal TEC. In this thesis, there are four distinct seasons which are March equinox, June solstice, September equinox and December solstice. Each season is represented by the monthly median value. Meaning, we take the median to each hourly data of 31-day TEC data in March predicted from the method described in Figure 1 in order to get the 24-hour seasonal TEC for March equinox, for example. Thus the 24 hours monthly median TEC values are cited as the seasonal TEC. For the seasonal comparison, we, hereafter, term the NN as the seasonal model.

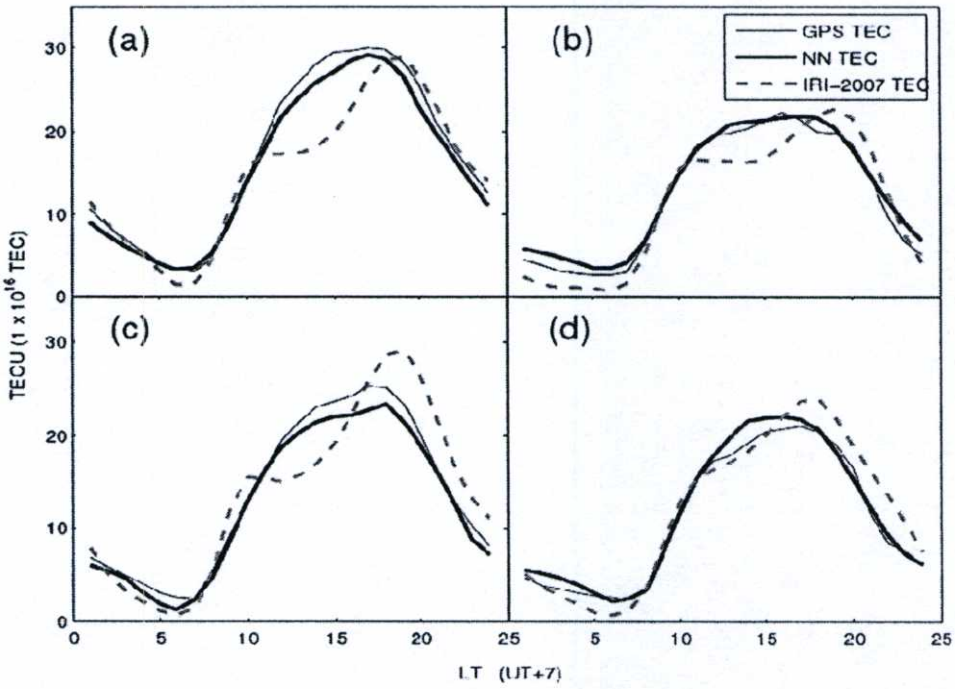

Figure 5.2 GPS TEC, NN TEC and IRI TEC at Chumphon station for (a) March (b) June (c) September (d) December.

Table 5.2 Background TEC, RMSE and normalized RMSE values of GPS TEC and predicted values (NN TEC and IRI-2007 TEC) for different seasons which are March (represent March equinox), June (represent June solstice), September (represent September equinox) and December (represent December solstice), respectively in 2007 over Chumphon station.

Season	Background TEC (TECU)	RMSE (TECU) between		Normalized RMSE between	
		NN TEC	IRI-2007 TEC	NN TEC	IRI-2007 TEC
March	16.923	1.385	4.025	0.081	0.237
June	12.163	1.107	2.485	0.091	0.204
September	13.639	1.208	3.513	0.088	0.257
December	11.083	1.012	2.135	0.091	0.192

For this model, the 5:9:1 architecture with 81-day mean SSN is still used. TEC in 2005, 2006, 2008 and 2009 are applied in the learning process while the seasonal TEC in 2007 is used as the target for this seasonal model. The NN TEC (seasonal TEC) is plotted to compare with the GPS TEC and the IRI-2007 TEC. Figure 5.2 depicts that the IRI TEC values are clearly underestimated during 0430 LT to 0630 LT and 1130 LT to 1630 LT for March equinox, during 0530 LT to 0730 LT and 1030 LT to 1630 LT for June solstice, during 0230 LT to 0530 LT and 1130 LT to 1530 LT for September equinox, and during 0330 LT to 0630 LT for December solstice, while during 1730 LT and 2130 LT for June solstice, during 1730 LT and 2330 LT for September equinox, and during 1530 LT and 2330 LT for December solstice, IRI-2007 TEC are overestimated. From this investigation, we can notice that the IRI-2007 model underestimates around the local pre-sunrise and the local midday, and overestimates around after the local sunset. For the rest of times, the IRI-2007 model predicts TEC quite well. When we take the seasonal NN TEC into account, we found that the NN performs quite well for seasonal TEC prediction. However, the NN underestimates TEC during 1130 LT to 2030 LT for March equinox, as well as during 1230 LT to 1830 LT for September equinox, and the NN overestimates TEC during 0030 LT to 0630 LT for June solstice and during 1230 to 1630 LT for December solstice. The shapes of the NN TEC and the GPS TEC for all seasons resemble each other. The RMSE values of the NN TEC and the IRI-2007 TEC are shown in Table 5.2. The best estimation for the NN occurs in March equinox with the normalized RMSE 0.081 while that for the IRI-2007 model occurs in December solstice with the normalized RMSE 0.192. The worst estimations occur in December solstice for the NN and in September equinox for the IRI-2007 model with the normalized RMSE 0.091 and 0.257, respectively.

5.3 0030 LT Comparison

The difference between the universal time and the local time of Chumphon is seven hours. We refer 0030 LT (1730 UT) as local midnight for this paper. To see if the NN is applicable for TEC prediction, the first comparison at 0030 LT in 2007 is then described. We show the comparison of 365-day variation of the GPS TEC, the NN TEC and the IRI-2007 TEC at local midnight in Figure 5.3. It is shown that the NN model predicts the TEC over Chumphon at 0030 LT for all year 2007 fairly well with the RMSE 1.996 TECU, and the normalized RMSE 0.334.

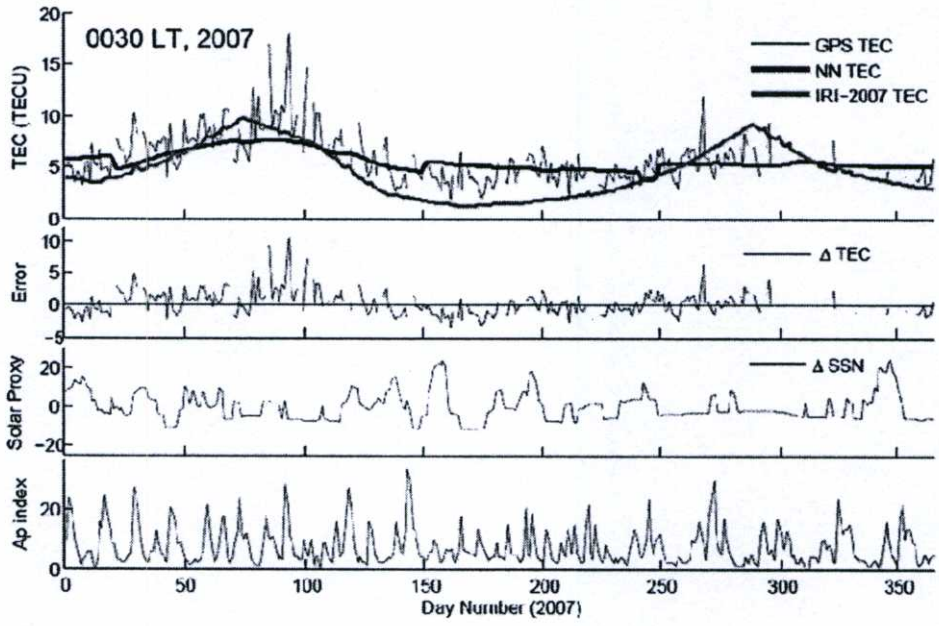

Figure 5.3 GPS TEC, NN TEC and IRI-2007 TEC, the difference between the GPS TEC and the NN TEC (Δ TEC), and the difference between daily SSN and 81-day mean SSN (Δ SSN), all at 0030 LT, and the Ap index, all in 2007 over Chumphon station.

The IRI-2007 TEC is underestimated at local midnight during midyear. The IRI-2007 model predicts TEC for Chumphon station at 0030 LT in year 2007 with the RMSE 2.469 TECU, and the normalized RMSE 0.413. The average TEC values of the GPS TEC, the NN model and the IRI-2007 model at local midnight in 2007 are equal to 5.971 TECU, 5.612 TECU and 4.729 TECU, respectively. The comparison results for local midnight reveal the worst estimation for both of the NN model and the IRI-2007 model. This may be as a result of the equatorial plasma bubble which always be observed during the night time and causes the drastically TEC variation. We presume that it contributes to the main reason why the worst estimation or prediction appears at local midnight.

5.4 0630 LT Comparison

The comparison between the GPS-TEC, the NN TEC and the IRI-2007 TEC at 0630 LT is made to investigate the TEC variation, the effectiveness of the proposed NN model and the IRI-2007

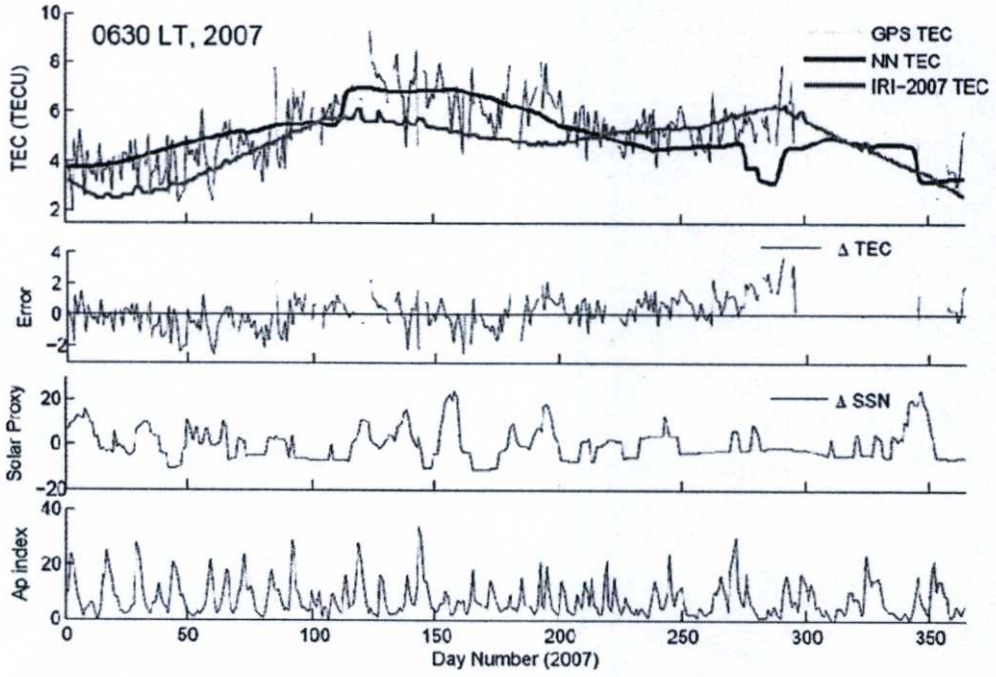

Figure 5.4 GPS TEC, NN TEC and IRI-2007 TEC, the difference between the GPS TEC and the NN TEC (Δ TEC), and the difference between daily SSN and 81-day mean SSN (Δ SSN), all at 0630 LT, and the Ap index, all in 2007 over Chumphon station.

model at local pre-sunrise. From an observation, the GPS TEC values at local pre-sunrise are quite low with the average TEC value at 5.287 TECU for all year 2007. To see the TEC prediction performance of the IRI-2007 and the NN model, TEC from the NN model is plotted against GPS TEC and IRI-2007 TEC as shown in Figure 5.4. We found that the NN is still able to predict TEC pretty well with the RMSE 1.084 TECU and the normalized RMSE 0.205 while the IRI-2007 model also predicts TEC pretty well with the RMSE 1.246 TECU and the normalized RMSE 0.235. The average TEC values of the NN model and the IRI-2007 model at local pre-sunrise in 2007 are equal to 5.064 TECU and 4.668 TECU, respectively.

5.5 1230 LT Comparison

The same procedure with two previous comparisons was applied for a 1230 LT which is referred as the local midday. The NN TEC and the IRI-2007 TEC at 1230 LT are compared to each

other by plotting the GPS TEC as shown in Figure 5.5. One can notice that both of the TEC predicted from the NN model and the IRI-2007 model have the same trend of data at local midday for year 2007. However, we can observe that the IRI-2007 TEC is evidently underestimated by both of the GPS TEC and the NN TEC, while the NN TEC agrees with the GPS TEC with the RMSE 2.718 TECU and the normalized RMSE 0.114. The RMSE of the IRI-2007 model is equal to 7.135 and the normalized RMSE is equal to 0.299 at local midday for all year at this station. The yearly average at local midday of the GPS TEC is 23.791 TECU while those for the NN model and the IRI-2007 model are 22.593 TECU and 17.741 TECU, respectively. The best estimation of the proposed NN model can be seen here, at local midday, among other comparisons at 0030 LT, 0630 LT, 1230 LT and 1830 LT as described in Table 5.3.

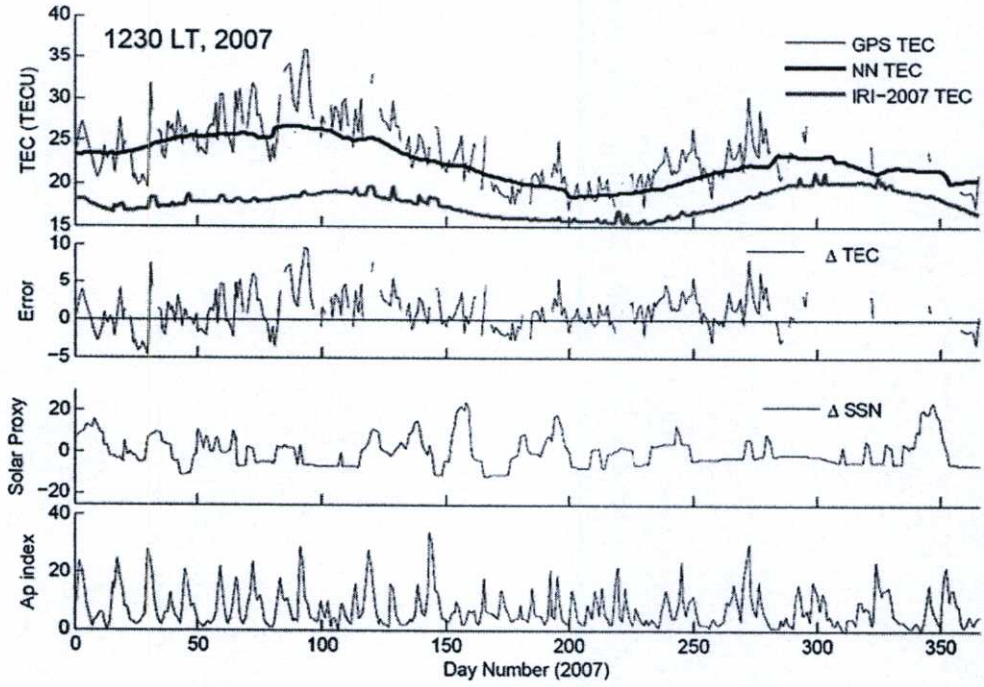

Figure 5.5 GPS TEC, NN TEC and IRI-2007 TEC, the difference between the GPS TEC and the NN TEC (Δ TEC), and the difference between daily SSN and 81-day mean SSN (Δ SSN), all at 1230 LT, and the Ap index, all in 2007 over Chumphon station.

5.6 1830 LT Comparison

The comparison of the NN TEC, the GPS TEC and the IRI-2007 TEC at local pre-sunset is shown in Figure 5.6. The trends of the NN TEC from the 1830 LT model and the IRI-2007 TEC are similar and follow the GPS TEC at local pre-sunset. If we consider only the RMSE value at 1830 LT, we will find that the RMSE of the NN TEC is pretty high with 3.300 TECU. However, this is affected from the high background TEC value at local pre-sunset hour which is equal to 20.939 TECU. To avoid this effect in the comparison, the normalized RMSEs are considered. The IRI-2007 model also comes along the high RMSE value, however, the normalized RMSE of which is equal to 0.211 which is the best approximation of the IRI-2007 model. The average TEC values for the NN model and the IRI-2007 model at local pre-sunset are equal to 18.934 TECU and 23.755 TECU, respectively. From Figure 5.6, we can notice that the IRI-2007 model distinctly overestimates TEC for the period after the 250th day at 1830 LT which may be the reason for the pretty high RMSE value.

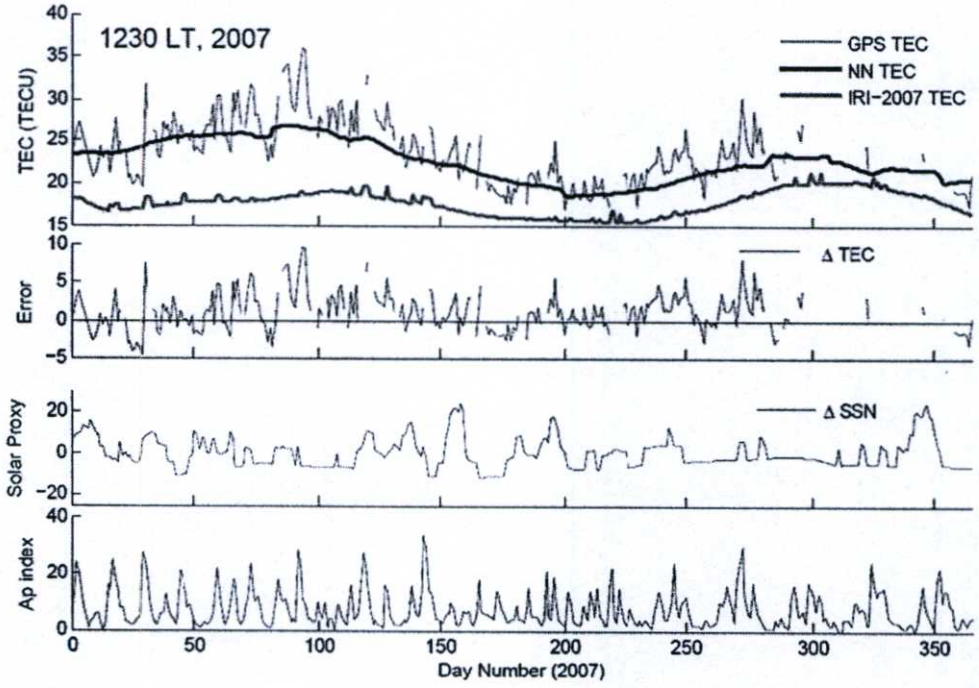

Figure 5.6 GPS TEC, NN TEC and IRI-2007 TEC, the difference between the GPS TEC and the NN TEC (Δ TEC), and the difference between daily SSN and 81-day mean SSN (Δ SSN), all at 1830 LT, and the Ap index, all in 2007 over Chumphon station.

Table 5.3 Average TEC, RMSE and normalized RMSE values of GPS TEC and predicted values (NN TEC and IRI-2007 TEC) for different times in 2007 which are 0030 LT, 0630 LT, 1230 LT and 1830 LT, respectively, over Chumphon station.

Time (LT)	Average TEC (TECU)			RMSE (TECU)		Normalized RMSE	
	GPS TEC	NN TEC	IRI-2007 TEC	NN TEC	IRI-2007 TEC	NN TEC	IRI-2007 TEC
0030	5.971	5.619	4.729	1.996	2.469	0.334	0.413
0630	5.287	5.064	4.668	1.084	1.246	0.205	0.235
1230	23.791	22.593	17.741	2.718	7.135	0.114	0.299
1830	20.939	18.934	23.755	3.300	4.433	0.157	0.211

The normalized RMSE values of the GPS TEC and the predicted values (NN TEC and IRI-2007 TEC) for each of the four comparisons in 5.3 to 5.6 over Chumphon station is compared and shown in Table 5.3. We found that our NN model can be used to predict TEC values at different times of the year 2007 over Chumphon, the equatorial latitude station. The minimum normalized RMSE value is 0.114 from the 1230 LT comparison, while the maximum one is 0.334 from the 0030 LT comparison. We can infer that the proposed NN model can give the best TEC approximation at local midday due to the smallest normalized RMSE value it gives. However, the NN TEC from the 0030 LT model needs to be leveled up to decrease the normalized RMSE value.

5.7 TEC Comparison on an Individual Day

For Figures 5.3 to 5.6, each of which includes (from top to bottom) the comparison between the GPS TEC, the NN TEC and the IRI-2007 TEC, the difference between the GPS TEC and the NN TEC (Δ TEC, the error of the NN model), the difference between daily SSN and 81-day mean SSN (Δ SSN), and the daily geomagnetic activity index, Ap, all in 2007. The positive error which are related to the solar proxy variation represented by Δ SSN are noticed on the 35th day of the 0030 LT comparison in Figure 5.3, and on the 195th day of 1230 LT comparison in Figure 5.6. For the 35th day in Figure 5.3, the Δ SSN is about 10 while the Δ TEC is about 3 TECU (the background TEC is equal to 5.971 TECU). The background TEC is an average GPS TEC value for all year 2007 at any

represented time. The Δ SSN is about 16 while the Δ TEC is about 5 TECU (the background TEC is equal to 23.791 TECU) on the 195th day in Figure 5.5. The trend of Δ TEC variation and Δ SSN variation resemble each other around 10 days before and after the 195th day of the 1230 LT comparison in Figure 5.5 as well. The TEC error corresponding to the largest Δ SSN at around 160th day is not prominent. Generally, daily errors caused by using 81-day mean SSN as a solar input are not very significant.

The positive error which are related to the geomagnetic activity index represented by the daily Ap index are noticed on the 40th and 85th days of the 0030 LT comparison in Figure 5.3, the 140th, 185th and 190th days of the 0630 LT comparison in Figure 5.4, the 17th, 30th, 60th, 65th, 70th, 195th, 271st and 277th days of the 1230 LT comparison in Figure 5.5, and the 30th, 72nd and 120th days of the 1830 LT comparison in Figure 5.6. The largest Δ TEC on the 85th day in Figure.5.3 and on the 120th day in Figure 5.6 are clearly related to the geomagnetic activity as well as during the 1st and 30th days of 1230 LT comparison in Figure 5.5 with three peaks resembling each other between Δ TEC and Ap variations. The negative error which are related to the solar proxy variation do not clearly appear in the study period but those related to the geomagnetic activity can be seen on the 132nd, 140th, 147th, and 170th days of the 0630 LT comparison in Figure 5.4. For the large positive error during the 270th and 290th days in Figure 5.4, it is absolutely not related to the solar proxy variation, however, it may be related to the geomagnetic activity index for some days. Another large positive error on the 340th day correlates to the peak of the geomagnetic activity index and the increasing of the Δ SSN on this day. Figure.5.7 compares daytime Δ TEC and Ap in more detail (for 1st to 100th days). The TEC increases occurred with a time delay by approximately one day, which strongly suggests a set up of disturbance dynamo [50]. The weakened daytime eastward electric field might suppress the fountain effect and cause density increase at the magnetic equator.

For the error unrelated to both of the solar proxy index and the geomagnetic activity index can be seen on the 270th day of the 0030 LT comparison in Figure 5.3. We presume that such error is attributed to other origins such as forcing below the ionosphere including coupling with planetary wave activities [51]. The remaining errors are affected from the large day-to-day variation of the TEC in an equatorial latitude region itself.

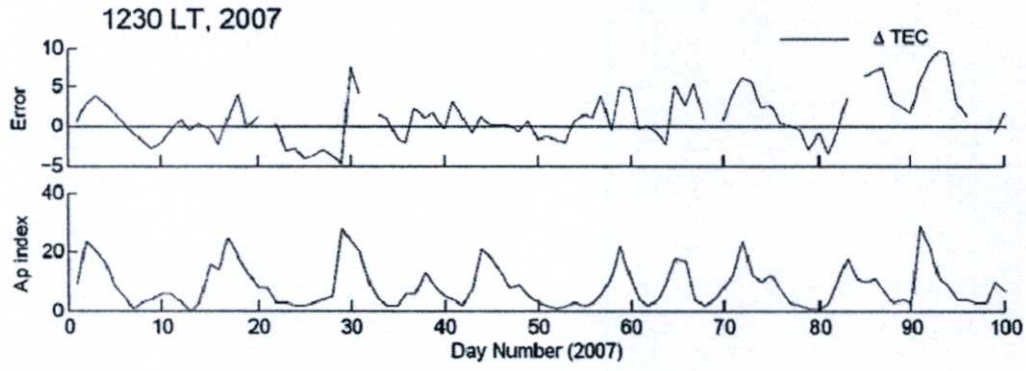

Figure 5.7 Comparison between the daytime Δ TEC and Ap index in more detail (for the 1st to 100th days), all in 2007 over Chumphon station.

5.8 Conclusions

The result is that the proposed NN model from all the comparisons described above can well predict TEC compared with the GPS TEC. For some periods, even though there is a considerable difficulty for the NN to learn in TEC prediction processes due to the large variations of TEC not only on equinox days but also on solstice days due to the large day-to night variation affected from the equatorial plasma bubble occurrence and the large scatter TEC data affected from the day-to-day TEC variation in an equatorial region, our model is still able to predict TEC quite well. Besides the TEC variation effect, three possible mechanisms including the geomagnetic activity index, the solar proxy and the other effect originated below the Earth's ionosphere which contributes to the TEC prediction error are introduced as error sources for an equatorial latitude region. For all comparisons, the NN model underestimates the GPS TEC which needs to be leveled up in the newer version, however, the NN TEC overall agrees with the GPS TEC. The IRI-2007 model underestimates the GPS TEC as shown in all comparisons except the estimation at 1830 LT that the IRI-2007 model overestimates. In this research, we show that the NN is the potentially effective method for the TEC prediction in an equatorial region.

Chapter 6

Conclusions

6.1 Summary

Existence of the ionospheric plasma, the charged particles which include free electrons and ions, is the reason why the Earth's ionosphere acts as an irregular and unstable medium. Several of the ionospheric phenomena are induced by the plasma variation. The satellite-based communications are affected from such phenomena like the plasma bubble occurrence. Various scales of ionospheric irregularity in the plasma bubble deteriorate the radio signal in the form of the radio scintillation and the loss of lock occurrences, for instance. Moreover, the radio signals with a shortwave band are degraded from the high levels of the sunspot activity which are proportional to the solar radiation on the ionosphere. Availability, integrity and reliability of the radio signal are of significance as it is concerned with our daily life in many aspects, essentially in the human safety issue for aeronautical navigation purpose. Loss of the satellite communication signal can be the serious problem. Understanding of the ionospheric effect on such communications thus becomes important.

One of the effective parameters which can manifest the characteristics of an electron density variation in the Earth's ionosphere is the TEC. This thesis has reviewed the TEC and its derivation. We have tried to model the TEC based on the NN. The TEC data over Chumphon which is used in this thesis are derived by NICT employing the method proposed by Otsuka.

The ionosphere-related problem is nonlinear and complicated. To deal with such a problem, NN is one of the good options. NN is an artificial intelligence system which is developed to imitate ability and intelligent of the human brain. TEC modeling based on the NN in this thesis is developed for Chumphon, the equatorial latitude station in Thailand. The multilayer NN with the supervised learning is developed in this thesis. The tangent sigmoid function with a back propagation algorithm is applied for this work. The proposed NN architecture is a five-nine-one architecture, representing five input nodes, nine hidden nodes and one output node, respectively. The input parameters of the NN include the day number, the hour number and the sunspot number which are normalized before passing through the NN process. All the NN processes are repeatedly run until satisfying the

maximum iteration defined by users or the threshold MSE. The output of the proposed NN is the hourly TEC. The RMSE and normalized RMSE are considered to investigate the NN efficiency.

For all comparisons, the NN model underestimates the GPS TEC which needs to be leveled up in the newer version, however, the NN TEC overall agrees with the GPS TEC. The IRI-2007 model underestimates the GPS TEC for all comparisons except at 1830 LT that the IRI-2007 model overestimates. We can deduce from the experimental results that the proposed NN model can well predict the TEC compared with the GPS TEC for all comparisons. Even though there is a considerable difficulty for the NN to learn in the TEC prediction processes due to the large variations of the TEC, not only on the equinox days, but also on the solstice days due to not only the day-to-day variation, but also the large day-to night variation of the TEC. The day-to-day variation causes the large scattering of the TEC data. The day-to-night variation is affected from the equatorial plasma bubble occurrence. We, in addition, suggest three possible mechanisms contributing to a prediction error, including the geomagnetic activity index, the solar proxy and the other effects originated below the Earth's ionosphere which contributes to the TEC prediction error. We conclude that the NN is the potentially effective method for the TEC prediction in an equatorial region.

6.2 Future Work Discussions

Even without any magnetic parameter included in the input space, our proposed NN model can predict TEC at Chumphon, equatorial latitude station during 2007 quite well. This may be due to the studied period during the low solar activity. However, some errors still include in the NN TEC. Moreover, the solar maximum is coming soon. Thus, for the model improvement, it would be beneficial to include the magnetic parameters and teach the NN with more study stations and longer period covering at least one solar cycle (11 years). In addition, the study of Maruyama [14] shows that other solar proxies besides the sunspot number may be more optimal; hence, we will experiment various options in the future work.

REFERENCES

[1] Watthanasangmechai, K., Supnithi, P., Lerkvaranyu, S., Maruyama, T., "Comparison of NN TEC with GPS TEC and IRI-2007 TEC over equatorial latitude station, Thailand," **Proceeding of the International Workshop on Information Communication Technology (ICT 2010)**, Bangkok, Thailand, W3B-1, August, 2010.

[2] Maruyama, T., "Regional reference total electron content model over Japan based on neural network mapping techniques," **Ann. Geophys.**, vol. 25, pp. 2609–2614, 2007.

[3] Tulunay, E., Ozkaptan, C., Tulunay, Y., "Temporal and spatial forecasting of the foF2 values up to twenty-four hours in advance," **Phys. Chem. Earth**, vol. 25, no. 4, pp. 281–285, 2000.

[4] Oyeyemi, E.O., McKinnell, L.A., Poole, A.W.V., "Near-real time foF2 predictions using neural networks," **J. Atmos. Solar Terrest. Physics.**, vol. 68, pp. 1807–1818, 2006.

[5] McKinnell, L.A., Poole, A.W.V., "Ionospheric variability and electron density profile studies with neural networks," **Adv. Space Res.**, vol. 27, no. 1, pp. 83–90, 2001.

[6] Maruyama, T., "Retrieval of in situ electron density in the topside ionosphere from cosmic radio noise intensity by an artificial neural network," **Radio Sci.**, vol. 37, no. 5, pp. 1077-1091, doi: 10.1029/2001RS002509, 2002.

[7] Tulunay, Y., Altuntas, E., Tulunay, E., Price, C., Ciloglu, T., Bahadirlar, Y., Senalp, E.T., "A case study on the ELF characteristirization of the Earthionosphere cavity: Forecasting the Schumann resonance intensities," **Adv. Space Res.**, vol. 70, pp. 669–674, 2008.

[8] Leandro, R.F., Santos, M.C., "Regional Computation of TEC using a Neural Network Model," **Poster presented at the joint Assembly of CGU, AGU, SEG and EEGS,** Montreal, 2004.

[9] Tulunay, Y., Tulunay, E., Senalp, E.T., "The neural network technique-2: an ionospheric example illustrating its application," **Adv. Space Res.**, vol. 33, pp. 988–992, 2004.

[10] Habarulema, J.B., McKinnell, L.A., Cilliers, P.J., "Prediction of global positioning system total electron content using neural networks over South Africa," **J. Atmos. Solar Terrest. Physics.**, vol. 69, no. 15, pp. 1842–1850, 2007.

[11] McKinnell, L.A., "Using neural networks to determine the optimum solar input for the prediction of ionospheric parameters," **Adv. Space Res.**, vol. 42, pp. 634–638, 2008.

[12] Habarulema, J.B., McKinnell, L.A., Opperman, B.D.L., "Toward a GPS-based TEC prediction model for Southern Africa with feed forward networks," **Adv. Space Res.**, vol. 44, pp. 82–92, 2009.

[13] Habarulema, J.B., McKinnell, L.A., Cilliers, P.J., Opperman, B.D.L., "Application of neural networks to South African GPS TEC modeling," **Adv. Space Res.**, vol. 43, no. 11, pp. 1711–1720, 2009.

[14] Maruyama, T., "Solar proxies pertaining to empirical ionospheric total electron content model," **J. Geophys. Res.**, vol. 115, doi:10.1029/2009JA014890, 2010.

[15] Watthanasangmechai, K., Supnithi, P., Lerkvaranyu, S., Maruyama, T., Srisupasitanon, W., "Hourly and seasonal TEC prediction with neural network at Chumphon equatorial lattitude station, Thailand," **Proceeding of the 25th International Technical Conference on Circuits/Systems, Computer and Communications (ITCCSCC)**, Pattaya, Thailand, pp. 796–799, 2010.

[16] Watthanasangmechai, K., Supnithi, P., Lerkvaranyu, S., Maruyama, "TEC prediction with neural network for equatorial latitude station in Thailand" **Earth Planets Space**, first revision, 2011.

[17] Bilitza, D., "A correction for the IRI topside electron density model based on Alouette/ISIS topside sounder data," **Adv. Space Res.**, vol. 33, no. 6, pp. 838–843, 2004.

[18] Coisson, P., Nava, B., Radicella, S.M., "On the use of NeQuick topside option in IRI-2007," **Adv. Space Res.**, vol. 43, no. 11, pp. 1688–1693, 2009.

[19] Yasukevich, Y., "Testing of IRI-2007 model using data of satellite altimeters Topex and Jason-1 and IRI-2001 modeling results," **Poster presented at 37th COSPAR Scientific Assembly**, Montreal, C41-0043-08, 3542, 2008.

[20] Bhattacharya, S., Dubey, S., Tiwari, R., Purohit, P. K. and Gwal, A. K., "Effect of Magnetic Activity on Ionospheric Time Delay at Low Latitude," **J. Astrophys. Astr.**, vol. 29, pp. 269–274, 2008

[21] M. Mosert, M. Gende, C. Brunini, R. Ezquer, and D. Altadill, "Comparisons of IRI TEC predictions with GPS and digisonde measurements at Ebro" ***Adv. Space Res.***, vol. 39, pp.841-847, 2007

[22] Tsugawa, T., "Observational Studies on Large-Scale Traveling Ionosphere Disturbances Using GPS Receiver Networks" Ph.D. dissertation, Kyoto university, 2004.

[23] Brown, B., **"HF Propagation tutorial"** [Online]. Available : http://www.astrosurf.com/luxorion/qsl-hf-tutorial-nm7m3.htm.

[24] Nishioka, M., "Study on meso-scale ionospheric structures at low – and mid – latitudes using data of GPS receiver networks and satellites" Ph.D. dissertation, Kyoto university, 2009.

[25] Maruyama, T., **Science of Space Environment**. Tadanori Ondoh and Katsushide Marubashi eds. 2001.

[26] Otsuka, Y., Ogawa, T., Saito, A., Tsugawa, T., Fukao, S., and Miyazaki, S., "A new technique for mapping of total electron content using GPS network in Japan," **Earth Planet. Sci.**, vol. 54, pp. 63-70, 2001.

[27] Khandagale, A., Gupta, "Communication Blackout: Causes and Measures," International Journal of Advanced Engineering Sciences and Technologies (IJAEST) vol. 3, no. 1, pp. 46-49, 2011.

[28] Anonymous, **"Solar Cycle"** [Online]. Available: http://en.wikipedia.org/wiki/Solar_cycle.

[29] Marshall Space Flight Center, **"Solar Physics"** [Online]. Available: http://solarscience.msfc.nasa.gov.

[30] Goodwin, G. L., Silby, J. H., Lynn, K. J., Breed, A. M., Essex, E. A., "GPS satellite measurements: ionospheric slab thickness and total electron content," **J. Atmos. Solar-Terr. Phys.**, vol. 57, no. 14, pp.1723-1732, 1995.

[31] Kenpankho, P., Watthanasangmechai, K., Supnithi, P., Tsugawa, T., Maruyama, T., "Comparison of GPS TEC measurements with IRI TEC prediction at an equatorial latitude station, Chumphon, Thailand," **Earth Planets Space**, doi:10.5047/eps.2011.01.010, in press, 2011.

[32] Blewitt, G., "An automatic editing algorithm for GPS data," **Geophys. Res. Lett.**, vol. 17, pp. 199-202, 1990.

[33] Sardon, E., A. Rius, and N. Zarraoa, "Estimation of the transmitter and receiver differential biases and the ionospheric total electron content from Global Positioning System observations," **Radio Sci.**, vol. 29, pp. 577–586, 1994.

[34] Ma, G., and Maruyama, T., "Derivation of TEC and estimation of instrumental biases from GEONET in Japan," **Ann. Geophys.**, vol. 21, pp.2083-2093, 2003.

[35] Bhuyan, P. K., Barah, R. R., "TEC derived from GPS network in India and comparison with the IRI," **J. Adv. Space Res.**, vol. 39, pp.830-840, 2007.

[36] Bilitza, D., Reinisch, B. W., "International Reference Ionosphere 2007: Improvements and new parameters," **Adv. Space Res.**, vol. 42, pp.599 -609, 2008.

[37] McKinnell, L. A., Friedrich, M., Steiner, R. J., "A new approach to modeling the daytime lower ionosphere at auroral latitudes," **Adv. Space Res.**, vol. 34, no. 9, pp.1943-1948, 2004.

[38] Space Environment Group, Applied Electromagnetic Research Center "**Radio Propagation Project**" [Online]. Available: http://wdc.nict.go.jp/IONO/index_E.html.

[39] Department of Public Works and Town & Country Planing, "**Public Service**" [Online]. Available: www.dpt.go.th.

[40] Miyazaki, S., Saito, T., Sasaki, M., Hatanaka, S., and Iimura, Y., "Expansion of GSI's Nationwide GPS Array, Bull." **Geographical Survey Institute**, vol. 43, pp. 23-34. 1997.

[41] Miyazaki, S., Hatanaka, S., Sasaki, M. and Tada, T., "The Nationwide GPS Array as an Earth Observation System, Bull." **Geographical Survey Institute**, vol. 44, pp. 11-22, 1998.

[42] National Geodetic Survey, "**Continuously Operating Reference Station (CORS),**" [Online]. Available: http://www.ngs.noaa.gov/CORS.

[43] Beutler, G., J. Kouba, and R. E. Neilan, "The International GPS Service: An interdisciplinary service in support of earth sciences," **Adv. Space Res.**, vol. 23, no. 4, pp. 631-653, 1999.

[44] Ho, C. M., Mannucci, A.J., Sparks, L., Pi, X., Lindqwister, U. J., Wilson, B. D., Iijima, B. A. and Reyes, M. J., "Ionospheric total electron content perturbations monitored by the GPS global network during two northern hemisphere winter storms," **J. Geophys. Res.**, vol. 103, no. A11, pp. 26409-26420, doi: 10.1029/98JA01237, 1998.

[45] Fausett, L., "Fundamentals of Neural Networks," **Prentice Hall International**, ISBN 0-13-042250-9, 1994

[46] Duda, R. O., Hart, P. E. and Stork, D. G., "Unsupervised Learning and Clustering," Ch. 10 in *Pattern classification* (2nd ed.), **Wiley**, New York, ISBN 0-471-05669-3, 2001.

[47] Sankar, A. B., Kumar, D. and Seethalakshmi, K., "Neural Network Based Respiratory Signal Classification Using Various Feed-Forward Back Propagation Training Algorithms," **European Journal of Scientific Research**, ISSN 1450-216X, vol. 49, no. 3 , pp.468-483, 2011.

[48] Tulunay, Y., Tulunay, E. and Senalp, E.T., "The neural network technique-1: a general exposition," **Adv. Space Res.**, vol. 33, pp. 983–987, 2004.

[49] McKinnell, L.A. and Poole, A.W.V., "The development of a Neural Network Based Short Term foF2 Forecast Program," **Adv. Space Res.**, vol. 25, no. 4, pp. 287–290, 2000.

[50] Scherliess, L. and Fejer, B. G., "Strom time dependence of equatorial disturbance dynamo zonal electric fields," **J. Geophys. Res.**, vol. 102, no. A11, pp. 24,037–24,046, 1997.

[51] Lastovicka, J., "Forcing of the ionosphere by waves from below," **J. Atmos. Sol. Terr. Phys.**, vol. 68, pp. 479–497, 2006.

APPENDICES

APPENDIX A

LIST OF PUBLICATIONS

Journals (To appear/published)

1. **Watthanasangmechai, K.**, Supnithi, P., Lerkvaranyu, S., Tsugawa, T., Nagatsuma, T., Maruyama, T., "TEC prediction with neural network for Thailand equatorial latitude station," ***Earth Planets, and Space***, in press, 2011.
2. P. Kenpankho, **K. Watthanasangmechai**, P. Supnithi, T. Tsugawa, and T. Maruyama, "Comparison of GPS TEC measurements with IRI TEC prediction at an equatorial latitude station, Chumphon, Thailand," ***Earth Planets, and Space***, doi:10.5047/eps.2011.01.010, in press, 2011.

Presentations (International poster presentation)

3. T. Tsugawa, **K. Watthanasangmechai**, H. Ishibashi, H. Kato, M. Nishioka, Y. Otsuka, A. Saito, T. Nagatsuma and K. T. Murata, "Observations of traveling ionospheric disturbances using GPS networks in the Southeast Asia," JpGU International Symposium 2011, Chiba, Japan, May 22 - 27, 2011.

Presentations (International oral presentation)

4. **K. Watthanasangmechai**, P. Supnithi, A. Mongkolkajid, T. Tsugawa and T. Maruyama, "Current Activities of TEC Monitoring and Prediction in Thailand,"SEALION International Symposium 2011, Bangkok, Thailand, pp. 58-59, Jan 27 - 28, 2011.
5. P. Kenpankho, **K. Watthanasangmechai,** P. Supnithi, T. Tsugawa, T. Maruyama, "Comparison of GPS TEC Measurements with IRI TEC Prediction at the Equatorial Latitude Station, Chumphon, Thailand," SEALION International Symposium 2011, Bangkok, Thailand, pp. 62-63, Jan 27 - 28, 2011.
6. **Kornyanat Watthanasangmechai**, Prasert Kenpankho, Pornchai Supnithi, Takuya Tsugawa, Takashi Maruyama, "Comparisons of GPS TEC and IGS TEC over four

SEALION sites," Society of Geomagnetism and Earth, Planetary and Space Sciences (SGEPSS) fall meeting, Okinawa, Japan, B005-34, Oct 30 - Nov 3, 2010.

7. **Kornyanat Watthanasangmechai**, Pornchai Supnithi, Somkiat Lerkvaranyu, Takashi Maruyama, "Comparison of NN TEC with GPS TEC and IRI-2007 TEC over equatorial latitude station, Thailand," 2010 International Workshop on Information Communication Technology (ICT2010), Bangkok, Thailand, August 2010.
8. P. Kenpankho, **K. Watthanasangmechai**, P. Supnithi, T. Tsugawa, T. Maruyama, "The comparison of TEC in Chumpon, Thailand with the IRI models," 2010 Asia-Pacific Radio Science Conference (AP-RASC'10), Toyama, Japan, September 2010.
9. **Kornyanat Watthanasangmechai**, Pornchai Supnithi, Somkiat Lerkvaranyu, Takashi Maruyama, Winai Srisupasitanon, "Hourly and seasonal TEC prediction with neural network at Chumphon equatorial lattitude station, Thailand," The 25th International Technical Conference on Circuits/Systems, Computers and Communications (ITC-CSCC 2010), Pattaya, Thailand, July 2010.
10. **K. Watthanasangmechai**, P. Supnithi, S. Lerkvaranyu, T. Maruyama, "TEC prediction with neural network for the equatorial latitude station in Thailand," IRI 2009 Workshop, Kagoshima, Japan, October 2009.
11. P. Kenpankho, **K. Watthanasangmechai**, P. Supnithi, T. Tsugawa, and T. Maruyama, "Equatorial solar and latitude dependence of TEC", IRI 2009 Workshop, Kagoshima, Japan, October 2009.
12. P. Kenpankho, **K. Watthanasangmechai** and P. Supnithi, "Solar and Latitude Dependence of TEC in Thailand," International Symposium on Antenna and Propagation (ISAP) 2009, Bangkok, Thailand, October 2009.

SEALION Symposium 2011

International Southeast Asia Low-Latitude Ionospheric Observation Network Symposium 2011

27-28 January 2011

Bangkok, Thailand

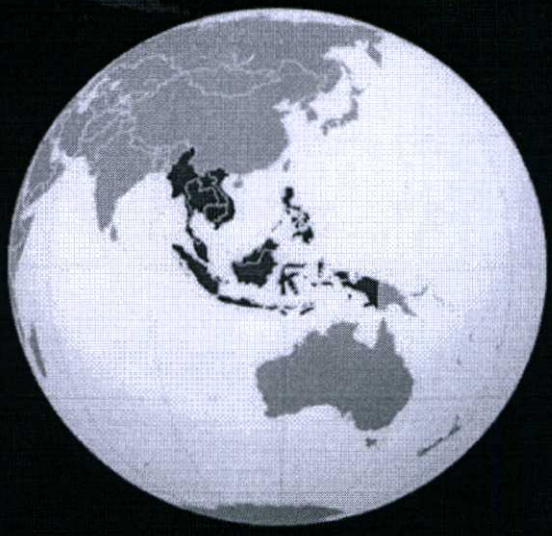

NiCT

Current Activities of TEC Monitoring and Prediction in Thailand

[#1]K. Watthanasangmechai, [1]P. Supnithi
[1]A. Mongkolkajid, [2]T. Tsugawa

and [2]T. Maruyama

[1]Faculty of Engineering, King Mongkut's Institute of Technology Ladkrabang Bangkok 10520, Thailand

[2]Space Environment Group, National Institute of Information and Communications Technology, Nukui-kita 4-2-1, Koganei, Tokyo 183-8795, Japan

[#1]kornyanat.watt@gmail.com

Abstract:

Since the earth's ionosphere is unstable and drastically changes in electron density, a number of ionospheric phenomena in the equatorial and low-latitude regions such as plasma enhancement and plasma bubble are frequently detected. The more plasma enhances the more time delay on GPA signal is noticed. The ionospheric disturbances affect the propagation of radio waves for broadcast and telecommunications. For the plasma bubble, it includes various scales of ionospheric irregularity. The several-hundred-meter scale irregularity causes the scintillation of radio signal. The scintillation degrades the GPS positioning/navigation accuracy, or cause the satellite communications break down. No satellite signal can be detected by the receivers due to the occurrences of loss-

of-lock (LOL). To investigate these phenomena, one parameter which can be used is GPS-derived TEC. Two-dimensional mapping technique is a powerful method for studying the generation and evolution of them. In this presentation, the TEC predicted by neural network (NN) model over equatorial-latitude station in Thailand will be discussed. The first development of two-dimensional TEC map over Thailand under the collaboration between National Institute of Information and Communications Technology (NICT), Japan, and King Mongkut's Institute of Technology Ladkrabang (KMITL), Thailand, will be demonstrated. The first data center of Thailand which is now undertaken by Communications and Storage Research Group (CSRG) at KMITL will finally be proposed.

Comparison of GPS TEC Measurements with IRI TEC Prediction at the Equatorial Latitude Station, Chumphon, Thailand

P. Kenpankho[1], K. Watthanasangmechai[1]
P. Supnithi[1], T. Tsugawa[2]
and T. Maruyama[2]

[1]Faculty of Engineering, King Mongkut's Institute of Technology Ladkrabang
Ladkrabang, Bangkok 10520, Thailand

[2]Space Environment Group, National Institute of Information and Communications Technology, Nukuikita
Koganei, Tokyo, 184-8795, Japan

Abstract:

In this work, the total electron content (TEC) derived from dual-frequency GPS receiver (GPS TEC) at the Chumpon station, Thailand, during 2004-2006 is analyzed. The diurnal, monthly and seasonal variation of the measure TEC is compared with the TEC from the IRI-2007 model as well as the TEC from the International GNSS service (IGS). Up to now, the TEC data from the equatorial latitudes are limited. The Chumphon station (10.72° N, 99.37° E) is located at the equatorial latitude and the dip latitude of 3° N. The TEC from the IRI-2007 model is based on the actual F2 plasma frequency (*fo*F2) measurement. The study shows that the IRI-2007 model agrees with the GPS TEC data mostly in the morning hours, but generally underestimates the GPS TEC. The

maximum differences are about 15 TECU during daytime and 5 TECU during night time. The underestimation is more evident at daytime than nighttime. The noon-bite out phenomena are clearly seen for the IRI-2007 TEC, but not on the IGS TEC and GPS TEC. The general underestimation is of the IRI-2007 model can be explained from the exclusion of the plasmasphere, whereas the large difference during noon bite-outs is caused by the difference in the slab thickness in the ionosphere between the IRI-2007 model and the actual measurement. When compared with the IGS model, the TEC measurements at Chumphon appear to be quite similar.

Key words: GPS TEC, IRI-2007 TEC, IGS TEC, TEC comparison, TEC measurement, TEC prediction, equatorial latitude

第128回 地球電磁気・地球惑星圏学会
総会・講演会（2010年 秋学会）

SGEPSS
Society of Geomagnetism and
Earth, Planetary and Space Sciences

開催期間：２０１０年１０月３０日（土）～１１月３日（水・祝）

総会・講演会：１０月３１日（日）～１１月３日（水・祝）

沖縄県市町村自治会館
Okinawa Jichikaikan

アウトリーチイベント：１０月３０日（土）
久茂地公民館
Kumoji Public Hall

大会概要 Outline
プログラム Program
著者索引 Authors
操作説明 Operation

主 催

地球電磁気・地球惑星圏学会

〒650-0044 神戸市中央区江戸町85-1
ベイ・ウイング神戸ビル10階
地球電磁気・地球惑星圏学会 事務局
E-mail: sgepss@pac.ne.jp
TEL: 078-332-3703　FAX: 078-332-2506

共催

独立行政法人情報通信研究機構
National Institute of Information and Communications Technology

後催

沖縄県、那覇市、沖縄県教育委員会、那覇市教育委員会
Okinawa Prefecture,Naha City,
Okinawa Prefectural Board of Education,Naha City Board of Education

Comparisons of GPS TEC and IGS TEC over four SEALION sites

Kornyanat Watthanasangmechai[1]; Prasert Kenpankho[1]; Pornchai Supnithi[1]; Takuya Tsugawa[2]; Takashi Maruyama[2]
[1] KMITL; [2] NICT

Global Positioning System (GPS) finds its applications in the navigational system as well as for the ionospheric observation. For the navigation purpose such as the Ground Based Augmentation System (GBAS), the ionospheric correction is simply incorporated in the pseudo-range correction. For the ionospheric observation, GPS-derived Total Electron Content (TEC) can describe the ionosphere ionization which varies over place and time. The satellite signals passing through the earth ionosphere to the ground-based GPS stations can suffer from the amplitude and phase fluctuation. The dispersion of two frequency GPS signals leads to the computation of the TEC by integrating the electron density along the propagation path. TEC measured by the dual-frequency JAVAD-GPS receivers installed at four GPS receiver stations in Thailand namely; Chiang Mai (18.76 deg N 98.93 deg E) located at the geomagnetic latitude 12.7 deg N, Bangkok (13.73 deg N 100.78 deg E) located at the geomagnetic latitude 6.7 deg N Chumphon (10.72 deg N 99.37 deg E) located at the geomagnetic latitude 3.0 deg N, and Phuket (7.90 deg N 98.39 deg E) located at the geomagnetic latitude 0.4 deg S are employed in this work. These four stations are part of the South East Asia Low-latitude Ionospheric Network (SEALION). SEALION has been conducted by National Institute of Information and Communications Technology (NICT) since 2003 for the purpose of monitoring and forecasting equatorial ionospheric disturbances, especially plasma bubbles. Several GPS receiver networks have been established and developed, one of which by the International GNSS Service (IGS), in recent years,

The IGS collects, archives, and distributes GPS observation data sets. It provides the GPS-based TEC map data via the ftp site: ftp://igscb.jpl.nasa.gov/. In order to verify the GPS TEC, it would be interesting to compare the GPS TEC with the IGS TEC on equinox and solstice days. In addition, we have ever compared the GPS TEC with the IGS TEC on equinox and solstice days in 2007 at Chumphon station in our previous work. The result reveals that the trends of the GPS TEC and IGS TEC are similarly. However, the IGS TEC values are higher than those from the GPS TEC about 2 TECU for year 2007. The noon-bite out phenomenon appears on March equinox day for IGS TEC only, but not for the rest.

To extend our research work into this study, we compare the GPS-TEC with the IGS TEC over four stations in Thailand. We use the IGS TEC map data at 20 deg N and 100 deg E, the nearest monitoring location to Chiang Mai station, at 15 deg N and 100 deg E, the nearest monitoring location to Bangkok station, and at 10 deg N and 100 deg E, the nearest monitoring location to Chumphon and Phuket stations. From this research, we find that the GPS TEC agree with the IGS TEC during the study period. The noon-bite out is not clearly seen on both of the IGS TEC and GPS TEC. This may be due to the height of the GPS satellite, about 22000 kilometers, which includes both of the ionosphere and the plasmasphere, the major parts which contribute to the TEC variation.

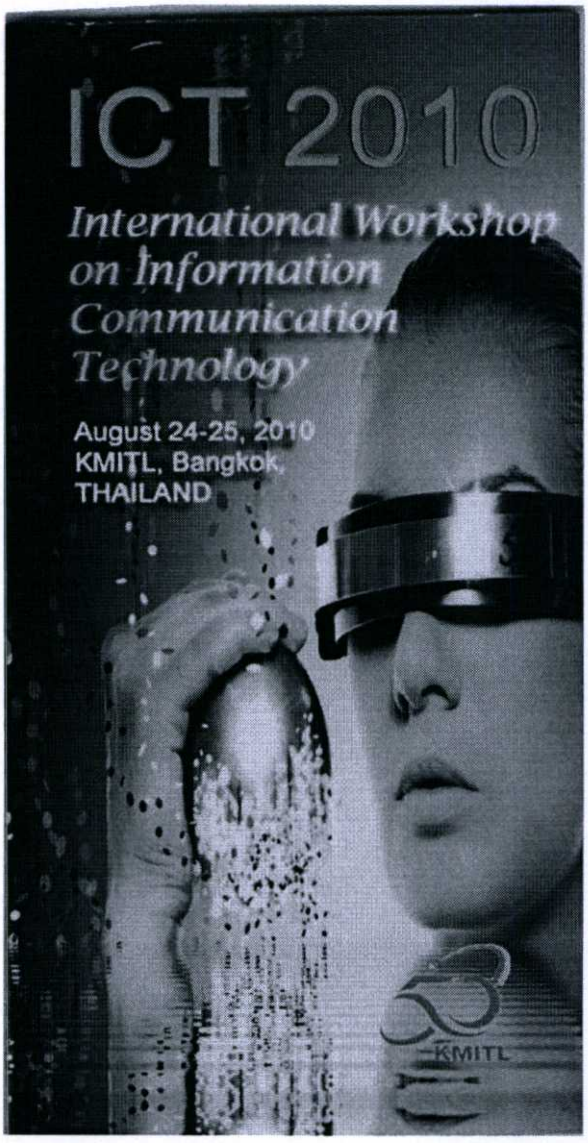
ICT 2010
International Workshop on Information Communication Technology
August 24-25, 2010
KMITL, Bangkok,
THAILAND
KMITL

Comparison of NN TEC with GPS TEC and IRI-2007 TEC over equatorial latitude station, Thailand

Kornyanat Watthanasangmechai*, Pornchai Supnithi*, Somkiat Lerkvaranyu*, Takashi Maruyama†
* Faculty of Engineering, King Mongkut's Institute of Technology Ladkrabang, Bangkok 10520, Thailand
E-mail: s2611215@kmitl.ac.th
† Space Environment Group, National Institute of Information and Communications Technology,
Nukui-kita, 4-2-1, Koganei, Tokyo 183-8795, Japan

***Abstract*— In this paper, the Global Positioning System Total Electron Content (GPS TEC) are presented. Data for Chumphon, the equatorial latitude station in Thailand, covering three-year period are used to train the feed forward neural network (NN). Levenberg-Marquardt back propagation is employed as the training function. The parameters affecting TEC are fed as the input of the NN called as the input space. The analysis is made by comparing the NN results with the GPS TEC and the TEC predicted by the most recent International Reference Ionosphere (IRI) model, IRI-2007 model. To investigate the performance of the NN, the root mean-square error (RMSE) comparisons are also described. The experimental results reveal that the proposed NN is able to predict the GPS TEC quite well even with the constraint limited of the available historical TEC data.**

I. INTRODUCTION

The ionosphere is the dispersive medium which affects to the GPS signal and other radio signals which propagate trough the earth atmosphere. Since it is the dispersive medium which is the irregular medium, through which the radio signals are subjected to refraction [11]. Total Electron Content (TEC) is one of the important parameters which can describe the ionosphere ionization and varies over place and time. In this paper, the TEC measurement for Chumphon station obtained from the JAVAD-GPS receiver is supported by the South East Asia Low Latitude Ionosphere Observation Network (SEALION) which is a joint project among the following institutions and countries: National Institute of Information and Communications Technology (NICT), Japan, King Mongkut's Institute of Technology Ladkrabang (KMITL), Thailand, Chiang Mai University (CMU), Thailand, National Institute of Aeronautics and Space (LAPAN), Indonesia, Hanoi Institute of Geophysics (HIG), Vietnamese Academy of Science and Technology, Vietnam, Center for Space Science and Applied Research (CSSAR), Chinese Academy of Sciences, China, and Kyoto University, Japan, observes, monitors and forecasts the ionospheric variation in the Asia Pacific region near the magnetic equator.

The International Reference Ionosphere (IRI) model is an empirical model which can be improved from the historical data. The neural network (NN) is the model which can learn and be improved from the historical data as well. A number of works employ the NN to predict the atmosphere parameters such as TEC and then compare with the observed data and the data from other models [6], [7], [8], [9], [14].

Thailand is located at the equatorial ionization anomaly (EIA) region which is the important region for the ionosphere study. However, the data covering this region are still scant. Besides, our previous works [7], [8] are focused on the NN interpolation ability for the lost TEC data in some duration. Thus, this work investigates the NN extrapolation for TEC prediction purpose. The NN results are compared with the observed GPS TEC data and the predicted data from the IRI-2007 model, the latest IRI model, to see the effectiveness of the proposed NN model. The RMSE comparisons are also described. Even with the constraint limited of the available data, our NN model still predicts the GPS TEC in 2009 over Chumphon quite well.

II. GLOBAL POSITIONING SYSTEM TOTAL ELECTRON CONTENT (GPS TEC)

TEC is defined as the total electron content (electron/m^2) of a vertical column of 1 m^2 cross-section [4], [12] called as a vertical TEC (VTEC) which varies over place and time. The height of the GPS satellites is about 22,000 km which includes both of the ionosphere and the plasmasphere. The TEC measurement for Chumphon station is obtained from the JAVAD-GPS receiver which receives two GPS signals with L_1 signal (f_1 = 1575.42 MHz) and L_2 signal (f_2 = 1227.60 MHz). For this work, the TEC measurement system consists of a microstrip antenna, an amplifier, a JAVAD TEC meter, and a computer unit as shown in Fig. 1. The slant TEC (STEC) data from the satellites to the receiver can be obtained from the difference between the pseudo ranges or the difference between the phases (L1 and L2) of the two frequencies [3]. Then the TEC can be computed from the STEC value and the zenith angle as described in our previous work [12]. Note that the height of the ionospheric layer for TEC calculation is assumed to be 400 kilometers [5].

III. INTERNATIONAL REFERENCE IONOSPHERE (IRI)

International Reference Ionosphere (IRI) [1] is an international project of NASA sponsored by the Committee on Space Research (COSPAR) and the International Union on Radio Science (URSI). It is an empirical model based on data

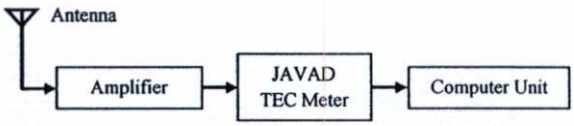

Fig. 1 TEC measurement system.

from the worldwide network of ionosonde stations, incoherent scatter radars, the ISIS and Alouette topside sounders, and in situ measurement on several satellites and rockets [10]. IRI predictions are most accurate in Northern mid-latitudes because of the generally high station density in this part of the globe. The steepest gradients, sharp peaks and deep valleys, of the ionospheric parameters are found at the low and high latitudes where are requiring a high station density to fully record and monitor the highly variable ionosphere. Due to the equatorial and the auroral regions have rather scant ionosonde coverage, partly because of the harsh climate conditions [2], and the lack of available local GPS TEC data which can be used for the model development, thus the IRI predictions are less accurate at equatorial and auroral latitude.

The IRI-2007 is the latest IRI model developed from the limitations of the previous IRI models. The topside profile which impacts on the TEC is specially improved. To overcome the shortcoming of the previous IRI models for the auroral region, one of the new features in the IRI-2007 is the NN model that was trained with a large volume of EISCAT incoherent scatter data and also with 115 profiles obtained from rocket borne wave propagation experiments [9].

The IRI-2007 TEC predictions are calculated from the IRI-2007 model via the IRI homepage by using latitude and longitude, date, period of time, and the upper boundary height, as the model input. We can access the IRI homepage at http://ccmc.gsfc.nasa.gov/modelweb/models/iri_vitmo.php. For this work, we set the upper boundary height to be 2,000 km, the maximum height of the IRI-2007 model, to include not only the ionosphere but also the plasmasphere as well.

IV. Neural Network (NN)

Neural network is the information processing system and modeled after human brain. It is compose of input unit, processing unit and output unit called as input layer, hidden layer and output layer, respectively. Each layer consists of node or neuron, the pattern of which is similar to the biological neural net. We employed the 5:9:1 NN architecture [7], as shown in Fig. 2, corresponding to five input parameters, nine cells in the hidden layer, and one output node. There are supervised and unsupervised learning for the neural network learning methodology, however, this work uses the supervised learning which needs training with the historical data. In order to teach the network to know the nonlinear data-pattern, we employ the feed-forward network with the back propagation algorithm to adjust the weight. After the network has known the pattern, the predicted output is compared with the target for computing an error. The error is then fed back to the network for improving the learning ability by weight

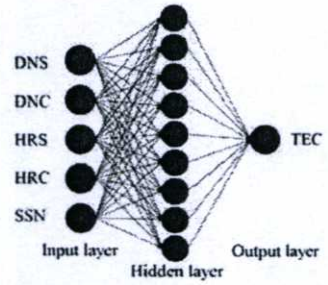

Fig. 2 The NN architecture for TEC prediction.

adjusting to reach the desired mean-square error. The expositions about the NN and its algorithm are well described in [7] and [15].

The input space for the proposed NN composes of the parameters affecting TEC which are day number (DN), hour number (HR), and sunspot number (SSN). The first two parameters are divided into sine and cosine components to let the data continue [7], [8]. The 27-day mean SSN data are used for representing the solar rotation and solar activity [7]. These input parameters are sent trough the input layer to process in the hidden layer. The Levenberg-Marquardt back propagation is applied as the training function. The TEC data during 2006 to 2008 are used as the NN target. To see if the NN is applicable to extrapolate the TEC, the TEC data in 2009 are used for the NN testing. The performance of the NN is considered from the RMSE.

V. Results and Analysis

A. *Hourly Comparison*

Most of our previous works are concern over the TEC interpolation; however, the TEC extrapolation has not been investigated. Thus, we focus on TEC prediction in 2009 from the NN that learns from TEC data in 2006, 2007 and 2008. The vertical TEC values obtained with the three techniques, GPS observing, IRI-2007 model, and NN model, for year 2009 over Chumphon (10.72 °N 99.37°E) are shown in Fig. 3, Fig. 4 and Fig. 5, respectively. We found that the GPS TEC which exhibits the usual diurnal variation of the maximum during 14h30 LT and 18h30 LT, the pre-sunset hours, and the minimum during 00h30 LT and 05h30 LT, the pre-sunrise hours, is quite agree with the NN TEC for all year 2009, however the NN TEC is rather smooth than the GPS TEC. As shown in Fig. 5, the predicted maximum IRI-2007 TEC values are occurred in the shorter period than the GPS TEC and the NN TEC. In Fig. 2, there are some periods, during the days 160th and 176th, for example, covered with the blue strips are ignored in the RMSE calculations, however, these periods can be fulfilled with the predicted TEC data from the NN model or the IRI-2007 model. If we take the RMSE into account, the NN RMSE is equal to 1.790 TECU and the IRI-2007 RMSE is equal to 3.568 TECU. This means our proposed NN improves the accuracy from the IRI-2007 model about 52.63% in year 2009.

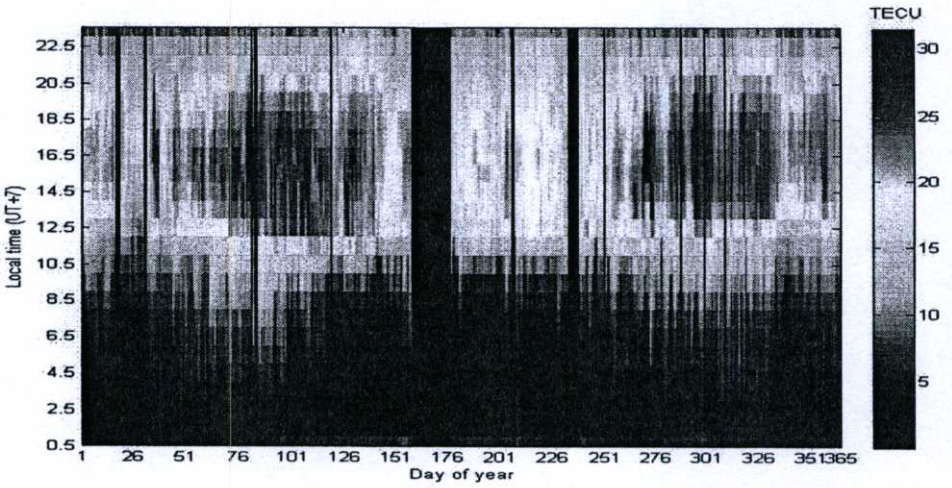

Fig. 3 The GPS TEC over Chumphon in 2009.

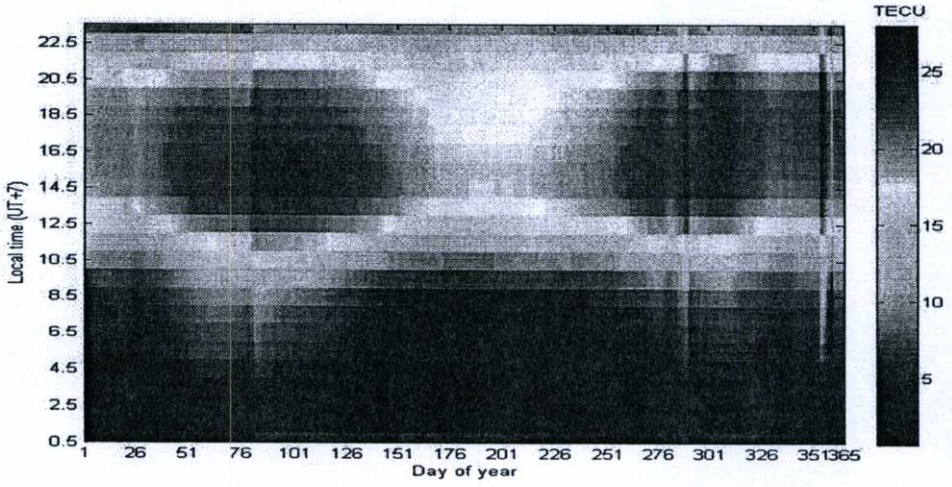

Fig. 4 The proposed NN TEC over Chumphon in 2009.

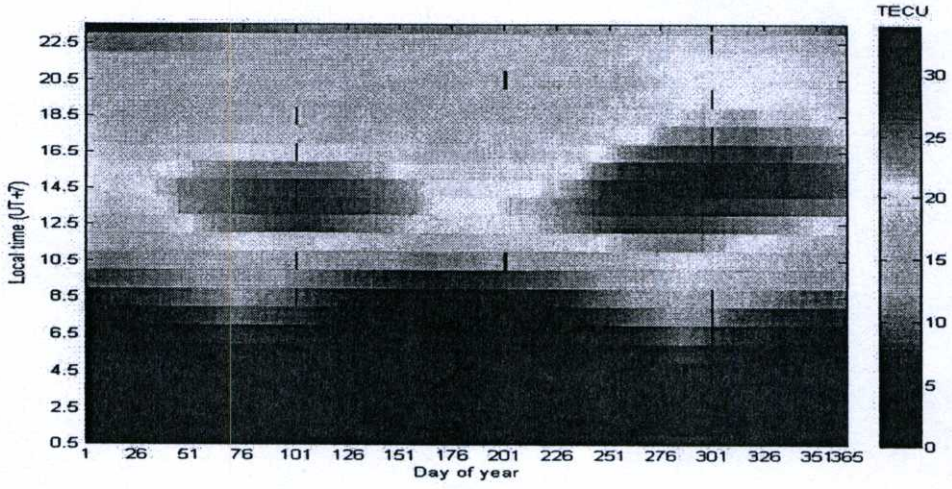

Fig. 5 The IRI-2007 TEC over Chumphon in 2009.

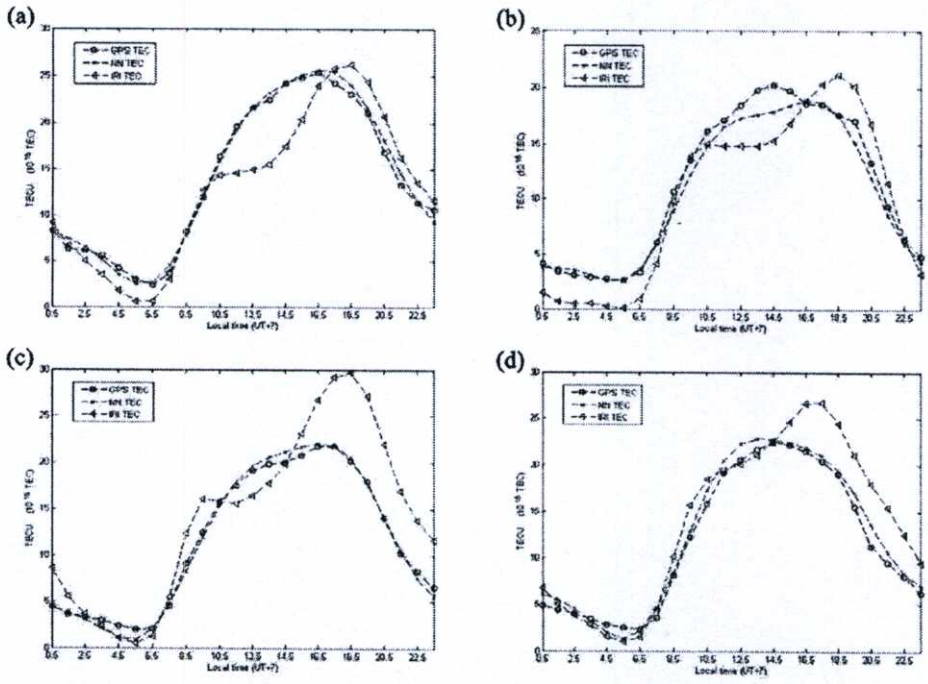

Fig. 6 GPS TEC, NN TEC and IRI-2007 TEC at Chumphon station for
(a) March equinox (b) June Solstice (c) September equinox (d) December solstice, all in 2009.

TABLE I
RMSE VALUES OF GPS TEC AND PREDICTED VALUES (NN TEC AND IRI-2007 TEC) FOR DIFFERENT SEASONS IN 2007 OVER CHUMPHON STATION.

Season	RMSE (TECU)	
	NN TEC	IRI-2007 TEC
March Equinox	0.957	4.025
June Solstice	0.770	2.485
September Equinox	2.105	3.513
December Solstice	2.012	2.135

B. Seasonal Comparison

In order to investigate a seasonal TEC variation, the TEC data are classified into March equinox (March, April, May), June solstice (June, July, August), September equinox (September, October, November), and December solstice (December, January, February). The monthly median values are used for representing the seasonal TEC as shown in Fig. 6. We can notice that the noon bite-out obviously seen from the IRI-2007 TEC is imperceptible appeared for the GPS TEC and the NN TEC due to the fact that the IRI-2007 TEC based on the ionogram and covered the electron up to only 2,000 km, the maximum values, which includes some parts of the plasmasphere, while the GPS TEC and the NN TEC based on the GPS satellites that orbit about 22,000 km above the earth which includes the major part of the plasmasphere. The trends of the NN TEC agree with those of GPS TEC quite well for all seasons. The large discrepancy values between the NN TEC and the GPS TEC are invisible. The IRI-2007 model overestimates TEC during 17h30 LT and 21h30 LT for all seasons and underestimates TEC during local midday for March Equinox, June solstice and September equinox. As shown in Table 1, the NN TEC gives the least RMSE (0.632 TECU) in September equinox and the most RMSE (1.080 TECU) in June solstice. The IRI-2007 model gives the least RMSE (2.683 TECU) in June solstice and the most RMSE (4.514 TECU) in September equinox. If we consider the RMSE comparison only in June solstice, the season which the most RMSE of the NN and the least RMSE of the IRI-2007 model occur, the proposed NN still predicts the GPS TEC more accurately than the IRI-2007 model. This is due to the proposed NN is trained with the historical local TEC data.

VI. CONCLUSIONS

This work investigates the TEC extrapolation performance of the NN. The comparisons of the NN TEC and the predicted TEC, the GPS TEC and the IRI-2007 TEC, are examined. The large discrepancy values between NN TEC and GPS TEC are invisible for all year 2009. However, the IRI-2007 model overestimates TEC during 17h30 LT and 21h30 LT for all seasons and underestimates TEC during local midday for March Equinox, June solstice and September equinox. This is due to the fact that the IRI-2007 TEC based on the ionograms and covered the electron up to only 2,000 km, the maximum

values, which includes some parts of the plasmasphere, while the GPS TEC and the NN TEC based on the GPS satellites that orbit about 22,000 km above the earth which includes the major part of the plasmasphere. Moreover, the NN is also trained with the historical local TEC data. Thus, this may be the reason why the proposed NN can predict the GPS TEC more accurately that the IRI-2007 model.

ACKNOWLEDGMENT

The authors are grateful to the National Institute of Information and Communications Technology (NICT) and King Mongkut's Institute of Technology Ladkrabang (KMITL) for technical and funding support through SEALION project. The IRI-2007 model available on the NASA website is extensively used and appreciated. In addition, we are grateful to Dr. Takuya Tsugawa, NICT, Japan, for kind advice and useful suggestions about the GPS TEC.

REFERENCES

[1] D. Bilitza, "A correction for the IRI topside electron density model based on Alouette/ISIS topside sounder data," *Adv. Space Res.*, vol. 33, no. 6, pp.838-843, 2004.

[2] D. Bilitza, B.W. Reinisch, "International Reference Ionosphere 2007: Improvements and new parameters," *Adv. Space Res.*, vol. 42, pp.599 -609, 2008.

[3] G. Blewitt, "An automatic editing algorithm for GPS data," *Geophys. Res. Lett.*, vol. 17, pp. 199-202, 1990.

[4] G. L. Goodwin, J. H. Silby, K. J. Lynn, A. M. Breed, E. A. Essex, "GPS satellite measurements: ionospheric slab thickness and total electron content," *J. Atmos. Solar-Terr. Phys.*, vol. 57, no. 14, pp.1723-1732, 1995.

[5] G. Ma and T. Maruyama, "Derivation of TEC and estimation of instrumental biases from GEONET in Japan," *Ann. Geophys.*, vol. 21, pp.2083-2093, 2003.

[6] J.B. Habarulema, L.A. McKinnell, P.J. Cilliers, B.D.L. Opperman, "Application of neural networks to South African GPS TEC modeling," *Adv. Space Res.*, vol. 43, no. 11, pp.1711-1720, 2009.

[7] K. Watthanasangmechai, P. Supnithi, S. Lerkvaranyu, T. Maruyama, W. Srisupasitanon, "Hourly and seasonal TEC prediction with neural network at Chumphon equatorial latitude station, Thailand," *Proceeding of the 25th International Technical Conference on Circuits/Systems, Computer and Communications (ITC-CSCC)*, Pattaya, Thailand, 2010.

[8] K. Watthanasangmechai, P. Supnithi, S. Lerkvaranyu, T. Nagatsuma, T. Tsugawa, T. Maruyama, "TEC prediction with neural network for Thailand equatorial latitude station" *J. EPS.*, unpublished.

[9] L. A. MaKinnell, M. Friedrich, R. J. Steiner, "A new approach to modeling the daytime lower ionosphere at auroral latitudes," *Adv. Space Res.*, vol. 34, no., 9, pp.1943-1948, 2004.

[10] P. K. Bhuyan, R. R. Barah, "TEC derived from GPS network in India and comparison with the IRI," *J. Adv. Space Res.*, vol. 39, pp.830-840, 2007.

[11] P. Kenpankho, K. Watthanasangmechai, P. Supnithi, "Solar and Latitude Dependence of TEC in Thailand," *Proceeding of The 2009 International Symposium on Antennas and Propagation (ISAP 2009)*, Bangkok, THAILAND, pp.189-192, 2009.

[12] P. Kenpankho, K. Watthanasangmechai, P. Supnithi, T. Tsugawa, T. Maruyama, "Comparison of GPS TEC measurements with IRI TEC prediction at an equatorial latitude station, Chumphon, Thailand," *J. EPS.*, unpublished.

[13] T. Maruyama, "Regional reference total electron content model over Japan based on neural network mapping techniques," *Ann. Geophys.*, vol. 25, pp.2609-2614, 2007.

[14] T. Maruyama, "Solar proxies pertaining to empirical ionospheric total electron content models," *J. Geophys. Res.*, vol. 115, A04306, doi:10.1029/2009 JA014890., 2010.

[15] Y. Tulunay, E. Tulunay, E. T. Senalp, "The neural network technique-1: a general exposition," *Adv. Space Res.*, vol. 33, pp.983-987, 2004.

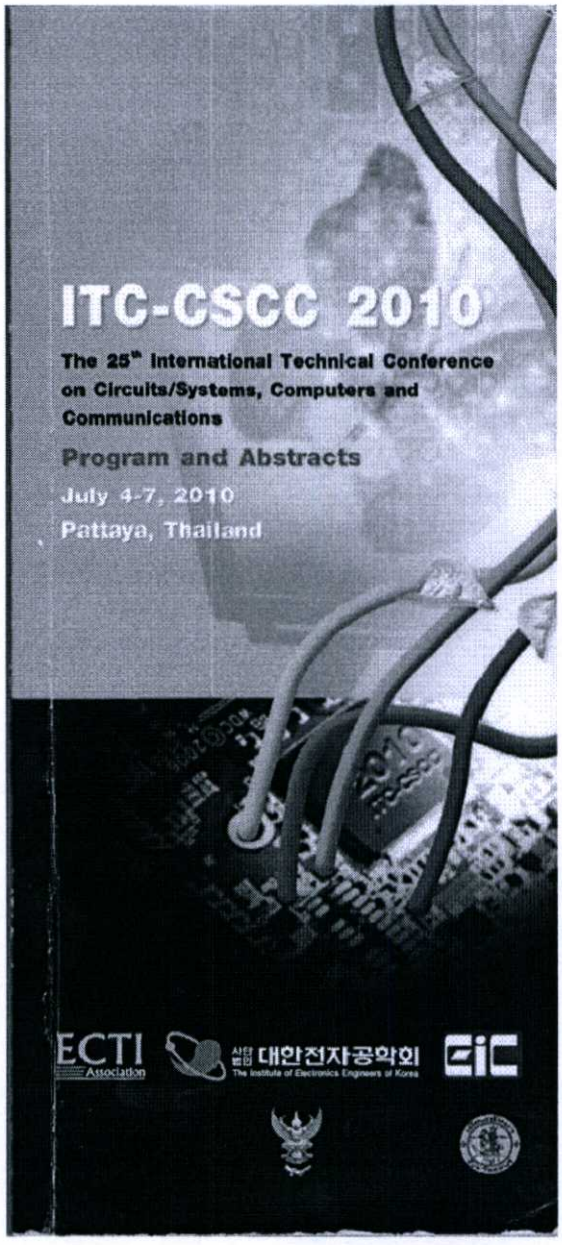
ITC-CSCC 2010
The 25th International Technical Conference on Circuits/Systems, Computers and Communications
Program and Abstracts
July 4-7, 2010
Pattaya, Thailand
ECTI Association
대한전자공학회
The Institute of Electronics Engineers of Korea
EIC

Hourly and seasonal TEC prediction with neural network at Chumphon equatorial lattitude station, Thailand

Kornyanat Watthanasangmechai[1], Pornchai Supnithi[2], Somkiat Lerkvaranyu[3], Takashi Maruyama[4], Winai Srisupasitanon[5]

[1, 2, 3] Faculty of Engineering, King Mongkut's Institute of Technology Ladkrabang, Bangkok 10520, Thailand
[4] Space Environment Group, National Institute of Information and Communications Technology, Nukui-kita, 4-2-1, Koganei, Tokyo 183-8795, Japan
[5] Phuket Technical College, Phuket 83000, Thailand
E-mail: [1]s2611215@kmitl.ac.th, [2]ksupornc@kmitl.ac.th, [3]somkiat@telecom.ac.th, [4]tmaru@nict.go.jp

ABSTRACT

This paper proposes the application of the neural network (NN) technique to interpolate hourly and seasonal total electron content (TEC) over Chumphon, Thailand, located at the equatorial lattitude. The feed forward network with supervised learning in this work has a single hidden layer with the back propagation algorithm applied for the prediction system. The parameters that influence TEC are used as the input space. The proposed NN is trained by the observed TEC values (GPS TEC) in 2006, 2008 and 2009 based on the available data. The predicted TEC values are compared with those derived from GPS data and the prediction by the recently updated International Reference Ionosphere model, IRI-2007. To examine the performance of NN, the root mean-square error (RMSE) of NN TEC and IRI-2007 TEC are compared. The results reveal that NN can predict GPS TEC quite well over Chumphon station.

1. INTRODUCTION

The total electron content (TEC), the line integral of the electron density along the propagation path from a satellite to a receiver, is one of the parameters which can investigate the ionosphere variability that affects to the GPS signal [4]. The variation of TEC over Chumphon (10.72 °N 99.37°E) are observed by the dual-frequency JAVAD-GPS receiver with f_1, 1575.42 MHz, and f_2, 1227.60 MHz. The equatorial region is an anomaly area at which the most significant discrepancy of experimental and modeled data was observed [10]. IRI-2007 model, the latest IRI model, is one of the ionospheric models which allow the TEC prediction [1]. A number of research works in the literature [5], [8] reported the comparison between the observed data, the IRI predicted data and the NN predicted data and already proved that the NN is one of the appropriate approaches to predict the ionospheric parameter such as TEC.

In the recent years, TEC computed from the GPS data have become available in Thailand and some neighboring countries through SEALION project among others. The availability of historic TEC data is important to the development of the IRI model [7] as well as the NN model which can learn from the prior data. Thus the research objectives are not only to predict and compare the TEC values, but also to develop the TEC database in the foreseeable future.

This work presents the NN application to predict TEC prediction. The NN results are compared to the observed values and the predicted values from the IRI-2007. To measure the effectiveness and the performance of our NN models, the RMSE values are then computed and compared.

2. IRI-2007 MODEL

International Reference Ionosphere (IRI) [1] is an international project of NASA sponsored by the Committee on Space Research (COSPAR) and the International Union on Radio Science (URSI). The IRI is bi-annually updated during special IRI workshops. The IRI-2007 [2], a new empirical standard model of the ionosphere, is improved from the limitations of the previous IRI models. We can access the site: http://ccmc.gsfc.nasa.gov/modelweb/models/iri_vitmo.php to obtain the IRI-2007 TEC. The electrons in the plasmasphere also affect to TEC, thus we set the upper boundary height for the model to be the maximum value, 2000 kilometres, to include not only the ionosphere but also the plasmasphere as well.

3. NEURAL NETWORK

Artificial neural network is an information processing system. It composes of input layer, hidden layer and output layer. Each layer consists of the processing unit called as node, unit, cell, or neuron. In order to teach the network to know the nonlinear data-pattern, we employ the feed-forward network with the back propagation algorithm to adjust the weight.

3.1. Training with backpropagation algorithm

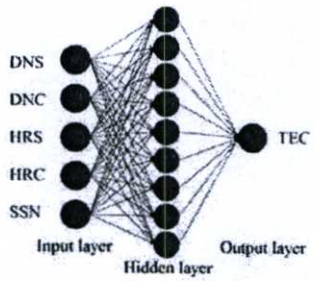

Fig. 1. The NN architecture for TEC prediction.

Within the context of the algorithm, this paragraph substantially relies on the book written by [6]. For this work, the algorithm is started by setting the initial weights and biases to be the small random values. Each input node (X_i, $i = 1,\ldots, n$) receives input signal x_i and broadcasts this signal to all nodes in the layer above, hidden layer. Each hidden node (Z_j, $j = 1, \ldots, p$) sums its weighted input signals as given by

$$z\_in_j = w_{0j} + \sum_{i=1}^{n} x_i w_{ij}, \quad (1)$$

where z_in_j is the net input to Z_j, w_{oj} is the bias on the hidden node j, x_i is the input signal from the input node i and w_{ij} is the bias from input node i to hidden node j.

We applied the hyperbolic tangent sigmoid function as an activation function for Z_j to compute the hidden output as Eq. (2).

$$z_j = TANSIG\left(z\_in_j\right) = \frac{2}{1+\exp\left(-2 \cdot z\_in_j\right)} - 1, \quad (2)$$

Then, the signal z_j is sent to all nodes in the layer above, output layer. Each output node (Y_k, $k = 1, \ldots, m$) sums its weighted input signals as given by

$$y\_in_k = w_{0k} + \sum_{j=1}^{p} z_j w_{jk}, \quad (3)$$

where y_in_k is the net input to Y_k, w_{ok} is the bias on the output node k, z_j is the input signal from the hidden node j and w_{jk} is the bias from hidden node j to output node k.

The linear transfer function, Eq. (4), is used as an activation function for Y_k to compute the output signals, y_k.

$$y_k = PURELIN\left(y\_in_k\right) = y\_in_k, \quad (4)$$

The Levenberg-Marquardt backpropagation (trainlm) is emploied as the training function for this work. It is not necessarily advantageous to keep the training on until the square error actually reaches a minimum [10]. As long as the error from testing process decreases, the training continues. The error is backpropagated to the nodes in the layer below. Each node, excluding the nodes in the input layer, updates its weights and biases. The validation process will be terminated if the error begins to increase.

3.2. NN input and output

This work applied the NN architecture as shown in Fig. 1 to predict the TEC for both of the hourly model and the seasonal model. The NN inputs include the parameters effecting to TEC which are hour number (diurnal variation), day number (seasonal variation) and sunspot number (SSN). To continue the data, we split both of the hour number and the day number to two cyclic components [5] as given by

$$DNS = \sin\left(\frac{2\pi \times DN}{365.25}\right), \quad DNC = \cos\left(\frac{2\pi \times DN}{365.25}\right), \quad (5)$$
$$HRS = \sin\left(\frac{2\pi \times HR}{24}\right), \quad DNC = \cos\left(\frac{2\pi \times HR}{24}\right)$$

where DNS, DNC, HRS, HRC are sine and cosine components of day number and hour number, respectively. Since the amplitude of short-term TEC variation is induced by solar rotation [9], one solar rotation is equal to 27 days, we choose the 27-day mean SSN for representing the solar activity.

The NN outputs shown in this paper are from the hourly model and the seasonal model. To see both of the NN model effectivenesses, the RMSE comparisons are described in this paper as well. RMSE is defined as:

$$RMSE = \sqrt{\frac{1}{N}\sum_{i=1}^{N}\left(TEC_{pred} - TEC_{meas}\right)^2}, \quad (6)$$

where N is the number of data points, TEC_{pred} is TEC predicted by a model and TEC_{meas} is TEC estimated from GPS observations.

4. RESULTS AND DISCUSSION

TEC can be computed from the slant TEC (STEC) value and the zenith angle [3]. The STEC data from the satellites to the receiver can be obtained from the difference between the pseudo ranges (P_1 and P_2) or the difference between the phases (L_1 and L_2) of the two signals. Note that the height of the ionospheric layer is assumed to be 400 kilometers [4].

4.1. Hourly model

To see the NN applicable for TEC prediction, the hourly model is then constructed. The data set for learning process includes the hourly TEC in 2006, 2008 and 2009, the low solar activity period, while the NN interpolates the hourly TEC in 2007. The hourly model outputs are compared with the hourly TEC from GPS and IRI-2007

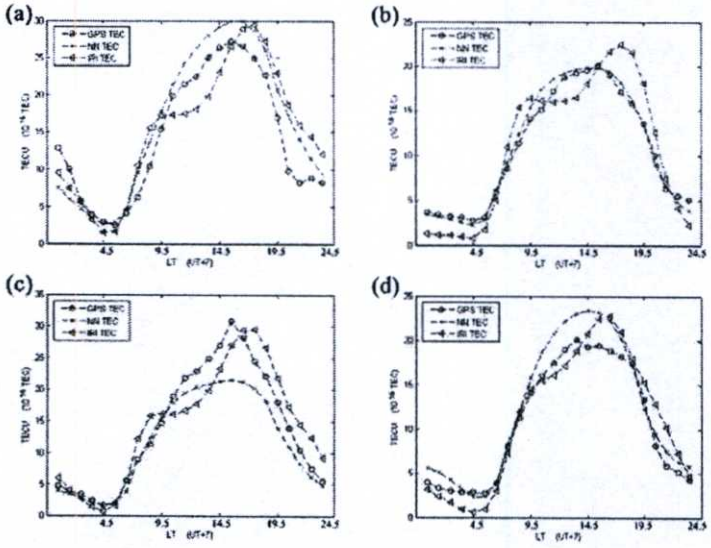

Fig. 2. GPS TEC, NN TEC and IRI-2007 TEC at Chumphon station (a) on 20 March 2007 (equinox day), (b) on 21 June 2007 (solstice day), (c) on 23 September 2007 (equinox day), (d) on 25 December 2007 (solstice day).

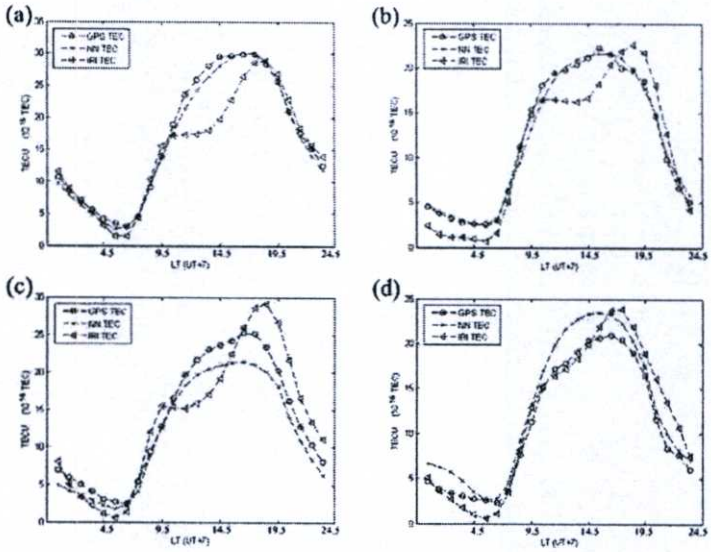

Fig. 3. GPS TEC, NN TEC and IRI-2007 TEC at Chumphon station for (a) March equinox (b) June Solstice (c) September equinox (d) December solstice, all in 2007.

model. We present only the results on equinox and solstice days in 2007. In 2007, equinox days occured on March 20 and September 23 while solstice days occurred on June 21 and December 22 (U.S. Naval Observatory, http://www.erh.noaa.gov/box/equinox.html), respectively. However, we show the results on December 25 instead of the lost data on December 22. NN TEC values are plotted versus the model values using IRI-2007 and the GPS TEC to show how close NN can predict four depicted days as shown in Fig. 2 (a)-(d). The NN TEC gives the least RMSE (0.830 TECU) on June 21, a solstice day, and the most RMSE (3.359 TECU) on September 23, an equinox day, as shown in Table 1. Alhough the maximum TEC on September 23 occurs around the same period, 13h30 LT to 17h30 LT, as the other days. The observed-TEC feature with the spike peak for September 23 is quite different from the usual one, the peak of which is a curve. Thus, we deduce that it may be the reason why NN could not perform well on September 23.

4.2. Seasonal model

Table 1
RMSE values of GPS TEC and predicted values (NN TEC and IRI-2007 TEC) for equinox and solstice days in 2007 over Chumphon station.

Date in 2005	RMSE (TECU) between GPS TEC and	
	NN TEC	IRI-2007 TEC
March 20	3.338	4.164
June 21	0.830	2.743
September 23	3.359	3.412
December 24	2.085	2.142

Table 2
RMSE values of GPS TEC and predicted values (NN TEC and IRI-2007 TEC) for different seasons in 2007 over Chumphon station.

Season	RMSE (TECU)	
	NN TEC	IRI-2007 TEC
March Equinox	0.957	4.025
June Solstice	0.770	2.485
September Equinox	2.105	3.513
December Solstice	2.012	2.135

The seasonal variation is generally considered to be one of the important factors for TEC variation, thus we undertake an analysis on seasonal TEC prediction in 2007 as well. The NN model constructed as the seasonal model includes four seasons which are March equinox, June solstice, September equinox and December solstice. The 24 hours monthly-median TEC values [8] are used to represent the seasonal TEC.

With the similar method to the hourly model, the seasonal model can interpolate the seasonal TEC values in 2007. As we expected, the seasonal model can predict the seasonal TEC quite well due to learning from the historic TEC data. The comparison results between NN TEC (seasonal TEC), GPS TEC and IRI-2007 TEC are presented in Fig. 3 (a)-(d). The trends of NN TEC agree with those of GPS TEC quite well for all seasons. The discrepancy values between NN TEC and GPS TEC are small, however NN model underestimates TEC after 11h30 LT for September equinox and overestimates TEC during 10h30 LT and 19h30 LT for December solstice. Even with the considerable difficulty for NN to learn the nonlinear TEC data-pattern which changes in amplitude drastically in equinox seasons due to a large effect from the sun which is perpendicular to the earth, the NN TEC still agrees with the GPS TEC during equinox seasons.

5. CONCLUSION

This analysis is made by making the comparison between GPS TEC, IRI-2007 TEC and NN TEC. The experimental results from our present work confirms that using the single hidden layer feed forward network with back propagation algorithm is suitable and sufficient for the TEC prediction purpose. The RMSE for the best estimation is equal to 0.770 TECU. The performances of our NN models are sastisfactory even with the constraint of limited available data.

6. ACKNOWLEDGEMENTS

We would like to thank the National Institute of Information and Communications Technology (NICT) and King Mongkut's Institute of Technology Ladkrabang (KMITL) for technical and funding support through SEALION project. The IRI-2007 model available on the NASA website is extensively used and appreciated. In addition, we are grateful to Prof. LeeAnne McKinnell, Rhodes University, South Africa, for kind advice and useful suggestions about NN input parameters.

7. REFERENCES

[1] D. Bilitza, "A correction for the IRI topside electron density model based on Alouette/ISIS topside sounder data," *Adv. Space Res.*, vol. 33, no. 6, pp.838-843, 2004.

[2] D. Bilitza, B.W. Reinisch, "International Reference Ionosphere 2007: Improvements and new parameters," Adv. Space Res., 42, 599 -609, 2008.

[3] G. Blewitt, "An automatic editing algorithm for GPS data," *Geophys. Res. Lett.*, vol. 17, pp. 199-202, 1990.

[4] G. Ma and T. Maruyama, "Derivation of TEC and estimation of instrumental biases from GEONET in Japan," *Ann. Geophys.*, vol. 21, pp.2083-2093, 2003

[5] J.B. Habarulema, L.A. McKinnell, P.J. Cilliers, B.D.L. Opperman, "Application of neural networks to South African GPS TEC modeling," *Adv. Space Res.*, vol. 43, no. 11, pp.1711-1720, 2009

[6] L. Fausett, *Fundamentals of Neural Networks*, Prentice Hall International, ISBN 0-13-042250-9, 1994

[7] M. Mosert, M. Gende, C. Brunini, R. Ezquer, and D. Altadill, "Comparisons of IRI TEC predictions with GPS and digisonde measurements at Ebro" *Adv. Space Res.*, vol. 39, pp.841-847, 2007

[8] T. Maruyama, "Regional reference total electron content model over Japan based on neural network mapping techniques," *Ann. Geophys.*, vol. 25, pp.2609-2614, 2007.

[9] T. Maruyama, "Solar proxies pertaining to empirical ionospheric total electron content models," *J. Geophys. Res.*, vol. 115, A04306, doi:10.1029/2009 JA014890., 2010.

[10] Y. Yasukevich, "Testing of IRI-2007 model using data of satellite altimeters Topex and Jason-1 and IRI-2001 modeling results," *37th COSPAR Scientific Assembly.*, Montréal, Canada., p.3542, July 2008.

IRI2009 Workshop

URSI/COSPAR INTERNATIONAL REFERENCE IONOSPHERE WORKSHOP

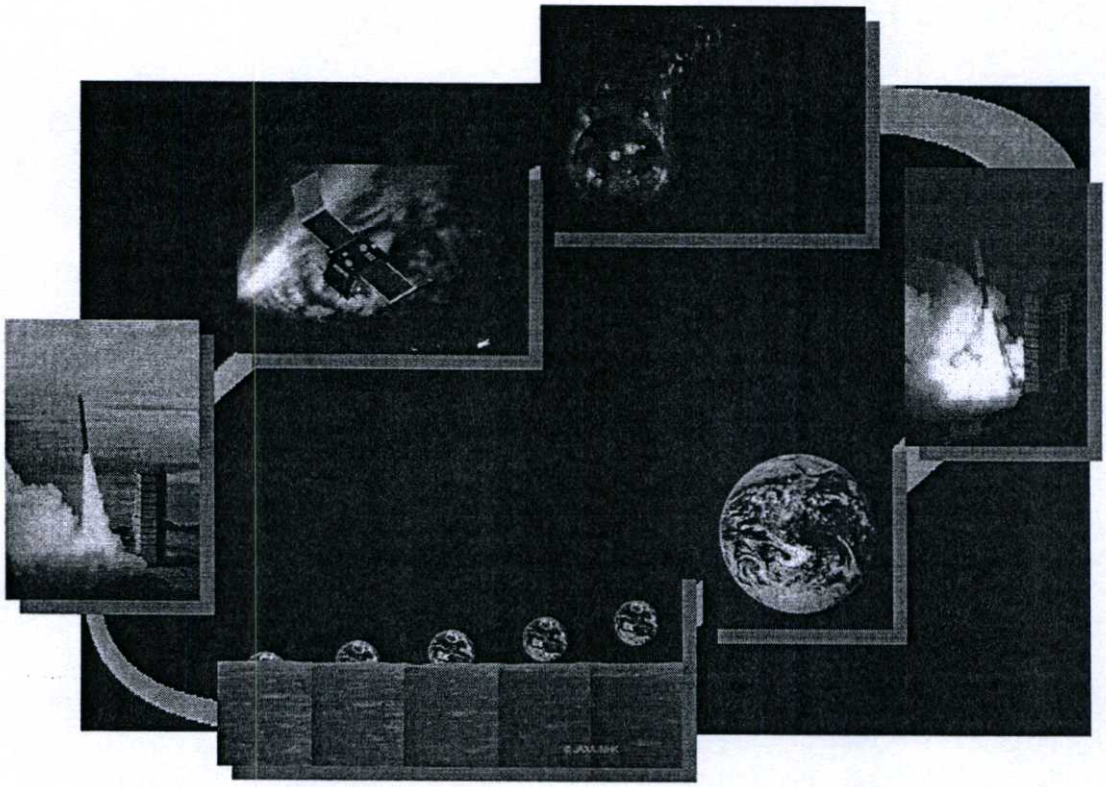

Inamori Hall, Kagoshima University,
Kagoshima, Japan
November 2-7, 2009

1-5 Monday, Nov. 2 11:10

Ionospheric Local Model based on Digisonde Measurements over Irkutsk

K.G. Ratovsky, A.V. Oinats

Institute of Solar-Terrestrial Physics, Lermontov st., 126a, P.O.Box 291, Irkutsk, 664033, Russia, ratovsky@iszf.irk.ru

The aim of the report is to present a Local Model (LM) creation technique which allows better prediction of the F2-layer parameters for single locality than the International Reference Ionosphere (IRI) model. The 27-day running medians of the parameters NmF2, hmF2, B0 and B1 measured with the DPS-4 Digisonde at Irkutsk (52.3N, 104.3E) have been used as inputs to create the LM. The LM is an empirical model based on assumption of linear dependence of the parameters on a solar activity proxy (the F10.7 index is chosen as the solar activity proxy). For each parameter (P) the LM consists of sets of two coefficients specifying the linear dependence on F10.7 index. The first coefficient is the P value under low (F10.7 = 70) solar activity and the second one is the derivative of the P with respect to F10.7. These coefficients are obtained by the linear regression of P on F10.7. The both coefficients are the functions of local time and month. To reproduce diurnal and seasonal variations we use B-spline approximation instead of a harmonic expansion. This allows noticeable improving the IRI prediction around the sunrise hours and providing more reliable solar activity dependence for the nighttime compared to IRI. The diurnal and seasonal behavior of the LM coefficients is compared with IRI model.

1-6 Monday, Nov. 2 11:25

TEC prediction with neural network for the equatorial latitude station in Thailand

Kornyanat Watthanasangmechai[a], Pornchai Supnithi[b], Somkiat Lerkvaranyu [c], Takashi Maruyama [d]

[a,b,c]Department of Telecommunications Engineering, King Mongkut's Institute of Technology Ladkrabang, Bangkok 10520, Thailand

[d]Space Environment Group, National Institute of Information and Communications Technology, Nukui-kita, 4-2-1, Koganei, Tokyo 183-8795, Japan

E-mail: [a] s2611215@kmitl.ac.th, [b] ksupornc@kmitl.ac.th, [c] somkiat@telecom.ac.th, [d] tmaru@nict.go.jp

Electron variation in the ionosphere has a significant effect on the radio signal propagating through the Earth's atmosphere. Total electron content (TEC) is one of the quantities which can describe the ionosphere ionization. In this paper, the TEC is measured by the JAVAD - GPS receiver installed at the GPS receiver station namely; Chumphon (10.72 °N 99.37°E), equatorial latitude station, Thailand. The TEC recorded during four years of low solar activity from 2005 to 2008 are used in this preliminary study. To predict the TEC with neural network (NN) model for equatorial latitude station, a feed forward network with back propagation algorithm was applied for this work. This NN model is composed of one input layer, one hidden layer and one output layer known as a single hidden layered feed forward network. The input layer consists of three nodes or neurons corresponding to three inputs while the hidden layer and the output layer consists of nine and one nodes or neurons, respectively. The performance of the NN model was considered from the mean-square error (MSE). To model the NN, the data set is divided into training, validating and testing sets. The training set is the TEC data in 2005, 2007 and 2008, while the TEC data in 2006 is reserved for the validating process. The input space was collected from the parameters that have an impact on the TEC data such as the hour number (diurnal variation), the month number (seasonal variation) and the Sunspot Number (SSN, measure of solar activity). In order to achieve an optimum NN architecture, the comparison between the MSE of a single hidden layered and a two hidden layered feed forward network was used. So as to validate the NN model, the NN TEC will be compared with the TEC from the global positioning system (GPS TEC) and the TEC from the International Reference Ionosphere model (IRI TEC).

From this research, we find that even though the single layered or the two layered feed forward network is used to reach the optimum NN architecture, the executed time, however, is surprisingly increased when the two hidden layered feed forward network is applied. It is the reason why we select the single hidden layered feed forward network for this work. The comparison of NN TEC, GPS TEC and IRI TEC has shown that the NN model predicts the TEC over Chumphon (10.72 °N 99.37°E),

equatorial latitude station, Thailand, fairly well. The IRI TEC is underestimates, while the NN TEC correlates to the GPS TEC at this station. Since the solar activity is one of the important parameters effecting on the TEC. The future works include expanding the input space in order to include most of the impact factors of the TEC, developing the GPS TEC database for perfectly boosting an efficiency of modeling the NN, and adding the studied stations within Thailand to develop the model which can be used for predicting the TEC all over Thailand, especially near the equatorial latitude area.

~~1-7~~ ~~Monday, Nov. 2~~ ~~11:40~~
(P-35) **Tuesday, Nov. 3** **16:00**

Regional ionosphere modeling from the combination of different satellite observation techniques

M.Schmidt (1), D.Dettmering (1), R.Heinkelmann (1), D.Bilitza (2,3)

(1)Deutsches Geodaetisches Forschungsinstitut (DGFI), Alfons-Goppel-Strasse 11, 80539 Muenchen, Germany, Email: schmidt@dgfi.badw.de, dettmering@dgfi.badw.de, heinkelmann@dgfi.badw.de
(2)Laboratory for Heliospheric Physics, GSFC, Greenbelt, Maryland, USA, Email: dieter.bilitza-1@nasa.gov
(3)Space Weather Laboratory, George Mason University, Fairfax, Virginia, USA, Email: dbilitza@gmu.edu

Electromagnetic measurements from various satellite missions are influenced on their way through the ionosphere by free electrons and thus, could be used to improve our knowledge on the distribution of the electron density in this region of the earth atmosphere and to provide a tool for correcting other measurements. At DGFI a procedure for multi-dimensional ionosphere modeling has been developed. It consists of a given reference part (e.g. IRI 2007) and an unknown correction part expanded in terms of multi-dimensional base functions. In the presented regional approach we use B-splines which allow additionally a so-called multi-resolution representation (MRR). The corresponding B-spline series coefficients are calculable from satellite measurements by parameter estimation. To take advantage of the different characteristics of the various measurement techniques we do a joint adjustment of COSMIC/FORMOSAT-3 GNSS measurements together with ground-based GNSS and measurements from dual-frequency radar altimetry. The weights for the different techniques are estimable by a variance component estimation (VCE); for the weights within a single technique different approaches will be discussed.

In this contribution we will introduce our approach and present results of the combination of different observation techniques. We will focus on vertical integrated electron density (vertical electron content, VTEC) models which will be compared to other VTEC maps available from a variety of institutions. Furthermore we will outline how the advantages of the MRR can be used, e.g. for near real-time processing.

P-27 Tuesday, Nov. 3 16:00

Equatorial solar and latitude dependence of TEC

P. Kenpankho[a], K. Watthanasangmechai[a], P. Supnithi[a], T. Tsugawa[b], and T. Maruyama[b]

[a]Faculty of Engineering, King Mongkut's Institute of Technology Ladkrabang, Bangkok 10520, Thailand
[b]Space Environment Group, National Institute of Information and Communications Technology, Nukuikita, Koganei, Tokyo, 184-8795, Japan

This study presents the influence of the solar flux index, daytime and nighttime on total electron content (TEC), and the dependence of TEC on different latitudes during 2005-2008. We analyze the median hourly values of TEC data from GPS-TEC measurements at four stations including Chiang Mai station (18.76°N, 98.93°E), Bangkok station (13.73°N, 100.78°E), Chumphon station (10.70°N, 99.30°E) and Phuket station (7.90°N, 98.39°E), located near the magnetic equator. During equinox, our results indicate that the daytime TEC is dependent on the solar activities and latitudes for four stations. There are positive correlation coefficients of daytime TEC with the solar activities and pair stations. For nighttime TEC, they are independent of the solar activity for all stations in 2007. There are negative correlation coefficients of nighttime TEC with the solar activities. During summer, the results indicate that the daytime TEC is quite dependent on the solar activities for four stations. There are positive correlation coefficients of daytime TEC with the solar activities. However, they are independent of TEC on the different latitudes. There are both negative and positive correlation coefficients of daytime and nighttime TEC with pair stations. During winter, TEC is quite dependent on the solar activities and latitudes for four stations. Nevertheless, in winter 2007, corresponding to the falling low solar activity, the nighttime TEC is independent on the solar activities for all stations.

Keywords: Total electron content; TEC; Equatorial TEC; Solar dependence of TEC; Latitude dependence of TEC

P-28 Tuesday, Nov. 3 16:00

Diurnal and seasonal variations of NmF2 at Thailand equatorial latitude and comparisons with IRI-2001 model

Noraset Wichaipanich[(a)], Pornchai Supnithi[(b)]

Faculty of Engineering, King Mongkut's Institute of Technology Ladkrabang, Bangkok 10520, Thailand.
E-mail: s1060038@kmitl.ac.th, [b] ksupornc@kmitl.ac.th

In 2003, a frequency modulated-continuous wave (FM/CW) ionosonde was installed at the equatorial latitude station at Chumphon province (Geographic latitude 10.72°N, Geographic longitude 99.37°E and Geomagnetic latitude 3.22°N), Thailand. It is one of the 5 SEALION (South East Asia Low-latitude Ionospheric Network) ionosondes (Maruyama et al., 2007). SEALION is an ionospheric observation network in Southeast Asia which has been conducted by National Institute of Information and Communication Technology (NICT), Japan, since 2003, for the purpose of monitoring and forecasting equatorial ionospheric disturbances, especially plasma bubbles. SEALION is a unique ionospheric observation network in having the conjugate observational points in the northern and southern hemispheres and around the magnetic equator.

In this paper, the maximum electron density of the F2 region (NmF2) are calculated from the observed critical frequency of the F2 region (foF2) and then compared with the IRI-2001 model. The foF2 data are obtained from bottomside ionogram recorded by the FM/CW ionosonde at Chumphon campus of King Mongkut's Institute of Technology Ladkrabang, Thailand, located near the magnetic equator. The measurement data during low solar activity from January 2004 to December 2006 are analyzed based on diurnal and seasonal variation. The results are then compared with the IRI-2001 model predictions. In this paper, the CCIR and URSI options are used to compare them with the observed NmF2. Our study shows that: In general, both the URSI and CCIR options of the IRI model give foF2 close to the measured ones, but the CCIR option produces a smaller range of deviation than the URSI option. The agreement during daytime is generally better than during nighttime. The best agreement between the observed NmF2 and the IRI model is obtained in June solstice. All comparative studies give feedback for new improvements of CCIR and URSI IRI models.

The 2009 International Symposium on Antennas and Propagation (ISAP 2009)

Final Program

October 20-23, 2009

Imperial Queen's Park Hotel, Bangkok, THAILAND

Organized by

Electrical Engineering/Electronics, Computer, Telecommunications, and Information Technology (ECTI) Association of Thailand

in cooperation with

King Mongkut's University of Technology North Bangkok (KMUTNB)

Technical Sponsors

IEICE,
IEEE Antennas and Propagation Society,
IEEE Geoscience and Remote Sensing Society,
IEICE Bangkok Section,
IEEE Thailand Section
IEEE MTT/AP/ED Thailand Chapter

Solar and Latitude Dependence of TEC in Thailand

[#]Prasert Kenpankho [1], Kornyanat Watthanasangmechai [2], and Pornchai Supnithi [3]
[1,2,3] Department of Telecommunication Engineering
King Mongkut's Institute of Technology Ladkrabang
Bangkok, 10520, Thailand
[1] kkpraser@kmitl.ac.th, [2] s2611215@kmitl.ac.th, [3] ksupornc@kmitl.ac.th

1. Introduction

The ionosphere is an upper atmospheric region, starting from an altitude of about 50 kilometers to more than 1000 kilometers. In this region, a fraction of the atmospheric particles is ionized, or the particles are separated into positive ions and free electrons. Since the ionosphere is an irregular medium, through which the radio signals are subjected to refraction. The parameters that have been studied on the ionosphere include TEC (Total Electron Content), NmF2 (the F2 layer peak electron density), hmF2 (the height maximum of the F2 layer) and foF2 (the ionospheric critical frequency). The TEC is one of the important parameters that indicate the ionospheric variation. The study of solar and latitude dependence of TEC have been carried out by previous works [1-4]. The TEC shows the diurnal, seasonal and solar activity variations with dependence on the location of the observation station. Kouris et al., [5] have found that TEC is independent of the solar activity and the correlation coefficients of TEC are correlated with the latitude.

The South East Asia Low Latitude Ionosphere Observation Network (SEALION) is a joint project among the following institutions and countries: National Institute of Information and Communications Technology (NICT), Japan, King Mongkut's Institute of Technology Ladkrabang (KMITL), Thailand, Chiang Mai University (CMU), Thailand, National Institute of Aeronautics and Space (LAPAN), Indonesia, Hanoi Institute of Geophysics (HIG), Vietnamese Academy of Science and Technology, Vietnam, Center for Space Science and Applied Research (CSSAR), Chinese Academy of Sciences, China, and Kyoto University, Japan, observes, monitors and forecasts the ionospheric variation in the Asia Pacific region near the magnetic equator. To study the solar and latitude dependence of total electron content (TEC) in the ionosphere, in this paper, we collect and analyze the TEC data from four observation stations in Thailand.

2. The Observation Setup

To study the solar and latitude dependence of TEC in Thailand, we have collected the TEC data from the four observation stations in Thailand: Chiang Mai, Bangkok, Chumphon, and Phuket with the geomagnetic latitudes as shown in Table 1. Note that Chumphon and Phuket stations are located at the geomagnetic equator, while Chiang Mai and Bangkok stations are in the equatorial ionization anomaly (EIA) region.

Table 1 : The Observation Stations in Thailand

Location	Latitude	Longitude	Geomagnetic Latitude
Chiang Mai	18.76 °N	98.93 °E	12.7 °
Bangkok	13.73 °N	100.78 °E	6.7 °
Chumphon	10.72 °N	99.37 °E	3.0 °
Phuket	7.90 °N	98.39 °E	-0.4 °

The TEC measurement for all stations are obtained from the JAVAD-GPS receivers. Each consists of a microstrip antenna, an amplifier and a TEC Meter JAVAD called as GPS-TEC. The microstrip antenna has a right-hand circularly polarized type and receives two GPS signals with L_1 signal (f_1=1575.42 MHz) and L_2 signal (f_2=1227.60 MHz). The signal from the amplifier is sent to the TEC Meter JAVAD with a built-in GPS receiver unit. The TEC Meter JAVAD works when it receives 4 to 12 GPS signals which are then converted to the TEC values.

3. Data and Methods

The TEC data have been recorded from the four stations from 2003 to 2007. For study the solar and latitude dependence of TEC, we use and analyze the TEC data in 2007 for this research. The TEC data are derived from the GPS signals. The GPS is a system in which signals transmitted by satellite are picked up by a ground based receiver, and these signals are used to determine the geographical position of the receiver. The GPS satellites generate a 10.23 MHz pseudorandom noise (PRN) code to modulate the carriers of the L_1 signal (f_1= 1575.42 MHz) and L_2 signal (f_2 = 1227.60 MHz) (called the P code). The slant TEC (STEC) data from satellites to a receiver can be obtained from the difference between the pseudo ranges and the difference between the phases (L_1 and L_2) of the two frequencies [6] as,

$$STEC=\frac{2\left(f_1 f_2\right)^2}{k\left(f_1^2-f_2^2\right)}\left(P_2-P_1\right), \tag{1}$$

and

$$STEC=\frac{2\left(f_1 f_2\right)^2}{k\left(f_1^2-f_2^2\right)}\left(L_1\lambda_1-L_2\lambda_2\right), \tag{2}$$

where k, related to the ionosphere refraction, is 80.62 (m^3/s^2), P_1 and P_2 are the pseudo ranges, λ_1 and λ_2 are the wavelengths corresponding to f_1 and f_2, respectively.

The TEC, in el/m^2, is computed from

$$TEC=STEC\times\cos\chi, \tag{3}$$

where the zenith angle χ is expressed as

$$\chi=\arcsin\left(\frac{R_E\cos a}{R_E+h}\right), \tag{4}$$

where a is the elevation angle of the satellite, R_E is the mean radius of the Earth, and h is the height of the ionospheric layer, which is assumed to be 400 kilometers [7].

4. Analysis and Results

The investigation has been conducted in order to understand the latitude dependence of TEC in Thailand. In this research, we analyze the median hourly values of TEC data from GPS-TEC measurements at four stations. We study the influence of the solar flux index, daytime and nighttime on TEC, and the dependence of TEC on different latitudes.

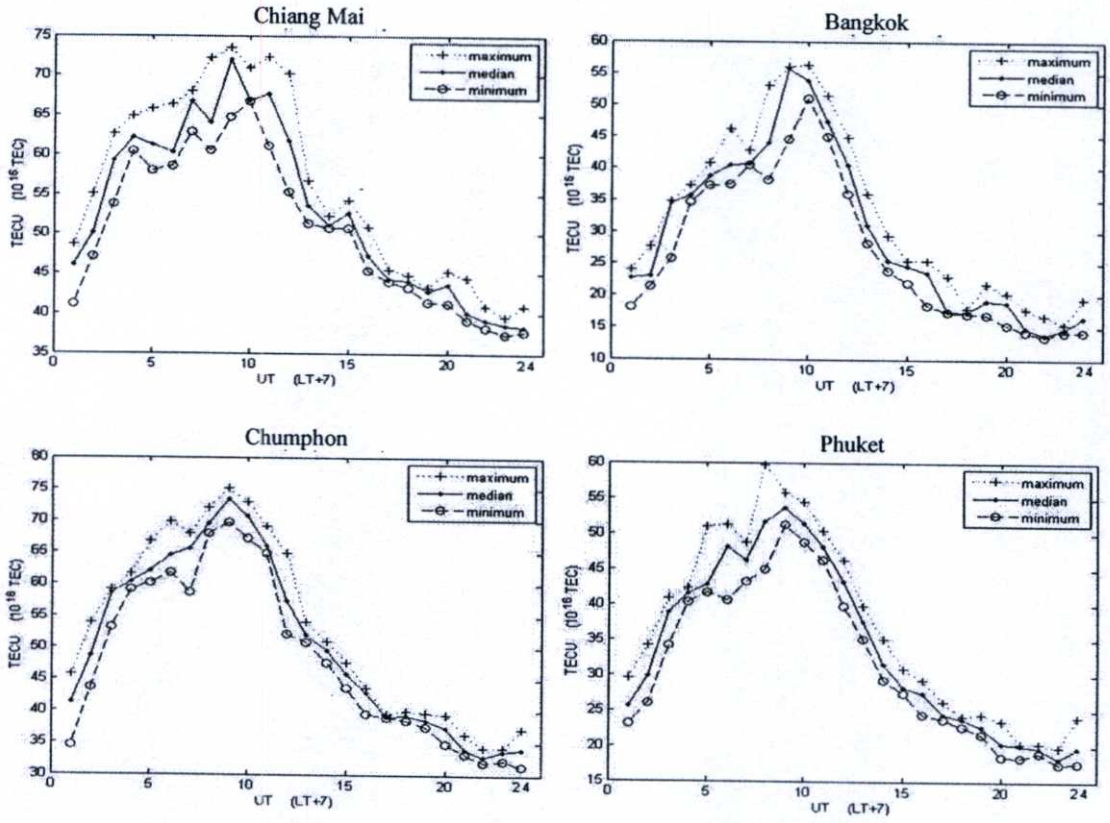

Figure 1 : The median diurnal values of TEC data from four stations in 2007

From Figure 1, Bangkok station has the lowest median value of TEC at 15 TECU (1 TECU = 10^{16} TEC) and Chiang Mai and Chumphon stations have the highest median value of TEC at 75 TECU. At 15:00 LT, Chumphon and Chiang Mai stations have almost the same maximum TEC values at about 75 TECU. At 06:00 LT, before sunrise, Chiang Mai station has the highest TEC value at 37.5 TECU, but Bangkok station has the lowest TEC value at 15 TECU.

Table 2 : The correlation coefficients from daytime and nighttime data of TEC and solar flux index at four locations in 2007

Location	Period	Jan	Feb	Mar	Apr	May	Jun	Jul	Aug	Sep	Oct	Nov	Dec
Chiang Mai	Day	0.48	-0.16	0.01	-0.28	0.49	-0.32	-0.71	0.22	0.00	0.21	0.47	0.68
	Night	0.35	0.22	0.35	-0.31	0.45	-0.32	-0.73	-0.10	-0.03	0.24	0.55	0.23
Bangkok	Day	0.32	-0.40	0.23	0.49	0.76	0.68	-0.06	0.20	0.12	-0.17	-0.53	0.75
	Night	0.33	0.11	0.50	-0.03	0.63	0.05	-0.24	0.19	-0.19	0.05	0.06	0.26
Chumphon	Day	0.33	-0.46	-0.11	0.06	-0.64	0.27	0.61	0.07	0.14	-0.40	-0.17	0.60
	Night	-0.53	0.00	-0.29	0.05	0.00	0.26	-0.09	0.10	-0.28	0.56	-0.88	0.29
Phuket	Day	0.56	-0.15	0.51	0.54	-0.04	0.68	0.51	-0.06	0.11	-0.17	-0.61	0.75
	Night	0.35	-0.10	0.60	-0.28	-0.09	0.25	-0.03	0.22	-0.40	0.05	-0.17	0.49

From Table 2, Phuket station has the most correlation coefficients above 0.30 from daytime and nighttime of TEC data and solar flux index, but Chumphon station has the least correlation coefficients above 0.3 in 2007. For daytime, Bangkok station has the highest positive correlation coefficient at 0.76 in May, but Chiang Mai station has the lowest negative correlation coefficient at -0.71 in July. For nighttime, Bangkok station has the highest positive correlation coefficient at 0.63 in May, but Chumphon station has the lowest negative correlation coefficient at -0.88 in November.

Table 3 : The correlation coefficients of TEC data for paired stations in 2007

Location	Cor.coef	Jan	Feb	Mar	Apr	May	Jun	Jul	Aug	Sep	Oct	Nov	Dec
Chiang Mai	Day	0.86	0.65	0.65	-0.11	0.39	-0.36	0.25	0.69	0.02	0.62	0.04	0.85
Bangkok	Night	0.89	0.16	0.46	0.39	0.49	0.02	0.36	0.59	0.01	-0.01	0.26	0.55
Chiang Mai	Day	0.33	-0.46	-0.11	0.06	-0.64	0.27	0.61	0.07	0.14	-0.40	-0.17	0.60
Chumphon	Night	0.58	0.01	-0.29	0.05	-0.01	0.26	-0.09	0.10	-0.28	0.56	-0.87	0.29
Chiang Mai	Day	0.67	0.33	0.46	-0.06	0.20	-0.25	-0.31	0.51	-0.07	0.46	-0.25	0.80
Phuket	Night	0.80	0.11	0.37	0.43	0.18	0.16	0.07	0.49	-0.05	0.04	0.01	0.49
Bangkok	Day	0.93	0.83	-0.01	-0.09	-0.85	0.62	0.37	-0.12	0.87	0.81	0.69	0.69
Chumphon	Night	0.09	0.00	-0.12	0.38	0.00	-0.16	0.86	0.08	0.92	0.43	-0.12	0.46
Bangkok	Day	0.80	0.71	0.75	0.64	0.08	0.91	0.43	0.79	0.83	0.83	0.72	0.93
Phuket	Night	0.86	0.85	0.85	0.85	0.15	0.79	0.73	0.87	0.84	0.73	0.84	0.80
Chumphon	Day	0.89	0.67	-0.18	0.13	0.01	0.58	0.86	0.04	0.82	0.82	0.62	0.68
Phuket	Night	0.01	0.02	-0.35	0.25	-0.01	-0.04	0.78	0.02	0.90	0.41	0.16	0.65

From Table 3, in December, the correlation coefficients for all paired stations are strongly correlated. The correlation coefficients for all compared stations in January and December are positively correlated. The correlation coefficients between Bangkok and Phuket stations have all positive correlation. For daytime, Bangkok and Phuket stations are strongly correlated. For nighttime, Bangkok and Phuket stations are mostly correlated. The correlation coefficients show that Bangkok and Phuket are a good paired station.

5. Conclusion

Our results of analyses have indicated that the total electron content is quite independent of the solar activity for four stations in Thailand. However, the correlation coefficients of total electron content are rarely correlated with the geomagnetic latitude.

Acknowledgments

The authors are grateful to the Space Environment Group, Applied Electromagnetic Research Center, National Institute of Information and Communications Technology (NICT), Japan for the necessary equipments and valuable cooperation.

References

[1] Bhonsle, R. V., Da Rosa , A. V., Garriott, O. K. Measurement of total electron content and equivalent slab thickness of the mid-latitude ionosphere, Radio Sc., 69D (7), 929, 1965.

[2] Huang , Y. N. Some result of ionospheric slab thickness observations at Lunping, J. Geophys., Res., 88, 5517, 1983.

[3] Davies, K., Liu, X. M. Ionospheric slab thickness in middle and low-latitudes, Radio Sci., 26(4), 997-1005, 1997.

[4] Gulyaea, T.L., Jayachandran, B., Krishnankutty, T.N. Latitudinal variation of ionospheric slab thickness. Adv. Space Res. 33, 862-865, 2004.

[5] S.S. Kouris, K.V. Polimeris, Lj.R.Cander, and L.Ciraolo,"Solar and latitude dependence of TEC and SLAB thickness," Journal of Atmospheric and Solar-Terrestrial Physics 70, 1351-1365. 2008.

[6] G. Blewitt, "An automatic editing algorithm for GPS data," Geophys. Res. Lett., 17, pp. 199-202, 1990.

[7] G. Ma and T. Maruyama, "Derivation of TEC and estimation of instrumental biases from GEONET in Japan," Ann. Geophys., vol. 21, pp. 2083-2093.

AUTHOR BIOGRAPHY

Author: Miss Kornyanat Watthanasangmechai

Date of Birth: August 26, 1987

Bachelor Degree: B.Eng. Telecommunications Engineering

Institute: Department of Telecommunications Engineering, Faculty of Engineering
King Mongkut's Institute of Technology Ladkrabang (KMITL)

Year of Graduation: 2009

Research Interests: Ionospheric Study in an Equatorial Latitude Area, Neural Networks for TEC Prediction, and Ground and Satellite Based Augmentation System.

Related Publications/ Presentations:

1. Watthanasangmechai, K., Supnithi, P., Lerkvaranyu, S., Tsugawa, T., Nagatsuma, T., Maruyama, T., "TEC prediction with neural network for Thailand equatorial latitude station," *Earth Planets, and Space*, in press, 2011.
2. P. Kenpankho, K. Watthanasangmechai, P. Supnithi, T. Tsugawa, and T. Maruyama, "Comparison of GPS TEC measurements with IRI TEC prediction at an equatorial latitude station, Chumphon, Thailand," *Earth Planets, and Space*, doi:10.5047/eps.2011.01.010, in press, 2011.
3. T. Tsugawa, K. Watthanasangmechai, H. Ishibashi, H. Kato, M. Nishioka, Y. Otsuka, A. Saito, T. Nagatsuma and K. T. Murata, "Observations of traveling ionospheric disturbances using GPS networks in the Southeast Asia," JpGU International Symposium 2011, Chiba, Japan, May 22 - 27, 2011.
4. K. Watthanasangmechai, P. Supnithi, A. Mongkolkajid, T. Tsugawa and T. Maruyama, "Current Activities of TEC Monitoring and Prediction in Thailand,"SEALION International Symposium 2011, Bangkok, Thailand, pp. 58-59, Jan 27 - 28, 2011.
5. P. Kenpankho, K. Watthanasangmechai, P. Supnithi, T. Tsugawa, T. Maruyama, "Comparison of GPS TEC Measurements with IRI TEC Prediction at the Equatorial Latitude

Station, Chumphon, Thailand," SEALION International Symposium 2011, Bangkok, Thailand, pp. 62-63, Jan 27 - 28, 2011.

6. Kornyanat Watthanasangmechai, Prasert Kenpankho, Pornchai Supnithi, Takuya Tsugawa, Takashi Maruyama, "Comparisons of GPS TEC and IGS TEC over four SEALION sites," Society of Geomagnetism and Earth, Planetary and Space Sciences (SGEPSS) fall meeting, Okinawa, Japan, B005-34, Oct 30 - Nov 3, 2010.
7. Kornyanat Watthanasangmechai, Pornchai Supnithi, Somkiat Lerkvaranyu, Takashi Maruyama, "Comparison of NN TEC with GPS TEC and IRI-2007 TEC over equatorial latitude station, Thailand," 2010 International Workshop on Information Communication Technology (ICT2010), Bangkok, Thailand, August 2010.
8. P. Kenpankho, K. Watthanasangmechai, P. Supnithi, T. Tsugawa, T. Maruyama, "The comparison of TEC in Chumpon, Thailand with the IRI models," 2010 Asia-Pacific Radio Science Conference (AP-RASC'10), Toyama, Japan, September 2010.
9. Kornyanat Watthanasangmechai, Pornchai Supnithi, Somkiat Lerkvaranyu, Takashi Maruyama, Winai Srisupasitanon, "Hourly and seasonal TEC prediction with neural network at Chumphon equatorial lattitude station, Thailand," The 25th International Technical Conference on Circuits/Systems, Computers and Communications (ITC-CSCC 2010), Pattaya, Thailand, July 2010.
10. K. Watthanasangmechai, P. Supnithi, S. Lerkvaranyu, T. Maruyama, "TEC prediction with neural network for the equatorial latitude station in Thailand," IRI 2009 Workshop, Kagoshima, Japan, October 2009.
11. P. Kenpankho, K. Watthanasangmechai, P. Supnithi, T. Tsugawa, and T. Maruyama, "Equatorial solar and latitude dependence of TEC", IRI 2009 Workshop, Kagoshima, Japan, October 2009.
12. P. Kenpankho, K. Watthanasangmechai and P. Supnithi, "Solar and Latitude Dependence of TEC in Thailand," International Symposium on Antenna and Propagation (ISAP) 2009, Bangkok, Thailand, October 2009.